MycoKeys 69: 1–31 (2020)
doi: 10.3897/mycokeys.69.33563
http://mycokeys.pensoft.net

RESEARCH ARTICLE

A peer-reviewed open-access journal
MycoKeys
Launched to accelerate biodiversity research

New species of *Pseudosperma* (Agaricales, Inocybaceae) from Pakistan revealed by morphology and multi-locus phylogenetic reconstruction

Malka Saba[1], Danny Haelewaters[2,3,4], Donald H. Pfister[2], Abdul Nasir Khalid[5]

1 *Department of Plant Sciences, Quaid-i-Azam University, Islamabad, 45320, Pakistan* **2** *Farlow Herbarium of Cryptogamic Botany, Harvard University, Cambridge, Massachusetts, USA* **3** *Department of Botany and Plant Pathology, Purdue University, West Lafayette, Indiana, USA* **4** *Faculty of Science, University of South Bohemia, České Budějovice, Czech Republic* **5** *Department of Botany, University of the Punjab, Lahore, Pakistan*

Corresponding author: Malka Saba (rustflora@gmail.com; msaba@qau.edu.pk)

Academic editor: Olivier Raspé | Received 3 February 2019 | Accepted 12 May 2020 | Published 10 July 2020

Citation: Saba M, Haelewaters D, Pfister DH, Khalid AN (2020) New species of *Pseudosperma* (Agaricales, Inocybaceae) from Pakistan revealed by morphology and multi-locus phylogenetic reconstruction. MycoKeys 69: 1–31. https://doi.org/10.3897/mycokeys.69.33563

Abstract

During fungal surveys between 2012 and 2014 in pine-dominated forests of the western Himalayas in Pakistan, several collections of *Pseudosperma* (Agaricales, Inocybaceae) were made. These were documented, based on morphological and molecular data. During this work, three new species came to light, which are here formally described as *Pseudosperma brunneoumbonatum*, *P. pinophilum* and *P. triacicularis*. These species belong in the genus *Pseudosperma fide* Matheny et al. (2019) = Pseudosperma clade *fide* Matheny (2005) = *Inocybe* sect. *Rimosae* s.s. *fide* Larsson et al. (2009). Macro- and micro-morphological descriptions, illustrations and molecular phylogenetic reconstructions of the studied taxa are provided. The new species are differentiated from their close relatives by basidiospore size and colouration of basidiomata. Molecular phylogenetic relationships are inferred using ITS (ITS1–5.8S–ITS2), nrLSU and mtSSU sequence data. All three newly-described taxa likely share an ectomycorrhizal association with trees in the genus *Pinus*. In addition, five names are recombined in *Inosperma*, *Mallocybe* and *Pseudosperma*. These are *Inosperma vinaceobrunneum*, *Mallocybe erratum*, *Pseudosperma alboflavellum*, *Pseudosperma friabile* and *Pseudosperma neglectum*.

Keywords

Ectomycorrhizal fungi, molecular systematics, phylogeny, *Pinus roxburghii*, southern Asia, taxonomy

Introduction

Inocybe (Fr.) Fr. (Agaricales, Inocybaceae) in the broad sense (sensu lato) is a highly diverse, ectomycorrhizal genus comprising about 735 known species worldwide (Ullah et al. 2018). *Inocybe* has a widespread distribution and is found commonly in temperate areas and, to a lesser extent, in the tropics (Matheny et al. 2009, Bougher et al. 2012, Matheny et al. 2012). Multi-locus phylogenies of the Inocybaceae by Matheny et al. (2002, 2009) and Matheny (2005) have confirmed that the family is monophyletic. Matheny (2005, 2009) recognised seven major clades within the Inocybaceae; clade names were given with a suggestion to recognise each informally at the generic rank within the family.

Inocybe section *Rimosae* sensu stricto (*fide* Larsson et al. 2009, = clade Pseudosperma *fide* Matheny 2005), traditionally placed in subgenus *Inosperma* (Kuyper 1986, Kobayashi 2002), is one of the seven major clades in the Inocybaceae. Species of this clade are typically characterised by a rimose pileus surface; furfuraceous to furfuraceous-fibrillose stipe; absence of metuloids and pleurocystidia; smooth, elliptical to indistinctly phaseoliform basidiospores; and cylindrical to clavate cheilocystidia. Unlike species in clades Mallocybe and Inosperma (*fide* Matheny 2005) and the genera *Auritella* Matheny & Bougher and *Tubariomyces* Esteve-Rav. & Matheny, all of which also lack pleurocystidia, the basidia of species in the Pseudosperma clade are hyaline and not necropigmented. The Nothocybe clade is represented by only one species, *I. distincta* K.P.D. Latha & Manim. This species also lacks pleurocystidia and can be differentiated based on molecular phylogenetic data (Latha et al. 2016). Some lineages in the Pseudosperma clade are composed of multiple cryptic species (Ryberg et al. 2008) and they form ectomycorrhizal associations with a broad range of host trees, both gymnosperms and angiosperms (Kuyper 1986, Stangl 1989, Jacobsson 2008).

Based on a six-locus phylogeny of the family *Inocybaceae*, Matheny et al. (2019) formally proposed genus names for the different clades: *Inocybe* sensu stricto, *Inosperma* (Kühner) Matheny & Esteve-Rav. (elevated from subgenus-level), *Mallocybe* (Kuyper) Matheny, Vizzini & Esteve-Rav. (elevated from subgenus-level), *Nothocybe* Matheny & K.P.D. Latha and *Pseudosperma* Matheny & Esteve-Rav., in addition to *Auritella* and *Tubariomyces* that were previously described. The authors decided to provide a formal generic system to name the different clades, because this allows better communication and provides the taxonomic precision needed for conservation issues and identification of biodiversity hot spots.

During an investigation of ectomycorrhizal fungi associated with pine species in Pakistan, three species of *Pseudosperma* with affiliation to sect. *Rimosae* s.s. were collected in the vicinity of pure stands of *Pinus roxburghii* Sarg. and *P. wallichiana* A.B. Jacks. The species were documented, based on morphological and molecular phylogenetic data. In this paper, we describe these taxa as new species, *P. brunneoumbonatum*, *P. pinophilum* and *P. triaciculare*. This is the first study in which a combination of morphological and multi-locus phylogenetic data was used to describe species of *Inocybe* sensu lato in sect. *Rimosae* s.s. – now genus *Pseudosperma* – from Pakistan.

Material and methods

Morphological studies

Basidiomata were collected, described and photographed in the field. Colours were compared to the Munsell Soil Color Charts (1975) guide. Collections were dried using a food dehydrator (at 39 °C for 7–9 hours). Microscopic characters were observed in the laboratory using hand-cut sections of basidiomata mounted in a 5% aqueous solution of potassium hydroxide (KOH) and in Congo red. Micromorphological analysis, photographs and measurements were made, using an Olympus BX40 light microscope with Olympus XC50 digital camera and Microsuite special edition software 3.1 (Soft imaging solutions GmbH). Thirty basidiospores were measured from each collection cited. Measurements include the range with extremes provided in parentheses. Q values (length/width ratios) and mean values (average basidiospore length and width) are also provided. Line drawings were made with a Leitz camera Lucida (Wetzlar, Germany). Collections of the newly-described species are deposited at LAH (University of the Punjab Herbarium, Lahore) and FH (Farlow Herbarium, Harvard University).

DNA extraction, PCR amplification and DNA sequencing

Genomic DNA was extracted from a 20 mg piece of dried tissue by a modified CTAB method (Lee et al. 1988). Loci examined during this study include the complete ITS region (ITS1–5.8S–ITS2) of the nuclear ribosomal RNA gene (hereafter ITS), the first ca. 900 bp of the nuclear 28S rRNA gene (nrLSU) and the mitochondrial small subunit rRNA gene (mtSSU).

Primers used for amplification were: ITS1F (Gardes and Bruns 1993) and ITS4 (White et al. 1990) for ITS; LR0R and LR5 for nrLSU (Vilgalys and Hester 1990); and MS1 and MS2 for mtSSU (White et al. 1990). The amplification reaction mixture contained 2.5 µl Econo buffer, 0.5 µl dNTPs, 1.25 µl each primer, 0.125 µl Econo Taq, 14.375 µl of deionised water and 5 µl of template DNA. Thermal profile of PCR for ITS was initial denaturation at 94 °C for 1 min.; then 35 cycles of denaturation at 94 °C for 1 min, annealing at 53 °C for 1 min and extension at 72 °C for 1 min; and final extension at 72 °C for 8 min. For nrLSU: 94 °C for 2 min; then 40 cycles of 94 °C for 1 min, 52 °C for 1 min and 72 °C for 1:30 min; and 72 °C for 5 min. For mtSSU: 95 °C for 10 min; then 30 cycles of 95 °C for 30 sec, 52 °C for 30 sec and 72 °C for 40 sec; and 72 °C for 7 min.

PCR products were run on 1% agarose gel, stained with ethidium bromide and bands were visualised under a UV transilluminator. Amplified PCR products of the ITS region were sent for purification and bidirectional sequencing to Macrogen (Republic of Korea). PCR products of 28S and 16S were purified using QIAquick PCR purification kit (Qiagen, Stanford, California) as per manufacturer's guidelines and sequencing reactions were performed using the Big Dye Terminator v3.1 Cycle Kit (Life Technologies, Carlsbad, California). Sequencing was carried out using the same primers as those used for PCR.

Sequence alignment and phylogenetic analysis

Sequences were manually edited and assembled in BioEdit v7.2.6 (Hall 1999). Generated ITS sequences were trimmed with the conserved motifs 5'–CATTA– and –GACCT–3' (Dentinger et al. 2011) and the alignment portion between these motifs was included in subsequent analyses. BLASTn searches were performed in NCBI GenBank. Three data matrices for phylogenetic inferences were prepared: a concatenated ITS–nrLSU–mtSSU dataset of *Rimosae* s.s. and Inosperma clades (dataset #1); a concatenated ITS–nrLSU–mtSSU dataset of *Rimosae* s.s. subclade A (dataset #2); and an extended nrLSU dataset of *Rimosae* s.s. subclade A (dataset #3). We applied the clade names used by Larsson et al. (2009) in the methods and results sections to maintain consistency and clarity.

Sequences were downloaded from NCBI GenBank (https://www.ncbi.nlm.nih.gov/genbank/). The majority of sequences were generated in the studies of Larsson et al. (2009) and Ryberg et al. (2008), complemented by nrLSU sequences from more recent papers and our newly-generated sequences (details and references in Table 1). Sequences were aligned by locus (ITS+nrLSU, mtSSU) using Muscle v3.7 (Edgar 2004), available in the Cipres Science Gateway (Miller et al. 2010). Ambiguously-aligned regions were detected and removed using trimAl v1.3 (Capella-Gutiérrez et al. 2009), with the following parameters: 60% gap threshold, 50% minimal coverage. The ITS1, 5.8S, ITS2 and nrLSU loci were extracted from the aligned ITS+nrLSU dataset. This allowed us to select substitution models for each region, which is important because there are different rates of evolution within and amongst these components and rDNA loci (e.g. Hillis and Dixon 1991, discussion in Haelewaters et al. 2018).

The data for each locus were concatenated in MEGA7 (Kumar et al. 2016) to create matrices of 2537 bp with sequence data for 123 isolates in the *Rimosae* s.s. and Inosperma dataset (#1); and of 2561 bp for 50 isolates in the *Rimosae* s.s. subclade A dataset (#2). The nrLSU dataset (#3) consisted of 1383 bp for 62 isolates belonging to *Rimosae* s.s. subclade A. Alignments generated during this study are available for download in NEXUS format from the figshare online repository (https://doi.org/10.6084/m9.figshare.c.4701338). Nucleotide substitution models were selected for each locus (ITS1, 5.8S, ITS2, nrLSU, mtSSU) using jModelTest2 (Darriba et al. 2012) by considering the Akaike Information Criterion (AIC). For both concatenated datasets #1 and #2, models were selected for ITS1, 5.8S, ITS2, nrLSU and mtSSU; for dataset #3, the best model was selected for nrLSU. Maximum likelihood was inferred for each dataset under partitioned models using IQ-tree (Nguyen et al. 2015, Chernomor et al. 2016). Ultrafast bootstrapping was done with 1000 replicates (Hoang et al. 2017).

Results

Nucleotide alignment datasets and phylogenetic inferences

Concatenated dataset #1 consisted of 2537 characters, of which 1448 were constant and 841 were parsimony-informative. A total of 123 isolates were included, of which

Naucoria bohemica Velen., *N. salicis* P.D. Orton and *N. submelinoides* (Kühner) Maire (Agaricales, Hymenogastraceae) served as outgroup taxa. The following models were selected by jModelTest2 (AIC): TIM2+I+G (ITS1, -lnL = 6194.8143), TPM2+I (5.8S, -lnL = 445.7026), GTR+G (ITS2, -lnL = 4445.9240), TIM3+I+G (nrLSU, -lnL = 10227.1599) and TVM+I+G (mtSSU, -lnL = 4034.3342). Concatenated dataset #2 consisted of 2561 characters, of which 2026 were constant and 399 were parsimony-informative. A total of 50 isolates were included, of which *P. obsoletum* (Romagn.) Matheny & Esteve-Rav. and *P. perlatum* (Cooke) Matheny & EsteveRav. (*Rimosae* s.s. subclade B, *fide* Larsson et al. 2009) served as outgroup taxa. The following models were selected by jModelTest2 (AIC): TPM2uf+G (ITS1, -lnL = 2070.5127), TrNef (5.8S, -lnL = 261.9437), TPM1uf+I+G (ITS2, -lnL = 1683.9167), TrN+I+G (nrLSU, -lnL = 4608.2667) and TIM2+G (mtSSU, -lnL = 1758.7165). Finally, dataset #3 consisted of 1383 characters, of which 1091 were constant and 205 were parsimony-informative. A total of 67 isolates were included, again with *N. bohemica*, *N. salicis* and *N. submelinoides* as outgroup taxa. For this single-locus dataset, the TrN+I+G model gave the best-scoring tree (nrLSU, -lnL = 5708.4547).

Six strongly supported clades (referred to as subclades A to F, *fide* Larsson et al. 2009) and two additional clades with maximum support were recovered in the ML analysis of the *Rimosae* s.s. and Inosperma clades (dataset #1, Figure 1). A strongly supported clade with 35 sequences corresponds with *Rimosae* s.s. subclade A and includes the following species: *P. bulbosissimum* (Kühner) Matheny & Esteve-Rav., *P. melliolens* (Kühner) Matheny & Esteve-Rav., *P. pinophilum* sp. nov., *P. rimosum* (Bull.) Matheny & Esteve-Rav. (s.s.), *P. sororium* (Kauffman) Matheny & Esteve-Rav. and *P. umbrinellum* (Bres.) Matheny & Esteve-Rav. In addition, numerous taxa on single branches and less-supported clades are recovered.

In all three phylogenetic reconstructions (Figures 1–3), there is high support (BS = 81–100) for the grouping of *P. pinophilum* sp. nov. with *P.* cf. *rimosum* from Europe (isolates JV8125 and PC080925). This clade is deeply nested in *Rimosae* s.s. subclade A (*fide* Larsson et al. 2009). *Pseudosperma brunneoumbonatum* sp. nov. is retrieved as sister to an undescribed species from Papua New Guinea (isolates TR104_05 and TR133_05) with high support (BS = 96–100). In both datasets #2 and #3, this clade, again, is deeply nested in *Rimosae* s.s. subclade A. In dataset #1, however, the clade *P. brunneoumbonatum* – *I.* sp. Papua New Guinea is placed between *Rimosae* subclades A and B (*fide* Larsson et al. 2009) with maximum support (Figure 1). *Pseudosperma triaciculare* sp. nov. is retrieved with high support (BS = 95–100) as an independent clade without clear affinities outside of *Rimosae* s.s. subclade A.

Our phylogenetic reconstructions (Figures 1–3) indicate that several undescribed species occur in *Rimosae* s.s. subclade A (see Discussion). All ML analyses recovered two new Pakistani species, *P. triaciculare* and *P. pinophilum*, as strongly-supported lineages nested within this subclade, whereas a third species, *P. brunneoumbonatum*, forms a strongly-supported clade outside of what is currently recognised as subclade A. These three new taxa from Pakistan can be distinguished, based on molecular phylogenetic data, as well as morphology and ecology.

Table 1. Isolates used in phylogenetic analyses, with geographic origin and GenBank accession numbers. Accession numbers of sequences generated during this study are in boldface. Explanation of datasets: #1 = concatenated ITS–nrLSU–mtSSU dataset of *Rimosae* s.s. and Inosperma clades, #2 = concatenated ITS–nrLSU–mtSSU dataset of *Rimosae* s.s. subclade A, #3 = extended nrLSU dataset of *Rimosae* s.s. subclade A (dataset #3). X under #1, #2, #3 = sequence(s) were used in the respective dataset. OUT = outgroup.

Species	Isolate	Geographic origin	GenBank		Reference(s)	Dataset		
			ITS/nrLSU	mtSSU		#1	#2	#3
Alnicola bohemica	EL71b-03	Sweden	FJ904179	FJ904243	Larsson et al. (2009)	OUT		OUT
Alnicola salicis	EL71a-03	Sweden	FJ904180		Larsson et al. (2009)	OUT		OUT
Alnicola submelinoides	TAA185174	Estonia	AM882885		Ryberg et al. (2008)	OUT		OUT
Conocybe siliginea	LÖ93-04	Sweden	DQ389731		Larsson and Orstadius (2008)	OUT		
Crepidotus calolepis	EL14-08	Sweden	FJ904178	FJ904242	Larsson et al. (2009)	X		
Crepidotus mollis	EL45-04	Sweden	AM882996		Ryberg et al. (2008)	X		
Inosperma adaequatum	PC2008-0014	Great Britain	FJ904177	FJ904240	Larsson et al. (2009)	X		
Inosperma adaequatum	MR00022	Sweden	AM882706	FJ904241	Ryberg et al. (2008), Larsson et al. (2009)	X		
Inosperma bongardii	EL123-04	Sweden	AM882941	FJ904186	Ryberg et al. (2008), Larsson et al. (2009)	X		
Inosperma cf. *calamistrata*	KHL13071	Costa Rica	AM882948		Ryberg et al. (2008)	X		
Inosperma cervicolor	SJ04024	Sweden	AM882939	FJ904185	Ryberg et al. (2008), Larsson et al. (2009)	X		
Inosperma cookei	MR00035	Sweden	AM882954		Ryberg et al. (2008)	X		
Inosperma cookei	EL191-06	Great Britain	FJ904173	FJ904234	Larsson et al. (2009)	X		
Inosperma cookei	EL70a-03	Sweden	AM882953		Ryberg et al. (2008)	X		
Inosperma cookei	EL73-05	Sweden	AM882955		Ryberg et al. (2008)	X		
Inosperma cookei	EL109-04	Sweden	AM882956	FJ904233	Ryberg et al. (2008), Larsson et al. (2009)	X		
Inosperma cf. *cookei*	EL104-04	Sweden	AM882952		Ryberg et al. (2008)	X		
Inosperma erubescens	TAA185164	Estonia	AM882950		Ryberg et al. (2008)	X		
Inosperma erubescens	KGN980714	Sweden	AM882951	FJ904239	Ryberg et al. (2008), Larsson et al. (2009)	X		
Inosperma erubescens	BH910707	Sweden	AM882949		Ryberg et al. (2008)	X		
Inosperma maculatum	EL74-05	Sweden	AM882959		Ryberg et al. (2008)	X		
Inosperma fulvum	EL78-03	Sweden	AM882962		Ryberg et al. (2008)	X		
Inosperma fulvum	EL166-08	Sweden	FJ904171	FJ904231	Larsson et al. (2009)	X		
Inosperma fulvum	EL114-06	Sweden	FJ904170		Larsson et al. (2009)	X		
Inosperma fulvum	SJ05029	Sweden	AM882994	FJ904230	Ryberg et al. (2008), Larsson et al. (2009)	X		
Inosperma fulvum	EL247-06	France	FJ904169		Larsson et al. (2009)	X		
Inosperma fulvum	PAM01100120	France	FJ904168		Larsson et al. (2009)	X		
Inosperma fulvum	SJ06007	Sweden	FJ904167		Larsson et al. (2009)	X		
Inosperma maculatum	MR00020	Sweden	AM882958		Ryberg et al. (2008)	X		
Inosperma maculatum	EL121-04	Sweden	AM882957	FJ904232	Ryberg et al. (2008), Larsson et al. (2009)	X		
Inosperma maculatum	EL58-03	Sweden	AM882963		Ryberg et al. (2008)	X		
Inosperma maculatum	EL126-04	Sweden	AM882964		Ryberg et al. (2008)	X		
Inosperma maculatum	EL182-08	Slovenia	FJ904172		Larsson et al. (2009)	X		

Species	Isolate	Geographic origin	GenBank		Reference(s)	Dataset		
			ITS/nrLSU	mtSSU		#1	#2	#3
Inosperma quietiodor	RP980718	Sweden	FJ936169	FJ904238	Larsson et al. (2009)	X		
Inosperma quietiodor	LAS97-067	Sweden	AM882974		Ryberg et al. (2008)	X		
Inosperma quietiodor	LAS94-023	Sweden	AM882961		Ryberg et al. (2008)	X		
Inosperma quietiodor	PAM01091310	France	FJ936168	FJ904237	Larsson et al. (2009)	X		
Inosperma quietiodor	EL115-04	Sweden	AM882960	FJ904236	Ryberg et al. (2008), Larsson et al. (2009)	X		
Inosperma quietiodor	JV20202	Norway	FJ904174	FJ904235	Larsson et al. (2009)	X		
Inosperma rhodiolum	PAM00090117	France	FJ904176		Larsson et al. (2009)	X		
Inosperma rhodiolum	EL223-06	France	FJ904175		Larsson et al. (2009)	X		
Inosperma subhirsutum	EL45-05	Norway		FJ904187	Larsson et al. (2009)	X		
Inosperma virosum	TBGT753	India	KT329458		Pradeep et al. 2016			X
Inosperma virosum	CAL1383	India	KY549138		K.P. Deepna Latha and P. Manihoman unpubl.			X
Mallocybe agardhii	EL88-04	Sweden	FJ904123	FJ904182	Larsson et al. (2009)	X		
Mallocybe dulcamara	EL89-06	Sweden	FJ904122	FJ904181	Larsson et al. (2009)	X		
Mallocybe fulvipes	EL37-05	Norway	AM882858	FJ904184	Ryberg et al. (2008), Larsson et al. (2009)	X		
Mallocybe terrigena	EL117-04	Sweden	AM882864	FJ904183	Ryberg et al. (2008), Larsson et al. (2009)	X		
Pseudosperma aestivum	BK18089706	USA, Utah	EU600847		Matheny et al. (2009)		X	X
Pseudosperma alboflavellum	TBGT11280	India	KP171058		Pradeep et al. (2016)			X
Pseudosperma arenicola	RC GB99-014	France	FJ904134	FJ904189	Larsson et al. (2009)	X		
Pseudosperma arenicola	EL238-06	France	FJ904133	FJ904188	Larsson et al. (2009)	X		
Pseudosperma breviterincarnatum	BK18089724	USA, Utah	EU555449		Matheny et al. (2009)			X
Pseudosperma breviterincarnatum	BK28080407	USA, Utah	EU555451		Matheny et al. (2009)			X
Pseudosperma breviterincarnatum	PBM1914	USA, Washington	JQ319677		Kropp et al. (2013)			X
Pseudosperma brunneoumbonatum	**MSM#0053**	**Pakistan**	**MG742419/ MG742420**	**n/a**	**This study**	**X**	**X**	**X**
Pseudosperma brunneoumbonatum	**MSM#00545**	**Pakistan**	**MG742421/ MG742422**	**n/a**	**This study**	**X**	**X**	**X**
Pseudosperma bulbosissimum	EL51-05	Norway	AM882764		Ryberg et al. (2008)	X	X	X
Pseudosperma bulbosissimum	EL66-05	Norway	AM882765	FJ904224	Ryberg et al. (2008), Larsson et al. (2009)	X	X	X
Pseudosperma bulbosissimum	EL37-06	Sweden	FJ904161	FJ904223	Larsson et al. (2009)	X	X	X
Pseudosperma bulbosissimum	EL75-07	Sweden	FJ904160	FJ904222	Larsson et al. (2009)	X	X	X
Pseudosperma bulbosissimum	EL88-06	Sweden	FJ904159	FJ904221	Larsson et al. (2009)	X	X	X
Pseudosperma bulbosissimum	EL30-06	Sweden	FJ904158	FJ904220	Larsson et al. (2009)	X	X	X
Pseudosperma cercocarpi	BK20069806	USA, Utah	EU600890		Matheny et al. (2009)			X
Pseudosperma cercocarpi	BK20069807	USA, Utah	JQ319683		Kropp et al. (2013)			X
Pseudosperma dulcamaroides	EL29-08	USA, Montana	FJ904127		Larsson et al. (2009)	X		
Pseudosperma dulcamaroides	EL112-06	Sweden	FJ904126	FJ904194	Larsson et al. (2009)	X		
Pseudosperma flavellum	EL56-08	Sweden	FJ904131	FJ904198	Larsson et al. (2009)	X		
Pseudosperma flavellum	EL137-05	Sweden	AM882776	FJ904199	Ryberg et al. (2008), Larsson et al. (2009)	X		
Pseudosperma flavellum	LAS89-030	Sweden	AM882775		Ryberg et al. (2008)	X		

Species	Isolate	Geographic origin	GenBank		Reference(s)	Dataset		
			ITS/nrLSU	mtSSU		#1	#2	#3
Pseudosperma cf. *flavellum*	GK080924	Great Britain	FJ904129	FJ904196	Larsson et al. (2009)	X		
Pseudosperma cf. *flavellum*	PAM05062502	France	FJ904128	FJ904195	Larsson et al. (2009)	X		
Pseudosperma cf. *flavellum*	EL118-05	Finland	AM882782		Ryberg et al. (2008)	X		
Pseudosperma cf. *flavellum*	BJ920829	Sweden	AM882774		Ryberg et al. (2008)	X		
Pseudosperma cf. *flavellum*	EL90-04	Sweden	AM882773		Ryberg et al. (2008)	X		
Pseudosperma griseorubidum	CAL1253	India	KT180327		Deepna Latha and Manimohan (2015)			X
Pseudosperma hygrophorus	EL97-06	Sweden	FJ904137	FJ904202	Larsson et al. (2009)	X		
Pseudosperma keralense	TBGT12854	India	KP171059		Pradeep et al. (2016)			X
Pseudosperma keralense	TBGT12828	India	KP171060		Pradeep et al. (2016)			X
Pseudosperma melliolens	PAM05052303	France	FJ904148	FJ904211	Larsson et al. (2009)	X	X	X
Pseudosperma melliolens	EL224-06	France	FJ904149		Larsson et al. (2009)	X	X	X
Pseudosperma cf. *microfastigiatum*	EL113-06	Sweden	FJ904156	FJ904217	Larsson et al. (2009)	X	X	X
Pseudosperma mimicum	EBJ961997	Sweden	FJ904124	FJ904191	Larsson et al. (2009)	X		
Pseudosperma mimicum	TK2004-114	Sweden	AM882781		Ryberg et al. (2008)	X		
Pseudosperma niveivelatum	BK21089714	USA, Utah	JQ319695		Kropp et al. (2013)		X	X
Pseudosperma niveivelatum	BK27089718	USA, Utah	EU600831		Matheny et al. (2009)		X	X
Pseudosperma niveivelatum	Stz12816	USA, Washington	JQ319696		Kropp et al. (2013)		X	X
Pseudosperma obsoletum	EL17-04	Sweden	AM882769	FJ904204	Ryberg et al. (2008), Larsson et al. (2009)	X	OUT	X
Pseudosperma obsoletum	BJ890915	Sweden	AM882770		Ryberg et al. (2008)	X	OUT	X
Pseudosperma occidentale	PBM525	USA, Washington	AY038321		Matheny et al. (2002)			X
Pseudosperma occidentale	BK27089703	USA, Utah	EU600893		Matheny et al. (2009)			X
Pseudosperma pakistanense	LAH35285	Pakistan	MG958608		Ullah et al. (2018)			X
Pseudosperma pakistanense	LAH35283	Pakistan	MG958609		Ullah et al. (2018)			X
Pseudosperma perlatum	BJ940922	Sweden	AM882772		Ryberg et al. (2008)	X	OUT	X
Pseudosperma perlatum	EL74-04	Sweden	AM882771	FJ904205	Ryberg et al. (2008), Larsson et al. (2009)	X	OUT	X
Pseudosperma pinophilum	**MSM#0046**	**Pakistan**	**MG742414/ MG742418**	**MG742416**	**This study**	**X**	**X**	**X**
Pseudosperma pinophilum	**MSM#0047**	**Pakistan**	**MG742417/ MG742415**	**MK474612**	**This study**	**X**	**X**	**X**
Pseudosperma rimosum	AO2008-0250	Great Britain	FJ904147	FJ904210	Larsson et al. (2009)	X	X	X
Pseudosperma rimosum	EL118-08	Sweden	FJ904146	FJ904209	Larsson et al. (2009)	X	X	X
Pseudosperma rimosum	EL102-04	Sweden	AM882761		Ryberg et al. (2008)	X	X	X
Pseudosperma rimosum	EL211-06	France	FJ904145		Larsson et al. (2009)	X	X	X
Pseudosperma rimosum	TK97-156	Sweden	AM882844		Ryberg et al. (2008)	X	X	
Pseudosperma rimosum	PAM03110904	France	FJ904144	FJ904208	Larsson et al. (2009)	X	X	X
Pseudosperma rimosum	EL75-05	Sweden	AM882762	FJ904207	Ryberg et al. (2008), Larsson et al. (2009)	X	X	X
Pseudosperma rimosum	SJ04007	Sweden	AM882763		Ryberg et al. (2008)	X	X	X
Pseudosperma rimosum	PAM06112703	Corsica	FJ904143	FJ904206	Larsson et al. (2009)	X	X	X
Pseudosperma cf. *rimosum*	EL71-04	Sweden	AM882786	FJ904193	Ryberg et al. (2008), Larsson et al. (2009)	X		

Species	Isolate	Geographic origin	GenBank		Reference(s)	Dataset		
			ITS/nrLSU	mtSSU		#1	#2	#3
Pseudosperma cf. *rimosum*	JD2008-0241	Great Britain	FJ904125	FJ904192	Larsson et al. (2009)	X		
Pseudosperma cf. *rimosum*	I116-06	Australia	FJ904142		Larsson et al. (2009)	X		
Pseudosperma cf. *rimosum*	PAM05061101	France	FJ904155	FJ904216	Larsson et al. (2009)	X	X	X
Pseudosperma cf. *rimosum*	JV26578	Estonia	FJ904154	FJ904215	Larsson et al. (2009)	X	X	X
Pseudosperma cf. *rimosum*	EL127-04	Sweden	AM882768	FJ904219	Ryberg et al. (2008), Larsson et al. (2009)	X	X	X
Pseudosperma cf. *rimosum*	TAA185135	Estonia	AM882766		Ryberg et al. (2008)	X	X	X
Pseudosperma cf. *rimosum*	JV22619	Estonia	FJ904157	FJ904218	Larsson et al. (2009)	X	X	X
Pseudosperma cf. *rimosum*	PC080925	Great Britain	FJ904153		Larsson et al. (2009)	X	X	X
Pseudosperma cf. *rimosum*	JV8125	Finland	FJ904152	FJ904214	Larsson et al. (2009)	X	X	X
Pseudosperma cf. *rimosum*	EL81-06	Sweden	FJ904135	FJ904190	Larsson et al. (2009)	X		
Pseudosperma sororium	Kuoljok0512	Sweden	FJ904150	FJ904212	Larsson et al. (2009)	X	X	X
Pseudosperma sororium	JV15200	Sweden	FJ904151	FJ904213	Larsson et al. (2009)	X	X	X
Pseudosperma sp.	TR138_05	Papua New Guinea	JN975009		Ryberg and Matheny (2012)	X	X	X
Pseudosperma sp.	TR133_05	Papua New Guinea	JQ319709		Kropp et al. (2013)	X	X	X
Pseudosperma sp.	TR104_05	Papua New Guinea	JN975011		Ryberg and Matheny (2012)	X	X	X
Pseudosperma squamatum	SJ08003	Sweden	FJ904136	FJ904201	Larsson et al. (2009)	X		
Pseudosperma squamatum	TK96-109	Sweden	AM882780		Ryberg et al. (2008)	x		
Pseudosperma squamatum	SJ85048	Norway	AM882778		Ryberg et al. (2008)	X		
Pseudosperma squamatum	PAM05052301	France	FJ904132	FJ904200	Larsson et al. (2009)	X		
Pseudosperma cf. *squamatum*	I93-04	Australia	FJ904141		Larsson et al. (2009)	X		
Pseudosperma cf. *squamatum*	I113-05	Australia	FJ904140		Larsson et al. (2009)	X		
Pseudosperma cf. *squamatum*	SJ92-010	Sweden	AM882785		Ryberg et al. (2008)	X		
Pseudosperma cf. *squamatum*	SM92-013	Sweden	AM882783		Ryberg et al. (2008)	X		
Pseudosperma cf. *squamatum*	SJ92-017	Sweden	AM882784		Ryberg et al. (2008)	X		
Pseudosperma cf. *squamatum*	Stordal18318	Norway	FJ904139		Larsson et al. (2009)	X		
Pseudosperma cf. *squamatum*	JV2609	Finland	FJ904138	FJ904203	Larsson et al. (2009)	X		
Pseudosperma triaciculare	**MSM#0039**	**Pakistan**	**MG742423/ MG742424**	**MG742425**	**This study**	**X**	**X**	**X**
Pseudosperma triaciculare	**MSM#0041**	**Pakistan**	**MG742429/ MG742430**	**MG742431**	**This study**	**X**	**X**	**X**
Pseudosperma triaciculare	**MSM#0040**	**Pakistan**	**MG742426/ MG742427**	**MG742428**	**This study**	**X**	**X**	**X**
Pseudosperma umbrinellum	JV13699	Finland	FJ904165	FJ904228	Larsson et al. (2009)	X	X	X
Pseudosperma umbrinellum	JV17954	Estonia	FJ904166	FJ904229	Larsson et al. (2009)	X	X	X
Pseudosperma umbrinellum	PC081010	Great Britain	FJ904164	FJ904227	Larsson et al. (2009)	X	X	X
Pseudosperma umbrinellum	PC080816	Great Britain	FJ904163	FJ904226	Larsson et al. (2009)	X	X	X
Pseudosperma umbrinellum	PAM01102912	France	FJ904162	FJ904225	Larsson et al. (2009)	X	X	X
Pseudosperma xanthocephalum	PAM00100606	France	FJ904130	FJ904197	Larsson et al. (2009)	X		

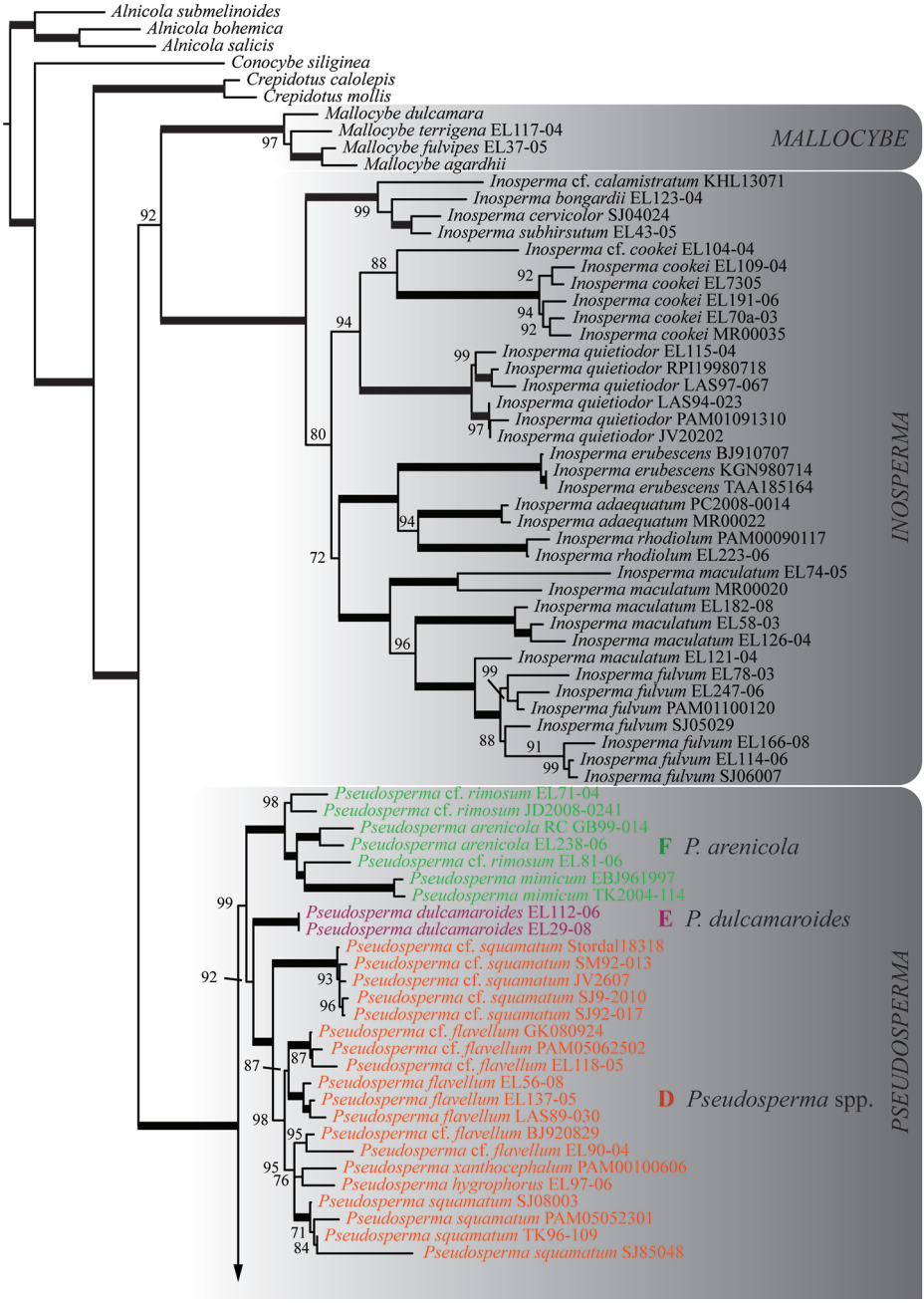

Figure 1. The best-scoring ML tree (-lnL = 27210.474) of the *Rimosae* s.s. and Inosperma clades, reconstructed from the concatenated ITS–nrLSU–mtSSU dataset. ML bootstraps (if ≥ 70) are presented above or in front of the branch leading to each node. Thick branches have maximum support (ML BS = 100). Subclade designations within sect. *Rimosae* s.s. follow Larsson et al. (2009) in the strict sense. Newly-described species are in boldface.

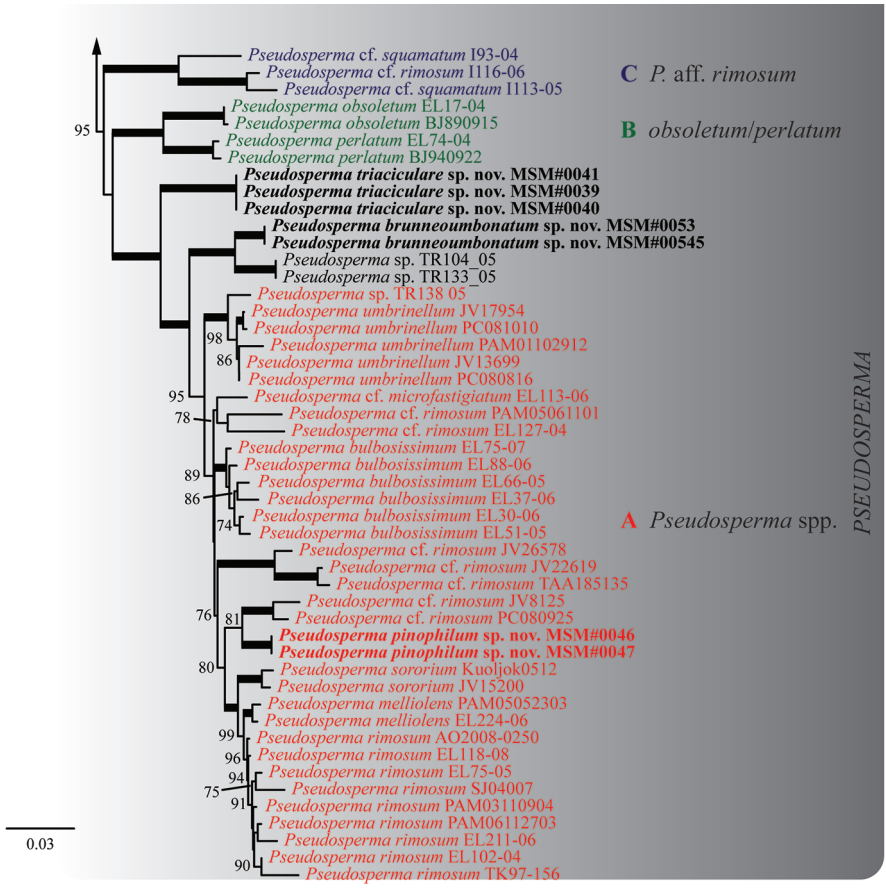

Figure 1. Continued.

Taxonomy

***Pseudosperma brunneoumbonatum* Saba & Khalid, sp. nov.**
MycoBank No: 822655
Figure 4

Diagnosis. Characterised by the dark brown umbo and basidiospores 10.3–15.3(–16.7) × 6.6–9.9 µm and an ecological association with *Pinus*.

Types. ***Holotype:*** Pakistan, Prov. Khyber Pakhtunkhwa, Abbottabad, Shimla, 14 Sep 2012, *leg.* M. Saba & A.N. Khalid; MSM#0053 (LAH 310032); GenBank accession nos. MG742419 (ITS), MG742420 (nrLSU). ***Paratype:*** *ibid.*, 6 Aug. 2014; MSM#00545 (LAH 31003); GenBank accession nos. MG742421 (ITS), MG742422 (nrLSU).

Etymology. From Latin, referring to dark brown colour of the umbo.

Description. ***Pileus*** 20–38 mm in diam., plane to broadly convex with an acute umbo; margin straight or flaring to deflexed; surface dry, dull, strongly rimose, cracked towards centre but disc smooth and unbroken; strong brown (5YR4/8), disc/umbo deep brown (5YR2/6). ***Lamellae*** regular, adnexed to sinuate, close, pale orange yellow (10YR8/4) or pale yellow (5Y9/4), becoming yellowish-brown with age, concolorous with stipe; edges even; lamelullae one tier; edges white and fimbrirate. ***Stipe*** 22–40 mm, central to slightly eccentric, equal, recurved squamulose, longitudinally fibrillose, pale yellow (5Y9/4) or light yellowish-brown (10YR7/4), veil not observed. Odour spermatic. Context white, lacking any colour changes where cut or bruised.

Basidiospores 10.3–15.3(–16.7) × 6.6–9.9 µm [x = 12.5 × 7.5 µm, Q = 1.2–1.96], smooth, phaseoliform or ellipsoid, thin-walled, pale brown to reddish-brown in KOH, apiculus present or absent, apex obtuse. ***Basidia*** 27–39 × 10.6–16 µm, clavate with refractive contents, primarily 4-sterigmate, less often 2-sterigmate, thin-walled, hyaline in KOH; sterigmata 3–6 µm long. ***Pleurocystidia*** absent. ***Cheilocystidia*** 24–35 × 14–29 µm, numerous, clavate, some catenate, hyaline to pale brown, thin-walled. ***Caulocystidia*** clavate or cylindrical, similar to cheilocystidia, infrequent. ***Pileipellis*** a cutis, hyphae cylindrical, 5–9 µm wide, thin-walled, pale brown in KOH, some with encrustations, septate. ***Lamellar trama*** of parallel hyphae, 5–10 µm wide; subhymenium of compact hyphae, 3–6 µm wide. ***Stipitipellis*** cylindrical hyphae, hyaline in mass in KOH. All structures inamyloid. ***Clamp connections*** present.

Habit and habitat. Occurring in August and September, solitary or in groups, scattered on the forest floor in stands of *Pinus roxburghii* (Pinaceae).

Notes. In all phylogenetic reconstructions (Figures 1–3), *P. brunneoumbonatum* sp. nov. is sister to *Pseudosperma* sp. (isolates TR104_05 and TR133_05). This undescribed species from high-elevations in Papua New Guinea is associated with *Castanopsis* (Fagaceae). Of the north temperate species, *P. brunneoumbonatum* is phylogenetically most closely related to *P. umbrinellum* (Figure 3, Table 2). In terms of morphology, *P. brunneoumbonatum* differs from *P. umbrinellum* by its strong brown pileus with an acute umbo (hazel to cinnamon brown) and somewhat larger basidiospores (measuring 10–13 × 5.5–6.5 µm in *P. umbrinellum*). Other related North American taxa are *P. aestivum* (Kropp, Matheny & Hutchison) Matheny & Esteve-Rav. and *P. niveivelatum* (D.E. Stuntz ex Kropp, Matheny & Hutchison) Matheny & Esteve-Rav. *Pseudosperma aestivum* can be separated by larger basidiomata and different pileus colouration (yellowish to pale yellow with yellow-brown centre), whereas *P. niveivelatum* has a white stipe and a non-rimose pileus with different colouration (covered with abundant white velipellis) (Kropp et al. 2013). *Pseudosperma perlatum* (Cooke) Matheny & Esteve-Rav. superficially resembles *P. brunneoumbonatum*. However, the slightly larger basidiospores, pale orange yellow stipe and a presumed association with *Pinus* distinguish the new species from *P. perlatum*, which is an associate of deciduous trees (Vauras and Huhtinen 1986). It differs from *I. rimosum* in having broader basidiospores.

Pseudosperma neoumbrinellum (T. Bau & Y.G. Fan) Matheny & Esteve-Rav. is an Asian species (described from China) with similar basidioma size and colouration (Bau and Fan 2018). The basidiospores of *P. brunneoumbonatum*, however, are remarkably larger.

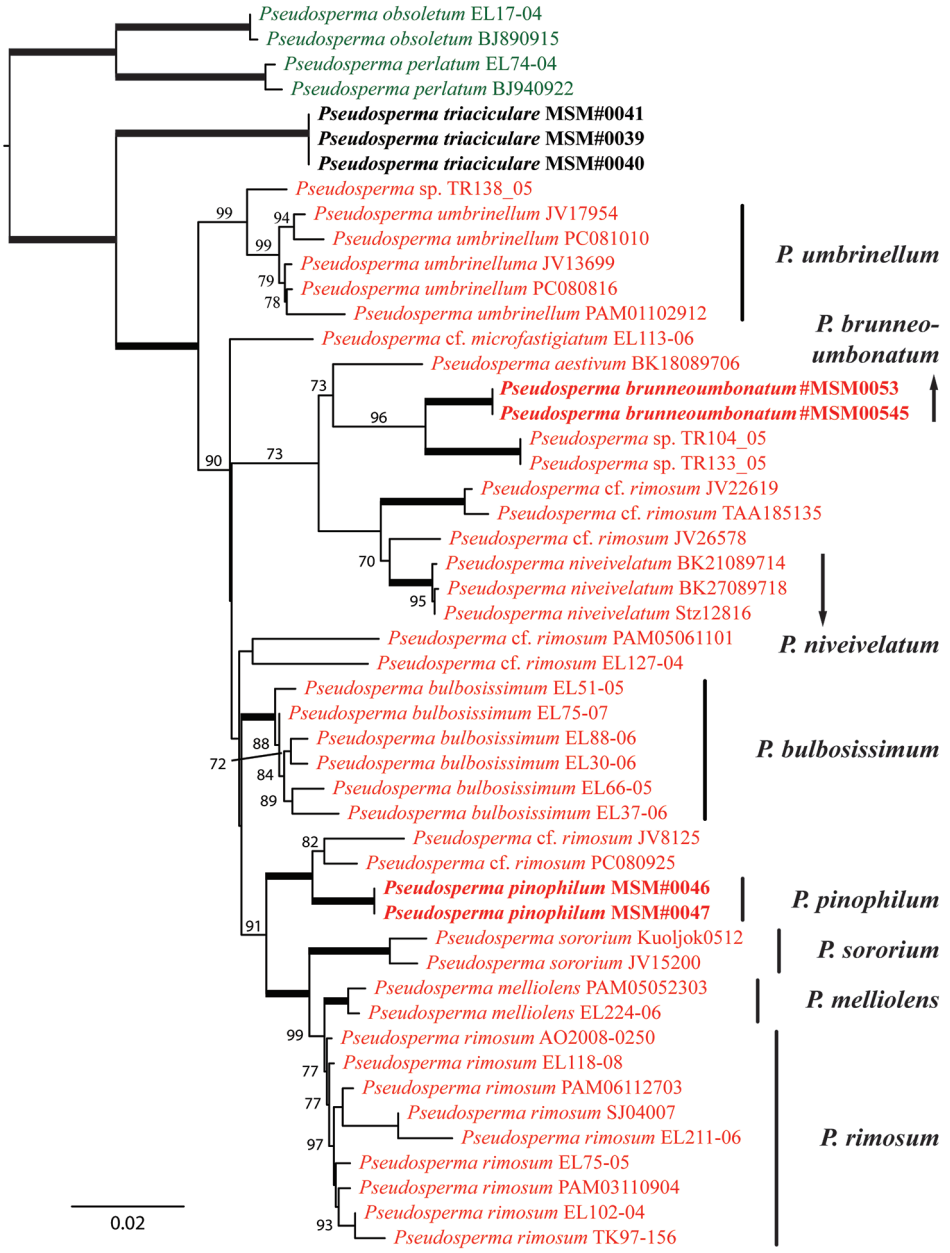

Figure 2. The best-scoring ML tree (-lnL = 9359.879) of *Rimosae* s.s. subclade A, reconstructed from the concatenated ITS–nrLSU–mtSSU dataset. ML bootstraps (if ≥ 70) are presented above or in front of the branch leading to each node. Thick branches have maximum support (ML BS = 100). Well-supported clades that represent described species within *Rimosae* s.s. subclade A are named. Newly-described species are in boldface.

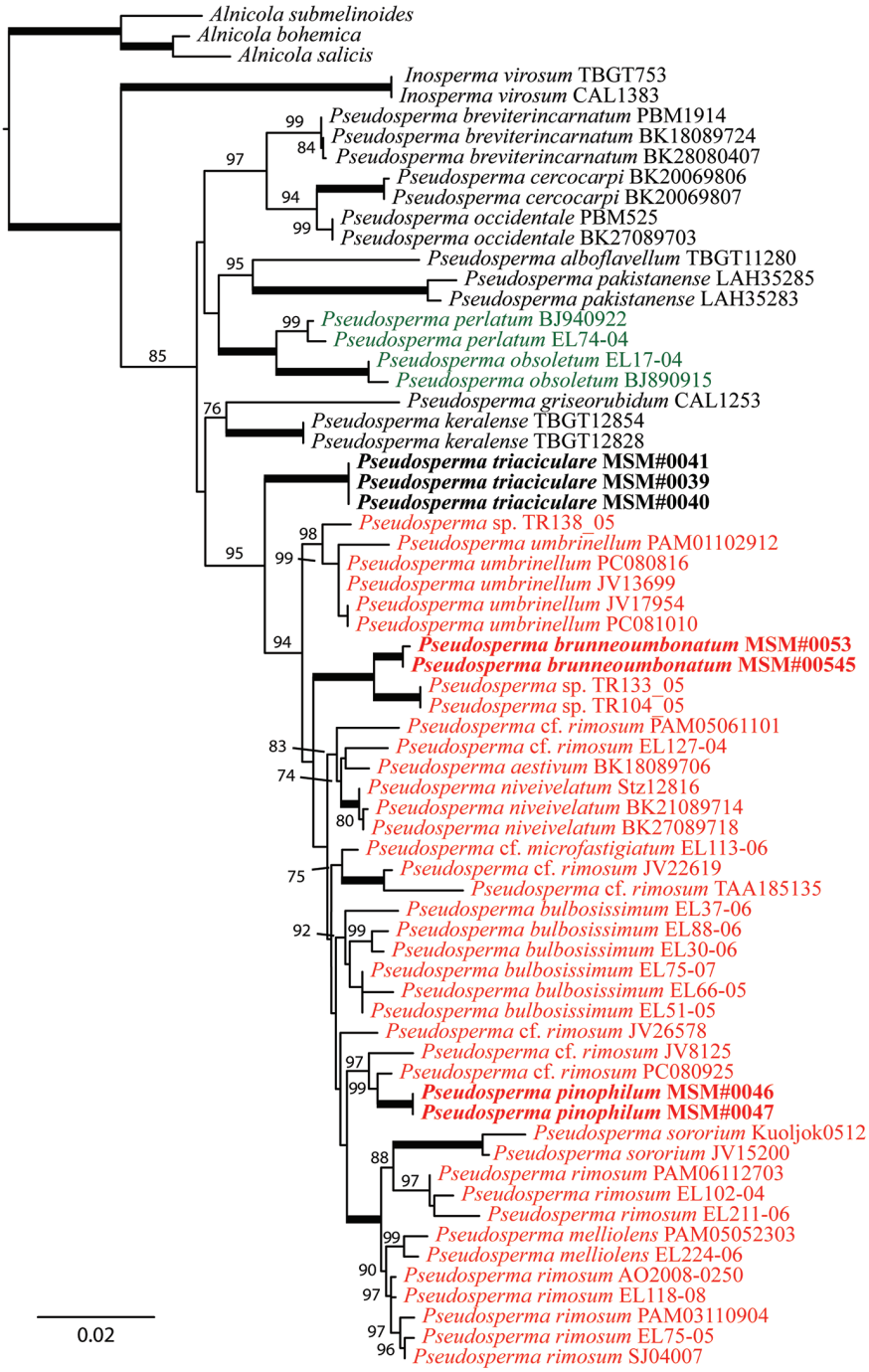

Figure 3. The best-scoring ML tree (-lnL = 5704.951) of *Rimosae* s.s. subclade A, complemented with recently-described species within sect. *Rimosae* s.s., reconstructed from the nrLSU dataset. ML bootstraps (if ≥ 70) are presented above or in front of the branch leading to each node. Thick branches have maximum support (ML BS = 100). Newly-described species are in boldface.

Table 2. Comparison of ecological and morphological characters among the three newly described Pakistani species of *Pseudosperma* and phylogenetically similar species *P. rimosum* and *P. umbrinellum*.

Species	*P. brunneoumbonatum*	*P. pinophilum*	*P. triacicularis*	*P. rimosum*	*P. umbrinellum*
Host association(s)	*Pinus*	*Pinus*	*Pinus*	*Abies*, *Alnus*, *Betula*, *Carpinus*, *Cedrus*, *Corylus*, *Fagus*, *Larix*, *Picea*, *Pinus*, *Populus*, *Quercus*, *Salix*, *Tilia*	*Helianthemum*, *Pinus*, *Populus*, *Quercus*
Pileus color	Strong brown (5YR4/8), disc/umbo deep brown (5YR2/6)	Strong brown throughout (5YR4/6 to 5YR4/8), with dark brown umbo	Brownish orange (5YR5/8) to fulvous	Highly variable, from pale to ochraceous yellow brown to dark brown, usually darkest around center; sometimes very conspicuous and bright yellow; sometimes blackish brown	Hazel to cinnamon brown, warm yellowish to reddish brown caps with a dark center and contrasting strongly rimose and lighter periphery
Umbo	Acute	Acute	Acute to subacute or obtuse	Acute	Blunt
Velipellis	Absent	Absent	Present	Absent	Absent
Basidiospores	10.3–15.3(–16.7) × 6.6–9.9 µm	(8.2–)9.4–15.8 × 6.3–8 µm	(7.7–)8.9–12.5 × 6.1–7.7 µm	9.5–12.5 × 6.0–7.0 µm	10.0–13.0 × 5.5–6.5 µm
Reference(s)	This paper	This paper	This paper	Kuyper (1986), Larsson et al. (2009)	Kuyper (1986), Larsson et al. (2009)

Pseudosperma himalayense (Razaq, Khalid & Kobayashi) Matheny & Esteve-Rav. was recently described from Pakistan (Liu et al. 2018) and is similar to *P. brunneoumbonatum* in having similar pileus size. This species was found at different localities in the western Himalayas, but always near *Pinus wallichiana*. *Pseudosperma himalayense* has a much longer stipe (50–80 mm vs. max. 40 mm in *P. brunneoumbonatum*); white to pale yellow, olive yellow or light brown pileus; and somewhat smaller basidiospores. *Pseudosperma pakistanense* (Z. Ullah, S. Jabeen, H. Ahmad & A.N. Khalid) Matheny & Esteve-Rav., another species described from Pakistan, can be differentiated by the presence of pleurocystidia, somewhat smaller basidiospores and phylogenetic placement (Ullah et al. 2018, Figure 3).

The following two species have not yet been recombined in *Pseudosperma*. However, phylogenetic evidence undoubtedly places both *I. neglecta* E. Horak, Matheny & Desjardin and *I. friabilis* Matheny & Kudzma in the newly-recognised genus *Pseudosperma* (Horak et al. 2015, Matheny and Kudzma 2019). The new combinations are presented at the end of the taxonomy section. *Inocybe neglecta* from Thailand was described in the Pseudosperma clade by Horak et al. (2015). While it also lacks pleurocystidia and has a strong brown umbonate pileus, it is different from *P. brunneoumbonatum* by the smaller pileus (12–18 mm vs. 20–38 mm) and smaller and differently-shaped basidiospores. In addition, *I. neglecta* is only known from the type locality, growing in a tropical montane forest dominated by *Lithocarpus* Blume and *Castanopsis* (D. Don) Spach (both in Fagaceae). *Inocybe friabilis*, described from North America in the Pseudosperma clade, resembles *P. brunneoumbonatum* by lacking pleurocystidia and having a similarly coloured pileus. However, *I. friabilis* has smaller basidiospores, is associated with *Quercus* and *Carya* and has an eastern United States distribution.

In *The taxonomic studies of the genus Inocybe*, Kobayashi (2002) discussed 136 species, of which 13 (including four varieties and three formae) in subgenus *Inosperma* section *Rimosae*. These are [all referred to as *Inocybe* in Kobayashi (2002)]: *Inosperma adaequatum* (Britzelm.) Matheny & Esteve-Rav., *I. aureostipes* (Kobayasi) Matheny & Esteve-Rav., *I. cookei* (Bres.) Matheny & Esteve-Rav., *I. erubescens* (A. Blytt) Matheny & Esteve-Rav. [as its synonym *I. patouillardii* Bres.], *I. maculatum* (Boud.) Matheny & Esteve-Rav., *Pseudosperma avellaneum* (Kobayasi) Matheny & Esteve-Rav., *P. bisporum* (Hongo) Matheny & Esteve-Rav., *P. flavellum* (P. Karst.) Matheny & Esteve-Rav., *P. macrospermum* (Hongo) Matheny & Esteve-Rav., *P. rimosum* [as its synonym *Inocybe fastigiata* (Schaeff.) Quél.], *P. squamatum* (J.E. Lange) Matheny & Esteve-Rav., *P. transiens* (Takah. Kobay.) Matheny & Esteve-Rav. and *P. umbrinellum*. Since no sequence data are available for *P. avellaneum*, *P. bisporum*, *P. macrospermum* and *P. transiens*, we will compare their morphology with the newly-proposed Pakistani species.

Pseudosperma avellaneum has a pale greyish ochraceous pileus, its basidiospores are smaller and its cheilocystidia are distinctly narrower (width 9.5–14.5 vs. 14–29 µm) compared to *P. brunneoumbonatum*. As the only species in sect. *Rimosae* (*sensu* Kobayashi 2002), *P. bisporum* is 2-sterigmate. In addition, this species has a generally shorter stipe (17–26 vs. 22–40 mm in *P. brunneoumbonatum*), the edges of its lamel-

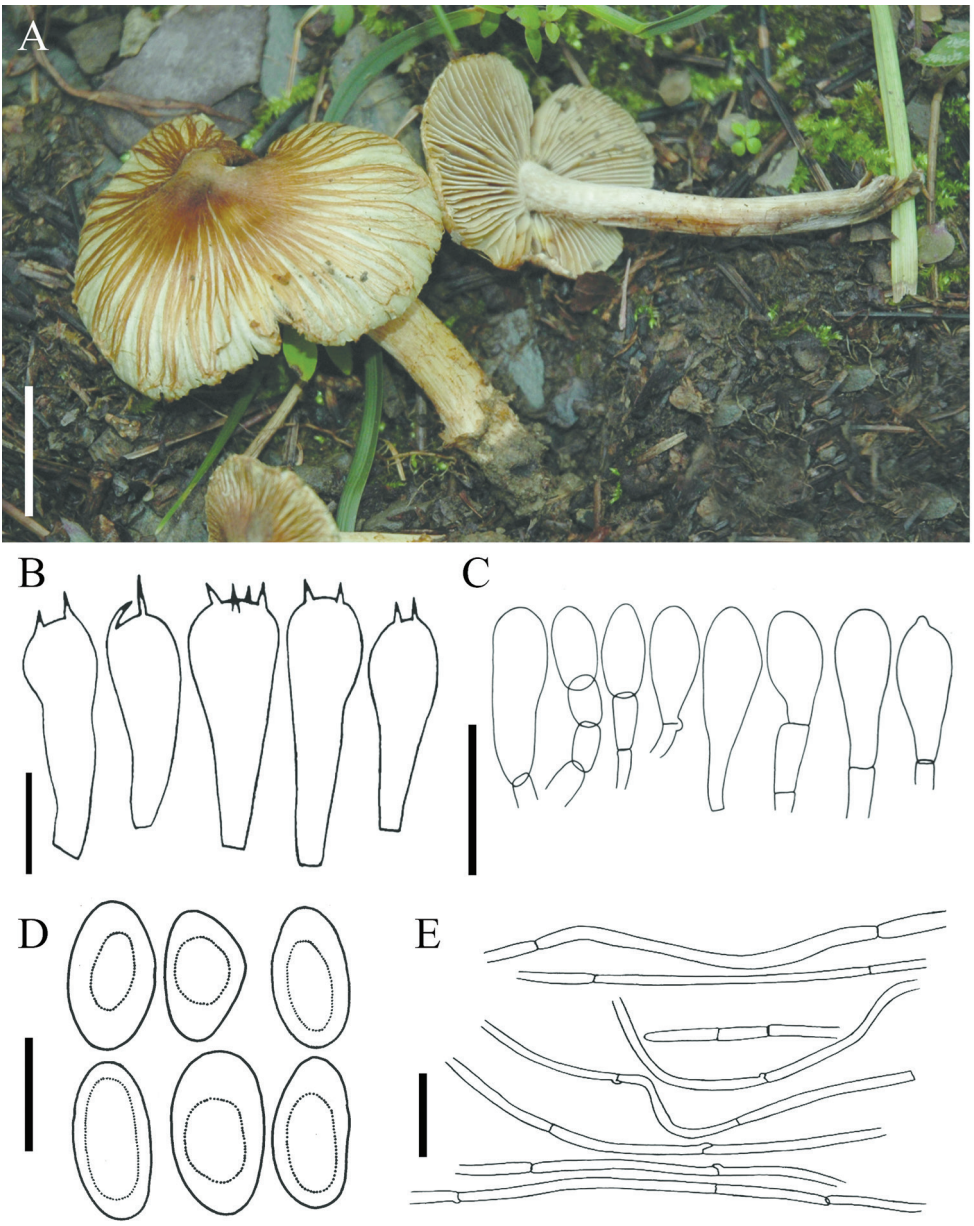

Figure 4. *Pseudosperma brunneoumbonatum*: **A** Basidiomata of holotype collection (LAH 310032) **B–E** microscopic characters: **B** basidia **C** cheilocystidia **D** basidiospores **E** pileipellis. Scale bars: 1 cm (**A**), 10 μm (**B**), 30 μm (**C, E**), 20 μm (**D**).

lae are serrate (with small teeth as a saw) and, again, the cheilocystidia are narrower (width 10.0–13.8 vs. 14–29 μm in *P. brunneoumbonatum*). Another Japanese species, *P. macrospermum*, is morphologically different in the following characters: the stipe has

a bulbous base, the basidia are shorter and narrower and its pileus is much smaller in diameter. Finally, *P. transiens* has a much longer stipe, its basidia are always narrower (up to 9.5 µm wide) and its cheilocystidia are both longer and narrower ((29–)38–52 × 9.5–13.8 µm) compared to *P. brunneoumbonatum*.

Pseudosperma pinophilum **Saba & Khalid, sp. nov.**
MycoBank No: 822656
Figure 5

Diagnosis. Characterised by the pale to light yellow equal stipe, basidiospores (8.2–)9.4–15.8 × 6.3–8 µm and an ecological association with *Pinus*.

Types. ***Holotype:*** Pakistan, Prov. Khyber Pakhtunkhwa, Abbottabad, Shimla, 14 Sep 2012, *leg.* M. Saba & A.N. Khalid; MSM#0046 (FH 00304582); GenBank accession nos. MG742414 (ITS), MG742418 (nrLSU), MG742416 (mtSSU). ***Paratype:*** Pakistan, Prov. Khyber Pakhtunkhwa, Shangla, Yakh Tangay, under *Pinus wallichiana*, 2 Sep 2013, *leg.* M. Saba & A.N. Khalid; MSM#0047 (LAH 310049); GenBank accession nos. MG742417 (ITS), MG742415 (nrLSU), MK474612 (mtSSU).

Etymology. From Greek, referring to an association with pine species.

Description. ***Pileus*** 16–31 mm in diam., convex, broadly convex or plane with an acute umbo; margin straight or flaring to deflexed; surface dry, dull, rimose, cracked towards centre, strong brown throughout (5YR4/6 to 5YR4/8) with dark brown umbo. ***Lamellae*** regular, adnexed to sinuate, close, white when young, light olivaceous at maturity; edges even. ***Stipe*** 54–70 mm, central, equal, longitudinally fibrillose, white with pale greenish-yellow (10Y9/4) or light yellow (5Y9/6) tinge or olivaceous tinge; veil not observed. Context white. Odour not distinctive.

Basidiospores (8.2–)9.4–15.8 × 6.3–8.0 µm [x = 13.5 × 7.6 µm, Q = 1.4–1.9], smooth, phaseoliform or ellipsoid, thin-walled, pale brown to golden brown in KOH, apiculus small and not distinctive, apex obutse. ***Basidia*** 21–40 × (9–)11–14 µm, clavate with refractive contents, primarily 4-sterigmate, less often 2-sterigmate, thin-walled, hyaline in KOH; sterigmata 2.5–4.0 µm long. ***Pleurocystidia*** absent. ***Cheilocystidia*** 25–47 × 10–20 µm, numerous, clavate or cylindrical, hyaline to pale brown in KOH, thin-walled. ***Caulocystidia*** not observed. ***Pileipellis*** a cutis of repent hyphae, hyphae cylindrical, 4–12 µm wide, thin-walled, pale brown in KOH, septate. ***Lamellar trama*** of parallel hyphae, 5–11 µm wide; subhymenium of compact hyphae, 3–6 µm wide. ***Stipitipellis*** cylindrical hyphae, 5–12 µm wide, hyaline in mass in KOH; all structures inamyloid. ***Clamp connections*** present.

Habit and habitat. Occurring in September, solitary or in groups, scattered on the forest floor in stands of *Pinus roxburghii* and *P. wallichiana* (Pinaceae).

Notes. Both *P. brunneoumbonatum* and *P. pinophilum* are placed in sect. *Rimosae* s.s. subclade A (Figures 1–3), which corresponds to *P. rimosum* senso lato, including the several *formae* and variations described for this species (Larsson et al. 2009). *Pseudosperma pinophilum* clusters with *P.* cf. *rimosum* (isolates JV1825 and PC080925). The pale yellow

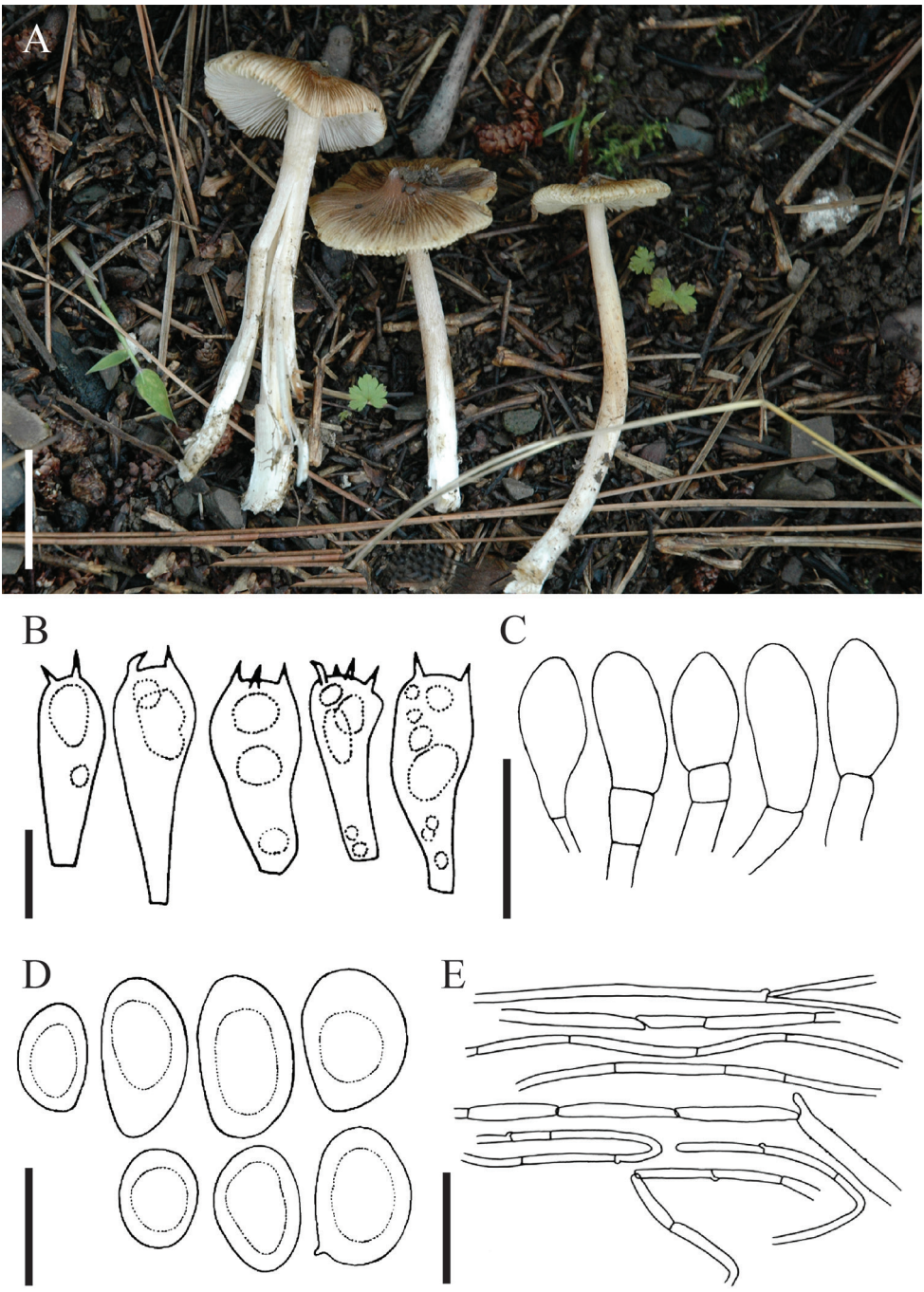

Figure 5. *Pseudosperma pinophilum*: **A** Basidiomata of holotype collection (FH 00304582) **B–E** microscopic characters: **B** basidia **C** cheilocystidia **D** basidiospores **E** pileipellis. Scale bars: 1 cm (**A**), 10 µm (**B, D**), 30 µm (**C, E**).

to light yellow tinged, equal stipe in *P. pinophilum* is very different compared to the white (rarely tinged with ochre), sub-bulbous stipe typical for *P. rimosum*. Moreover, *P. pinophilum* has broader basidiospores ((8.2–)9.4–15.8 × 6.3–8.0 μm) compared to *P. rimosum* (9–11(–13) × 4.5–6.0 μm). Also *P. brunneoumbonatum* has broader – and generally larger – basidiospores (10.3–15.3(–16.7) × 6.6–9.9 μm) compared to *P. rimosum*. *Pseudosperma sororium* is relatively closely related to *P. pinophilum* and can be differentiated in having different pileus colouration (greyish-brown to pinkish-grey or pale pinkish-beige) and measurement of basidiospores (10–12.5 × 5.5–6.0 μm) (Kauffman 1926).

Two more species of *Pseudosperma* are known from Pakistan; both *P. himalayense* and *P. pakistanense* were described, based on material collected in Pakistan. *Pseudosperma himalayense* was found near *Pinus wallichiana* trees, but an ITS sequence generated from root tips (GenBank acc. no. HG796995) confirmed an ectomycorrhizal association with *Quercus incana* (Liu et al. 2018). It can be distinguished from *P. pinophilum* by the pale yellowish to camel brown, fibrillose pileus; longer cheilocystidia (43–60 μm vs. 25–47 μm); and much thicker pileipellis. In addition, *P. himalayense* was resolved as sister to *P.* cf. *microfastigiatum* (Kühner) Matheny & Esteve-Rav. in Liu et al.'s (2018) ITS phylogeny. *Pseudosperma pakistanense* was found in a mixed conifer-dominated forest with some deciduous trees, under *Quercus incana* (Ullah et al. 2018). This species can be differentiated from the new species by the presence of pleurocystidia, the smaller stipe (50 mm vs. 54–70 mm in *P. pinophilum*) and its phylogenetic position (Ullah et al. 2018). In our nrLSU phylogeny, *P. pakistanense* was retrieved as sister to *P. alboflavellum* (C.K. Pradeep & Matheny) Haelew. (Figure 3).

The Japanese species in sect. *Rimosae* without sequence data from Kobayashi (2002), *P. avellaneum*, *P. bisporum*, *P. macrospermum* and *P. transiens*, are also different from *P. pinophilum* in their morphology. *Pseudosperma avellaneum* has smaller basidiospores and the pileipellis hyphae are almost hyaline (vs. pale brown in *P. pinophilum*). *Pseudosperma bisporum* has lamellae with serrate edges, its stipe is much shorter (17–26 vs. 54–70 mm in *P. pinophilum*), the basidia are 2-sterigmate, the cheilocystidia are usually shorter (max. 31 μm in length) and the pileipellis hyphae are smaller in diameter. *Pseudosperma macrospermum* has a smaller pileus diameter, a shorter stipe, narrower basidia, usually shorter cheilocystidia and pileipellis hyphae that are smaller in diameter. Finally, both the basidiospores (4.8–6.5 vs. 6.3–8.0 μm in *P. pinophilum*) and basidia (8.8–9.5 vs. (9–)11–14 μm in *P. pinophilum*) of *P. transiens* are narrower. In addition, the cheilocystidia of *P. pinophilum* are hyaline to pale brown in KOH, whereas in *P. transiens*, they are "rarely filled with yellowish brown contents" (Kobayashi 2002).

Pseudosperma triaciculare **Saba & Khalid, sp. nov.**
MycoBank No: 822657
Figure 6

Diagnosis. Characterised by the acutely umbonate brownish-orange to fulvous pileus, the presence of a pale velipellis coating on the pileus, septate cheilocystidia and an ecological association with *Pinus*.

Types. ***Holotype:*** Pakistan, Prov. Khyber Pakhtunkhwa, Mansehra, Batrasi, under *Pinus roxburghii*, 3 Aug 2014, *leg.* M. Saba & A.N. Khalid; MSM#0039 (LAH 310054); GenBank accession nos. MG742423 (ITS), MG742424 (nrLSU), MG742425 (mtSSU). ***Paratypes:*** *ibid.*, 3 Aug 2014; MSM#0040 (LAH 310055); GenBank accession nos. MG742426 (ITS), MG742427 (nrLSU), MG742428 (mtSSU). *Ibid.*, 3 Aug 2014; MSM#0041 (LAH 310056); GenBank accession nos. MG742429 (ITS), MG742430 (nrLSU), MG742431 (mtSSU). Pakistan, Prov. Khyber Pakhtunkhwa, Abbottabad, Shimla, 14 Sep 2012, *leg.* M. Saba & A.N. Khalid; MSM#0038 (FH 00304561).

Etymology. From Latin, meaning "three-needled," with reference to the association with the three-needled pine *Pinus roxburghii*.

Description. ***Pileus*** 12–29 mm in diam., conical when young, plane to convex at maturity, with acute to subacute or obtuse umbo; margin radially rimose, straight or flaring to uplifted; surface dry, dull, colour brownish-orange (5YR5/8) to fulvous, presence of a pale velipellis coating over the disc. ***Lamellae*** regular, adnexed to sinuate, close, pale orange yellow (10YR8/4), edges even; two tiers of lamelullae. ***Stipe*** 19–60 mm, central, equal, fibrillose, white with pale orange yellow tinge (10YR8/4). Odour mild, not diagnostic.

Basidiospores (7.7–)8.9–12.5 × 6.1–7.7 µm [x = 10.2 × 6.9 µm, Q = 1.64–2.2], smooth, mostly elliptic, thin-walled, yellowish-brown in KOH, apiculus present small and indistinctive. ***Basidia*** 24–36 × (9–)10–13 µm, clavate to broadly clavate with refractive contents, 4-sterigmate, thin-walled, hyaline in KOH; sterigmata 2.5–4.0 µm long. ***Pleurocystidia*** absent. ***Cheilocystidia*** cylindrical to clavate, septate, some with sub-capitate apices, terminal cells 23–54 × 9–16 µm, non-encrusted, hyaline, thin-walled. ***Caulocystidia*** 36–98 × 7–14 µm, cylindrical, non-encrusted, hyphoid, thin-walled. ***Pileipellis*** a cutis, hyphae cylindrical, 6–12 µm wide, thin-walled, golden brown or yellowish-brown in KOH, without encrustations, septate. ***Lamellar trama*** of parallel hyphae, 6–12 µm wide; subhymenium of compact hyphae, 3–6 µm wide. ***Stipitipellis*** cylindrical hyphae, 2–12 µm wide, hyaline in mass in KOH; all structures inamyloid. ***Clamp connections*** present.

Habit and habitat. Occurring in August to September, solitary or in groups, scattered on the forest floor in stands of *Pinus roxburghii* (Pinaceae).

Notes. *Pseudosperma triaciculare* has been found in association with *Pinus roxburghii*, the three-needled pine. This new species forms a distinct monophyletic group without clear affinities outside of *Rimosae* s.s. subclade A (Figures 1–3). Some of the unique features of this species are the umbonate brownish-orange to pale orange yellow pileus; cylindrical to clavate cheilocystidia; and cylindrical, non-encrusted, hyphoid caulocystidia. Allied species include *P. brunneoumbonatum*, *P. griseorubidum* (K.P.D. Latha & Manim.) Matheny & Esteve-Rav., *P. keralense* [synonym *I. rimulosa* C.K. Pradeep & Matheny] and *P. umbrinellum*. *Pseudosperma triaciculare* shares the same presumed *Pinus* association and shape of basidiomata with *P. brunneoumbonatum*, but can be distinguished by its brownish-orange pileus and smaller basidiospores. *Pseudosperma umbrinellum* is differentiated from *P. triaciculare* by the presence of an obtuse umbo (acute in *P. triaciculare*), yellowish- or reddish-brown pileus (brownish-orange in *P. triaciculare*), somewhat narrower basidiospores (5.5–6.5 µm vs. 6.1–7.7 µm) and a broad host range, including species in Cistaceae, Fagaceae, Pinaceae and Salicaceae (Larsson et al. 2009).

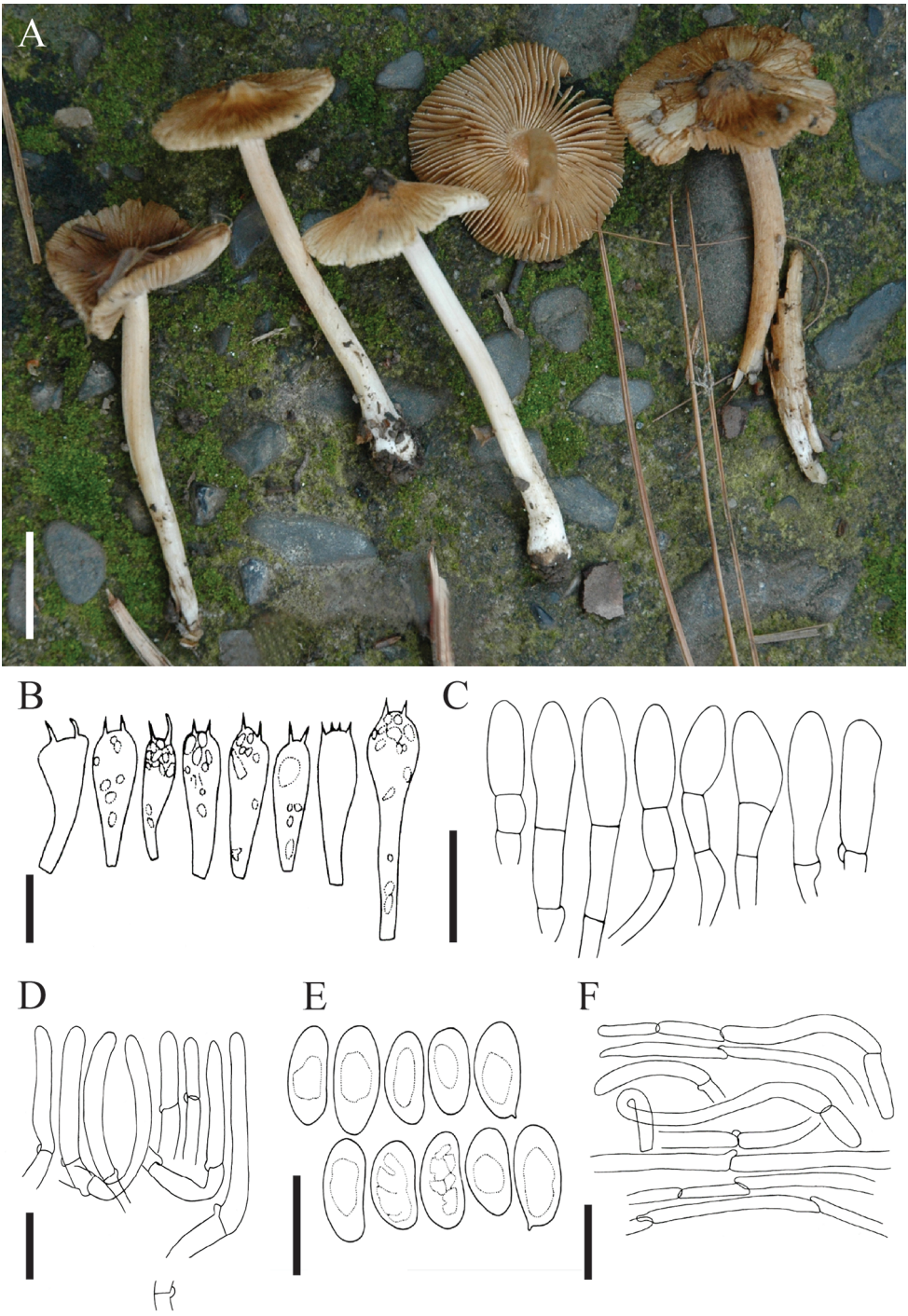

Figure 6. *Pseudosperma triaciculare*: **A** Basidiomata of paratype collection (FH 00304561) **B–F** microscopic characters: **B** Basidia **C** cheilocystidia **D** caulocystidia **E** basidiospores **F** pileipellis. Scale bars: 1 cm (**A**), 10 µm (**B, E**), 30 µm (**C, D, F**).

Pseudosperma triaciculare is most closely related to *P. griseorubidum* and *P. keralense*, described recently from tropical India (Latha and Manimohan 2015, Pradeep et al. 2016, Figure 3). *Pseudosperma griseorubidum* can be differentiated by its pileus, which is greyish-red and rarely with an umbo. In addition, *P. griseorubidum* is associated with members of Dipterocarpaceae (Latha and Manimohan 2015). The differences between *P. keralense* and *P. triaciculare* are more subtle. *Pseudosperma keralense* can be separated based on the following features: its lamellae have serrate edges and its basidiospores are narrower on average (6.1 vs. 6.9 µm in *P. triaciculare*). It is also phylogenetically clearly different; the ITS sequence of the holotype collection (GenBank acc. no. KM924523) is 84.11% identical to the holotype of *P. triaciculare*, whereas the LSU (KM924518) is 95.13% identical.

Other similar Asian species include *P. himalayense*, *P. neoumbrinellum*, *P. pakistanense* and *P. yunnanense* (T. Bau & Y.G. Fan) Matheny & Esteve-Rav. *Pseudosperma triaciculare* resembles *P. neoumbrinellum* in its pileus and basidiospores. However, it is easily differentiated by the characteristic brownish-orange to fulvous colouration of its pileus, whereas the pileus of *P. neoumbrinellum* is chocolate to dark brown in colour (Bau and Fan 2018). In addition, the shape and size of caulocystidia in these two species are very different: 20–48 × 10–17 µm in *P. neoumbrinellum* vs. 36–98 × 7–14 µm in *P. triaciculare*. *Pseudosperma triaciculare* is different from the recently-described *P. himalayense* from Pakistan (Liu et al. 2018) by the presence of a velipellis and a shorter stipe (16–60 vs. 50–80 µm). *Pseudosperma pakistanense* is separated from *P. triaciculare* by the absence of velipellar hyphae (unless the authors referred to the velipellis by their description of "[pileus] sometimes peeling off in the form of fine threads"), presence of pleurocystidia and a generally wider stipitipellis lacking caulocystidia (Ullah et al. 2018). Finally, *P. yunnanense*, described from China, also has velipellar hyphae, but its basidiomata are much larger in size (pileus 30–60 mm in diam., stipe 60–70 mm) and it lacks caulocystidia (Bau and Fan 2018). We did not include *P. yunnanense* in our phylogenetic analyses, but blasted the ITS sequence of the holotype collection (GenBank acc. no. MH047250) against *P. triaciculare*, resulting in 89.09% identity. *Pseudosperma yunnanense* is phylogenetically most similar to *P. perlatum*.

Finally, *P. avellaneum*, *P. bisporum*, *P. macrospermum* and *P. transiens* from Kobayashi's (2002) morphological *Inocybe* treatment are all different from *P. triaciculare*. Of all four, *P. avellaneum* is probably most difficult to separate from the new species: its pileus is pale greyish-ochraceous, the stipe is less slender and – this seems the best character for separating both species – no caulocystidia were observed. *Pseudosperma bisporum* has lamellae with serrate edges, 2-sterigmate basidia and pileipellis hyphae that are smaller in diameter. In addition, again, no caulocystidia were observed in this species. Compared to *P. triaciculare*, the basidiospores of *P. macrospermum* are longer (10.5–)14.0–15.5(–18.3) vs. (7.7–)8.9–12.5) µm, its basidia are narrower (8.8–9.5(–12.5) vs. (9–)10–13 µm) and its cheilocystidia are wider (16–18 vs. 9–16 µm). *Pseudosperma transiens* has basidiospores (4.8–6.5 vs. 6.1–7.7 µm) and basidia (8.8–9.5 vs. (9–)10–13 µm) that are both narrower than those in *P. triaciculare*. In addition, the pileus of *P. transiens* is coloured brown to dark brown, whereas *P. triaciculare* has a brownish-orange to fulvous pileus.

New combinations

During our studies of *Inocybe* sensu lato, we came across species of *Inocybe* that had not been recombined in the appropriate genera after Matheny et al. (2019) proposed a new generic system. Five names are recombined in *Inosperma*, *Mallocybe* and *Pseudosperma*.

***Inosperma vinaceobrunneum* (Matheny, Ovrebo & Kudzma) Haelew., Index Fungorum 436: 1 (2020).**
Index Fungorum No: IF557431

≡ *Inocybe vinaceobrunnea* Matheny, Matheny and Kudzma, J. Torrey Bot. Soc. 146(3): 227 (2019). [Basionym]

Note. This combination was made, based on a four-locus phylogeny (ITS, nrLSU, rpb1, rpb2). *Inosperma vinaceobrunneum* was retrieved in a clade with two other species (*I. rodiolum* (Bres.) Matheny & Esteve-Rav. and an undescribed species), sister to *I. adaequatum* (Matheny and Kudzma 2019).

***Mallocybe erratum* (E. Horak, Matheny & Desjardin) Haelew., comb. nov.**
Index Fungorum No: IF557512

≡ *Inocybe errata* E. Horak, Matheny & Desjardin, Phytotaxa 230(3): 210 (2015). [Basionym]

Note. This combination is based on phylogenetic evidence of the holotype (Horak et al. 2015). Based on both nrLSU-alone and nrLSU–rpb1–rpb2 datasets, it is placed deep in *Mallocybe*. It is highly supported as a sister species to an undescribed Zambia species ("*I. microdulcamara*" nom. prov.), both sister to *M. heimii* (Bon) Matheny & Esteve-Rav. (Matheny et al. 2009, Horak et al. 2015).

***Pseudosperma alboflavellum* (C.K. Pradeep & Matheny) Haelew., Index Fungorum 436: 1 (2020).**
Index Fungorum No: IF557432

≡ *Inocybe alboflavella* C.K. Pradeep & Matheny, Pradeep et al., Mycol. Progr. 15: 13 (2016). [Basionym]

Note. This combination was made, based on phylogenetic placement of the isotype (Pradeep et al. 2016, this study). In our nrLSU phylogeny, it was retrieved as a sister species to *P. pakistanense* with high support (Figure 3).

Pseudosperma friabile **(Matheny & Kudzma) Haelew., Index Fungorum 436: 1 (2020).**
Index Fungorum No: IF557433

≡ *Inocybe friabilis* Matheny & Kudzma, J. Torrey Bot. Soc. 146(3): 226 (2019). [Basionym]

Note. This combination was made, based on phylogenetic evidence. *Pseudosperma friabile* is most closely related to *P. gracilissimum* (Matheny & Bougher) Matheny & Esteve-Rav. and *P. keralense* (K.P.D. Latha & Manim.) Matheny & Esteve-Rav., deep in the Pseudosperma clade (*fide* Matheny 2005, Matheny and Kudzma 2019).

Pseudosperma neglectum **(E. Horak, Matheny & Desjardin) Haelew., comb. nov.**
Index Fungorum No: IF557513

≡ *Inocybe neglecta* E. Horak, Matheny & Desjardin, Phytotaxa 230(3): 208 (2015). [Basionym]

Note. The combination of *I. neglecta* in genus *Pseudosperma* is made, based on phylogenetic evidence. Horak et al. (2015) presented the phylogenetic reconstruction of an nrLSU dataset and found high statistical support for the Pseudosperma clade (*fide* Matheny 2005) including *P. neglectum*. While *P. neglectum* was retrieved as sister to the remaining members of the Pseudosperma clade, there was no support for this relationship. The same result was also found by Kropp et al. (2013). In addition, blasting the ITS sequence of the holotype (GenBank acc. no. EU600829) against sequences from type materials, resulted in *P. occidentale* (Kropp, Matheny & Hutchison) Matheny & Esteve-Rav. and *P. illudens* (Matheny, Bougher & G.M. Gates) Matheny & Esteve-Rav. with the highest percentages of identity (96.46% and 96.28%, respectively).

Discussion

Pakistan is located in southern Asia. This country is geographically diverse, ranging from the mountainous northern part, where the Himalayas meet their westernmost end, to the southern part with the coastal area along the Arabian Sea. Following the Köppen-Geiger classification system for climate, 20 types can be found in Pakistan – including four arid, six temperate, eight cold and even two polar (Beck et al. 2018). Note that despite this diversity in climate types, most of the country has a hot desert climate (*BWh*, Peel et al. 2007). Pakistan has a very rich flora; in an ongoing effort to write the *Flora of Pakistan*, S.I. Ali and colleagues identified 5,521 plant species in 1,572 genera thus far (Ali 2008). When keeping the ratio between vascular plants and fungi (1:6) in mind (*sensu* Hawksworth 1991), this number of plants only hints at the true potential of in-depth mycological studies in Pakistan, which has been traditionally under-explored.

The multiple geographic features, different climates and plant species richness in Pakistan are suggestive of a high diversity of fungal species. In recent years, many papers have been published, describing new species from different fungal groups collected in Pakistan (e.g. Razaq et al. 2012, Nawaz et al. 2013, Thongklang et al. 2014, Qasim et al. 2015a, 2015b, Sarwar et al. 2015, Hussain et al. 2016, 2017, 2018, Jabeen et al. 2016, Farooqi et al. 2017, Naseer et al. 2018, Ullah et al. 2018, Saba et al. 2019a, 2019b, Kiran et al. 2020). Thirty-five species of *Inocybe* sensu lato are reported from Pakistan (Ahmad et al. 1997, Ilyas et al. 2013, Saba et al. 2015, Jabeen et al. 2016, Farooqi et al. 2017, Razaq and Shahzad 2017, Naseer et al. 2018, Ullah et al. 2018, Song et al. 2019, this study). The genus *Pseudosperma* is poorly known in Pakistan, with only three species that were known before this study: *P. himalayense*, *P. rimosum* and *P. pakistanense* (Ahmad et al. 1997, Liu et al. 2018, Ullah et al. 2018).

In his dissertation about smooth-spored species of *Inocybe* from Europe, Kuyper (1986) presented a key to species of sect. *Rimosae*. He included 12 species [all as *Inocybe*]: *Inosperma adaequatum*, *I. cookei*, *I. erubescens*, *I. maculatum*, *I. quietiodor* (Bon) Matheny & Esteve-Rav., *I. reisneri* (Velen.) Matheny & Esteve-Rav., *Pseudosperma arenicola* (R. Heim) Matheny & Esteve-Rav., *P. flavellum*, *P. mimicum* (Massee) Matheny & Esteve-Rav., *P. rimosum* (sensu lato), *P. squamatum* and *I. vinosistipitatum* (Grund & D.E. Stuntz) Matheny & Esteve-Rav. Kuyper (1986) followed a conservative approach for *P. rimosum* – citing 31 species and varieties as synonyms and allowing considerable morphological plasticity and broad ecological amplitude. Larsson et al. (2009) followed a less conservative approach and recognised *P. obsoletum*, *P. perlatum* and *P. umbrinellum* as separate species in their identification key of Maculata and *Rimosae* s.s. clades in north-western Europe. These three species were amongst the synonymies of *P. rimosum* as treated by Kuyper (1986). Following both keys, our newly described taxa are most similar to *P. rimosum* and *P. umbrinellum* (Table 2). From our phylogenetic analyses, it is obvious that both *P. rimosum* and *P. umbrinellum* are separated from our Pakistani species. Other, more recently described taxa of *Pseudosperma* are also differentiated from the newly-proposed species, based on morphology, molecular phylogeny and geographic distribution.

Our phylogenetic analyses revealed that several undescribed species or collections that have not yet been properly identified occur in *Rimosae* s.s. subclade A (Larsson et al. 2009, Kropp et al. 2012). These are represented by singleton clades and clades including tentatively (cf.) or unidentified isolates. For example, isolates TR104_05 and TR133_05 represent an undescribed species from Papua New Guinea. In addition, isolates JV1825, PC080925, JV22619 and TAA185135 were identified as *P.* cf. *rimosum*, but represent at least two different species, either undescribed or previously described, but without available DNA sequence data. The isolate JV26578, which forms a singleton clade with unresolved position in our phylogenetic analyses, was also identified as *P.* cf. *rimosum*, but this identification is again inaccurate. We agree with Larsson et al. (2009) that more taxa need be sampled before the diversity and evolutionary relationships in this section can be fully understood.

Data availability

All holotype and paratype collections of the new species are deposited at LAH and FH. The sequences generated during this study are deposited in NCBI GenBank under accession numbers MG742414–MG742431. The sequence alignments generated in the present study are available from figshare (https://doi.org/10.6084/m9.figshare.c.4701338).

Acknowledgements

We are highly indebted to the Higher Education Commission (HEC), Islamabad, Pakistan, for funding this project under Phase II, Batch I, Indigenous PhD fellowships programme for 5000 scholars and through the International Research Support Initiative Program (IRSIP). We thank P. Brandon Matheny (University of Tennessee-Knoxville, USA), Olivier Raspé (Botanic Garden Meise, Belgium) and Martin Ryberg (Uppsala University, Sweden) for critically reviewing the manuscript. Finally, we acknowledge the efforts of Meike Piepenbring and Carola Glatthorn (Goethe-Universität Frankfurt, Germany) to provide us with necessary literature during the COVID-19 pandemic and subsequent lockdown.

References

Ahmad S, Iqbal SH, Khalid AN (1997) Fungi of Pakistan. Sultan Ahmad Mycological Society Pakistan, 1–248.

Ali SI (2008) Significance of flora with special reference to Pakistan. Pakistan Journal of Botany 40(3): 967–971.

Bau T, Fan Y-G (2018) Three new species of *Inocybe* sect. *Rimosae* from China. Mycosystema 37: 693–702.

Beck HE, Zimmermann NE, McVicar TR, Vergopolan N, Berg A, Wood EF (2018) Present and future Köppen-Geiger climate classification maps at 1-km resolution. Scientific Data 5: 180214. https://doi.org/10.1038/sdata.2018.214

Bougher NL, Matheny PB, Gates GM (2012) Five new species and records of *Inocybe* (Agaricales) from temperate and tropical Australia. Nuytsia 22(2): 57–74.

Capella-Gutiérrez S, Silla-Martínez JM, Gabaldón T (2009) TrimAl: a tool for automated alignment trimming in large-scale phylogenetic analyses. Bioinformatics 25: 1972–1973. https://doi.org/10.1093/bioinformatics/btp348

Chernomor O, Von Haeseler A, Minh BQ (2016) Terrace aware data structure for phylogenomic inference from supermatrices. Systematic Biology 65: 997–1008. https://doi.org/10.1093/sysbio/syw037

Darriba D, Taboada GL, Doallo R, Posada D (2012) jModelTest 2: more models, new heuristics and parallel computing. Nature Methods 9(8): 772. https://doi.org/10.1038/nmeth.2109

Dentinger BT, Didukh MY, Moncalvo JM (2011) Comparing COI and ITS as DNA barcode markers for mushrooms and allies (Agaricomycotina). Plos One 6(9): e25081. https://doi.org/10.1371/journal.pone.0025081

Edgar RC (2004) MUSCLE: multiple sequence alignment with high accuracy and high throughput. Nucleic Acids Research 32: 1792–1797. https://doi.org/10.1093/nar/gkh340

Farooqi A, Aqdus F, Niazi AR, Jabeen S, Khalid AN (2017) *Inocybe ahmadii* sp. nov. and a new record of *I. leptocystis* from Pakistan. Mycotaxon, 132(2): 257–269. https://doi.org/10.5248/132.257

Gardes M, Bruns TD (1993) ITS primers with enhanced specificity for basidiomycetes - application to the identification of mycorrhizae and rusts. Molecular Ecology 2(2): 113–118. https://doi.org/10.1080/10635150802429642

Haelewaters D (2020) Nomenclatural novelties. Index Fungorum 436: 1.

Haelewaters D, Dirks AC, Kappler LA, Mitchell JK, Quijada L, Vandegrift R, Buyck B, Pfister DH (2018) A preliminary checklist of fungi at the Boston Harbor islands. Northeastern Naturalist 25(Special Issue 9): 45–76. https://doi.org/10.1656/045.025.s904

Hall TA (1999) BioEdit: A user-friendly biological sequence alignment editor and analysis program for Windows 95/98/NT. Nucleic Acids Symposium Series 41: 95–98.

Hawksworth D (1991) The fungal dimension of biodiversity: magnitude, significance, and conservation. Mycological Research 95(6): 641–655. https://doi.org/10.1016/S0953-7562(09)80810-1

Hillis DM, Dixon MT (1991) Ribosomal DNA: Molecular evolution and phylogenetic inference. The Quarterly Review of Biology 66: 411–453. https://doi.org/10.1086/417338

Hoang DT, Chernomor O, Von Haeseler A, Minh BQ, Vinh LS (2017) UFBoot2: Improving the ultrafast bootstrap approximation. Molecular Biology and Evolution 35: 518–522. https://doi.org/10.1093/molbev/msx281

Horak E, Matheny PB, Desjardin DE, Soytong K (2015) The genus *Inocybe* (Inocybaceae, Agaricales, Basidiomycota) in Thailand and Malaysia. Phytotaxa 230(3): 201–238. https://doi.org/10.11646/phytotaxa.230.3.1

Hussain S, Yousaf N, Afshan NS, Niazi AR, Ahmad H, Khalid AN (2016) *Tulostoma ahmadii* sp. nov. and *T. squamosum* from Pakistan. Turkish Journal of Botany 40(2): 218–225. https://doi.org/10.3906/bot-1501-9

Hussain S, Ahmad H, Khalid AN, Niazi AR (2017) *Parasola malakandensis* sp. nov. (Psathyrellaceae; Basidiomycota) from Malakand, Pakistan. Mycoscience 58(2): 69–76. https://doi.org/10.1016/j.myc.2016.09.002

Ilyas S, Razaq A, Khalid AN (2013) *Inocybe nitidiuscula* and its ectomycorrhizae with *Alnus nitida* from Galyat, Pakistan. Mycotaxon 124: 247–254. https://doi.org/10.5248/124.247

Jabeen S, Ahmad I, Rashid A, Khalid AN (2016) *Inocybe kohistanensis*, a new species from Pakistan. Turkish Journal of Botany 40(3): 312–318. https://doi.org/10.3906/bot-1501-17

Jacobsson S (2008) Key to *Inocybe*. In: Knudsen H, Vesterholt J (Eds) Funga Nordica. Agaricoid, boletoid and cyphelloid genera. Nordsvamp, Copenhagen, 868–906.

Kauffman CH (1926) The genera *Flammula* and *Paxillus* and the status of the American species. American Journal of Botany 13(1): 11–32. https://doi.org/10.1002/j.1537-2197.1926.tb05862.x

Kiran M, Sattar A, Zamir K, Haelewaters D, Nasir Khalid A (2020) Additions to the genus *Chroogomphus* (Boletales, Gomphidiaceae) from Pakistan. MycoKeys 66: 23–38. https://doi.org/10.3897/mycokeys.66.38659

Kobayashi T (2002) The taxonomic studies of the genus *Inocybe*. Nova Hedwigia 124: 1–246.

Kropp BR, Matheny PB, Hutchison LJ (2013) *Inocybe* section *Rimosae* in Utah: phylogenetic affinities and new species. Mycologia 105(3): 728–747. https://doi.org/10.3852/12-185

Kuyper TW (1986) A revision of the genus *Inocybe* in Europe. I. Subgenus *Inosperma* and the smooth-spored species of subgenus *Inocybe*. Persoonia Suppl. 3: 1–247.

Kumar S, Stecher G, Tamura K (2016) MEGA7: Molecular Evolutionary Genetics Analysis version 7.0 for bigger datasets. Molecular Biology and Evolution 33(7): 1870–1874. https://doi.org/10.1093/molbev/msw054

Larsson E, Ryberg M, Moreau PA, Mathiesen ÅD, Jacobsson S (2009) Taxonomy and evolutionary relationships within species of section *Rimosae* (*Inocybe*) based on ITS, LSU and mtSSU sequence data. Persoonia 23: 86–98. https://doi.org/10.3767/003158509X475913

Latha KPD, Manimohan P (2015) *Inocybe griseorubida*, a new species of *Pseudosperma* clade from tropical India. Phytotaxa 221(2): 166–174. https://doi.org/10.11646/phytotaxa.221.2.6

Lee SB, Milgroom MG, Taylor JW (1988) A rapid, high yield mini-prep method for isolation of total genomic DNA from fungi. Fungal Genetics Reports 35(1): 23. https://doi.org/10.4148/19

Liu L-N, Razaq A, Atri NS, Bau T, Belbahri L, Chenari Bouket A, Chen L-P, Deng C, Ilyas S, Khalid AN, Kitaura MJ, Kobayashi T, Li Y, Lorenz AP, Ma Y-H, Malysheva E, Malysheva V, Nuytinck J, Qiao M, Saini MK, Scur MC, Sharma S, Shu L-L, Spirin V, Tanaka Y, Tojo M, Uzuhashi S, Valério-Júnior C, Verbeken A, Verma B, Wu R-H, Xu J-P, Yu Z-F, Zeng H, Zhang B, Banerjee A, Beddiar A, Bordallo JJ, Dafri A, Dima B, Krisai-Greilhuber I, Lorenzini M, Mandal R, Morte A, Nath PS, Papp V, Pavlík J, Rodríguez A, Ševčíková H, Urban A, Voglmayr H, Zapparoli G (2018) Fungal systematics and evolution: FUSE 4. Sydowia 70: 211–286.

Matheny PB (2005) Improving phylogenetic inference of mushrooms with RPB1 and RPB2 nucleotide sequences (*Inocybe*; Agaricales). Molecular Phylogenetics and Evolution 35(1): 1–20. https://doi.org/10.1016/j.ympev.2004.11.014

Matheny PB (2009) A phylogenetic classification of the Inocybaceae. McIlvainea 18(1): 11–21.

Matheny PB, Aime MC, Bougher NL, Buyck B, Desjardin DE, Horak E, Kropp BR, Lodge DJ, Soytong K, Trappe JM, Hibbett DS, Hibbett DS (2009) Out of the Palaeotropics? Historical biogeography and diversification of the cosmopolitan ectomycorrhizal mushroom family Inocybaceae. Journal of Biogeography 36(4): 577–592. https://doi.org/10.1111/j.1365-2699.2008.02055.x

Matheny PB, Hobbs AM, Esteve-Raventós F (2019) Genera of Inocybaceae: New skin for the old ceremony. Mycologia 112(1): 83–120. https://doi.org/10.1080/00275514.2019.1668906

Matheny PB, Kudzma LV (2019) New species of *Inocybe* (Inocybaceae) from eastern North America. Journal of the Torrey Botanical Society 146(3): 213–235. https://doi.org/10.3159/TORREY-D-18-00060.1

Matheny PB, Liu YJ, Ammirati JF, Hall BD (2002) Using RPB1 sequences to improve phylogenetic inference among mushrooms (*Inocybe*, Agaricales). American Journal of Botany 89(4): 688–698. https://doi.org/10.3732/ajb.89.4.688

Matheny PB, Pradeep CK, Vrinda KB, Varghese SP (2012) *Auritella foveata*, a new species of Inocybaceae (Agaricales) from tropical India. Kew Bulletin 67(1): 119–125. https://doi.org/10.1007/s12225-012-9329-9

Miller MA, Pfeiffer W, Schwartz T (2010) Creating the CIPRES Science Gateway for inference of large phylogenetic trees. Proceedings of the Gateway Computing Environments Workshop (GCE), 14 Nov 2010, 1–8. https://doi.org/10.1109/GCE.2010.5676129

Munsell Soil Color Charts (1975) Munsell Color Company. Baltimore, Maryland.

Naseer A, Khalid AN, Smith ME (2018) *Inocybe shawarensis* sp. nov. in the *Inosperma* clade from Pakistan. Mycotaxon 132(4): 909–918. https://doi.org/10.5248/132.909

Nawaz R, Khalid AN, Hanif M, Razaq A (2013) *Lepiota vellingana* sp. nov. (Basidiomycota, Agaricales), a new species from Lahore, Pakistan. Mycological Progress 12(4): 727–732. https://doi.org/10.1007/s11557-012-0884-0

Nguyen L-T, Schmidt HA, Von Haeseler A, Minh BQ (2015) IQ-TREE: A fast and effective stochastic algorithm for estimating maximum likelihood phylogenies. Molecular Biology and Evolution 32: 268–274. https://doi.org/10.1093/molbev/msu300

Peel MC, Finlayson BL, McMahon TA (2007) Updated world map of the Köppen-Geiger climate classification, Hydrology and Earth System Sciences 11(5): 1633–1644. https://doi.org/10.5194/hess-11-1633-2007

Pradeep CK, Vrinda KB, Varghese SP, Korotkin HB, Matheny PB (2016) New and noteworthy species of *Inocybe* (Agaricales) from tropical India. Mycological progress 15(3): 24. https://doi.org/10.1007/s11557-016-1174-z

Qasim T, Amir T, Nawaz R, Niazi AR, Khalid AN (2015) *Leucoagaricus lahorensis*, a new species of *L.* sect. *Rubrotincti*. Mycotaxon 130(2): 533–541. https://doi.org/10.5248/130.533

Qasim T, Khalid AN, Vellinga EC, Razaq A (2015) *Lepiota albogranulosa* sp. nov. (Agaricales, Agaricaceae) from Lahore, Pakistan. Mycological Progress 14(5): 24. https://doi.org/10.1007/s11557-015-1037-z

Razaq A, Khalid AN, Vellinga EC (2012) *Lepiota himalayensis* (Basidiomycota, Agaricales), a new species from Pakistan. Mycotaxon 121: 319–325. https://doi.org/10.5248/121.319

Razaq A, Shahzad S (2017) Additions to the diversity of mushrooms in Gilgit-Baltistan, Pakistan. Pakistan Journal of Botany 49(SI): 305–309.

Ryberg M, Nilsson RH, Kristiansson E, Töpel M, Jacobsson S, Larsson E (2008) Mining metadata from unidentified ITS sequences in GenBank: a case study in *Inocybe* (Basidiomycota). BMC Evolutionary Biology 8(1): 50. https://doi.org/10.1186/1471-2148-8-50

Saba M, Ahmad I, Khalid AN (2015) New reports of *Inocybe* from pine forests in Pakistan. Mycotaxon 130(3): 671–681. https://doi.org/10.5248/130.671

Saba M, Haelewaters D, Fiaz M, Khalid AN, Pfister DH (2019a) *Amanita mansehraensis*, a new species in section Vaginatae from Pakistan. Phytotaxa 409(4): 189–201. https://doi.org/10.11646/phytotaxa.409.4.1

Saba M, Haelewaters, D, Iturriaga T, Ashraf T, Khalid AN, Pfister DH (2019b) *Geopora ahmadii* sp. nov. from Pakistan. Mycotaxon 134(2): 377–389. https://doi.org/10.5248/134.377

Sarwar S, Saba M, Khalid AN, Dentinger BM (2015) *Suillus marginielevatus*, a new species and *S. triacicularis*, a new record from Western Himalaya, Pakistan. Phytotaxa 203(2): 169–177. https://doi.org/10.11646/phytotaxa.203.2.6

Smith AH, Stuntz DE (1950) New or noteworthy fungi from Mt. Rainier National Park. Mycologia 42(1): 80–134. https://doi.org/10.1080/00275514.1950.12017817

Song J, Liang J-F, Mehrabi-Koushki M, Krisai-Greilhuber I, Ali B, Bhatt VK, Cerna-Mendoza A, Chen B, Chen Z-X, Chu H-L, Corazon-Guivin MA, da Silva GA, De Kesel A, Dima B, Dovana F, Farokhinejad R, Ferisin G, Guerrero-Abad JC, Guo T, Han L-H, Ilyas S, Justo A, Khalid AN, Khodadadi-Pourarpanahi S, Li T-H, Liu C, Lorenzini M, Lu J-K, Mumtaz AS, Oehl F, Pan X-Y, Papp V, Qian W, Razaq A, Semwal KC, Tang L-Z, Tian X-L, Vallejos-Tapullima A, van der Merwe NA, Wang S-K, Wang C-Q, Yang R-H, Yu F, Zapparoli G, Zhang M, Antonín V, Aptroot A, Aslan A, Banerjee A, Chatterjee S, Dirks AC, Ebrahimi L, Fotouhifar K-B, Ghosta Y, Kalinina LB, Karahan D, Maiti M, Mookherjee A, Nath PS, Panja B, Saha J, Ševčíková H, Voglmayr H, Yazıcı K, Haelewaters D (2019) Fungal Systematics and Evolution 5. Sydowia 71: 141–245.

Stangl J (1989) Die Gattung *Inocybe* in Bayern. Hoppea 46: 5–388.

Thongklang N, Nawaz R, Khalid AN, Chen J, Hyde KD, Zhao R, Parra LA, Hanif M, Moinard M, Callac P (2014) Morphological and molecular characterization of three *Agaricus* species from tropical Asia (Pakistan, Thailand) reveals a new group in section *Xanthodermatei*. Mycologia 106(6): 1220–1232. https://doi.org/10.3852/14-076

Ullah Z, Jabeen S, Ahmad H, Khalid AN (2018). *Inocybe pakistanensis*, a new species in section *Rimosae* s. str. from Pakistan. Phytotaxa 348(4): 279–288. https://doi.org/10.11646/phytotaxa.348.4.4

Vauras J, Huhtinen S (1986) Finnish records on the genus *Inocybe* ecology and distribution of four calciphilous species. Karstenia 26(2): 65–72. https://doi.org/10.29203/ka.1986.246

Vilgalys R, Hester M (1990) Rapid genetic identification and mapping of enzymatically amplified ribosomal DNA from several *Cryptococcus* species. Journal of Bacteriology 172(8): 4238–4246. https://doi.org/10.1128/JB.172.8.4238-4246.1990

White TJ, Bruns TD, Lee SB, Taylor JW (1990) Analysis of phylogenetic relationships by amplification and direct sequencing of ribosomal RNA genes. In: Innis MA, Gelfand DH, Sninsky JJ, White TJ (Eds) PCR Protocols: a guide to methods and applications. Academic Press, San Diego, 315–322. https://doi.org/10.1016/B978-0-12-372180-8.50042-1

MycoKeys 69: 33–52 (2020)
doi: 10.3897/mycokeys.69.53205
http://mycokeys.pensoft.net

RESEARCH ARTICLE

A peer-reviewed open-access journal
MycoKeys
Launched to accelerate biodiversity research

Novel species of *Huntiella* from naturally-occurring forest trees in Greece and South Africa

FeiFei Liu[1,2], Seonju Marincowitz[1], ShuaiFei Chen[1,2], Michael Mbenoun[1], Panaghiotis Tsopelas[3], Nikoleta Soulioti[3], Michael J. Wingfield[1]

1 *Department of Biochemistry, Genetics and Microbiology (BGM), Forestry and Agricultural Biotechnology Institute (FABI), University of Pretoria, Pretoria 0028, South Africa* **2** *China Eucalypt Research Centre (CERC), Chinese Academy of Forestry (CAF), ZhanJiang, 524022, GuangDong Province, China* **3** *Institute of Mediterranean Forest Ecosystems, Terma Alkmanos, 11528 Athens, Greece*

Corresponding author: ShuaiFei Chen (shuaifei.chen@gmail.com)

Academic editor: R. Phookamsak | Received 13 April 2020 | Accepted 4 June 2020 | Published 10 July 2020

Citation: Liu FF, Marincowitz S, Chen SF, Mbenoun M, Tsopelas P, Soulioti N, Wingfield MJ (2020) Novel species of *Huntiella* from naturally-occurring forest trees in Greece and South Africa. MycoKeys 69: 33–52. https://doi.org/10.3897/mycokeys.69.53205

Abstract

Huntiella species are wood-infecting, filamentous ascomycetes that occur in fresh wounds on a wide variety of tree species. These fungi are mainly known as saprobes although some have been associated with disease symptoms. Six fungal isolates with typical culture characteristics of *Huntiella* spp. were collected from wounds on native forest trees in Greece and South Africa. The aim of this study was to identify these isolates, using morphological characters and multigene phylogenies of the rRNA internal transcribed spacer (ITS) region, portions of the β-tubulin (BT1) and translation elongation factor 1α (TEF-1α) genes. The mating strategies of these fungi were also determined through PCR amplification of mating type genes. The study revealed two new species; one from *Platanus orientalis* in Greece and one from *Colophospermum mopane* and *Senegalia nigrescens* in South Africa. These novel taxa have been provided with the names, *H. hellenica* **sp. nov.** and *H. krugeri* **sp. nov.**, respectively. The former species was found to have a homothallic and the latter a heterothallic mating system.

Keywords

Ceratocystidaceae, *Ceratocystis moniliformis* Complex, *Colophospermum mopane*, *Huntiella*, *Platanus orientalis*, saprobes, *Senegalia nigrescens*

Introduction

Huntiella species are members of the family Ceratocystidaceae (Microascales, Sordariomycetes) as defined by De Beer et al. (2014). This family includes 15 genera, namely *Ambrosiella*, *Berkeleyomyces*, *Bretziella*, *Catunica*, *Ceratocystis*, *Chalaropsis*, *Davidsoniella*, *Endoconidiophora*, *Huntiella*, *Meredithiella*, *Phialophoropsis*, *Solaloca*, *Tielaviopsis*, *Toshiolenlla* and *Wolfgangiella* (De Beer et al. 2014, 2017; Mayers et al. 2015, 2020; Nel et al. 2018). The type species of *Huntiella*, *H. moniliformis*, was first isolated from a sweetgum (*Liquidambar styraciflua*) in Texas, USA (Von Schrenk 1903). It was initially described as *Ceratostomella moniliformis* (Hedgcock 1906) and later transferred to *Ceratocystis* (Moreau 1952). When the family Ceratocystidaceae was redefined (De Beer et al. 2014), *Huntiella* was established as a distinct genus, which can be distinguished from *Ceratocystis* and other members of the Ceratocystidaceae, based on their unique morphological features (Davidson 1935; Van Wyk et al. 2006; Wingfield et al. 2013). Most *Huntiella* spp. are easily recognised by a relatively-thick collar plate connecting the ascomatal necks and bases and ascomatal bases that are rough and ornamented with conical spines (Hedgcock 1906). In addition, aleurioconidia are rarely found in *Huntiella* species unlike most species of *Ceratocystis sensu stricto* with which they were previously confused (Hedgcock 1906; De Beer et al. 2014; Mbenoun et al. 2016).

Many species in the Ceratocystidaceae are important pathogens of woody plants, including agricultural, fruit and forest tree crops (Kile 1993; Roux and Wingfield 2009). These pathogens result in a multiplicity of symptoms, such as branch and stem cankers, vascular staining, wilt, root rot, die-back and fruit rot (Kile 1993; Harrington 2004; Roux and Wingfield 2009). *Huntiella* spp. are generally considered saprobes or weak pathogens associated with relatively-minor lesions or sap stain of timber (Van Wyk et al. 2004, 2006, 2011; Tarigan et al. 2010; Kamgan Nkuekam et al. 2012; Chen et al. 2013; Mbenoun et al. 2016; Liu et al. 2018). However, there have been a few reports of more severe disease symptoms and even mortality caused by *Huntiella* spp. (Cristobal and Hansen 1962; De Errasti et al. 2015)

Huntiella species are most commonly isolated from freshly-made wounds on trees, to which they are vectored by insects, especially sap-feeding beetles in the Nitidulidae (Heath et al. 2009; Kamgan Nkuekam et al. 2012; Mbenoun et al. 2016, 2017). It has been suggested that the relationship between *Huntiella* species and sap beetle is symbiotic and mutually beneficial, as the insects benefit from essential nutritional supplementation from their fungal partners, while the fungi benefit from transportation and access to scanty and ephemeral substrates (Mbenoun et al. unpublished data). Moreover, one species (*H. bhutanensis*) is found in association with the bark beetle *Ips schmutzenhoferi* (Van Wyk et al. 2004), which is similar to various important species of *Endoconidiophora* (De Beer et al. 2014), although the nature of insect-fungus interaction in this association is unknown.

Huntiella spp. are particularly interesting in terms of their mating biology. *Huntiella fecunda* and *H. moniliformis* were, for example, shown to exhibit a unisexual mating system, unlike the many heterothallic species found in this genus (Wilson et al. 2015; Liu et al. 2018). More recent studies have revealed a diversity of mating systems

in *Huntiella* spp., including those that are homothallic, heterothallic and unisexual (Wilson et al. 2015; Liu et al. 2018). Efforts are consequently being made to collect these fungi, providing a basis for future fungal genetics studies, but also, together with genomics data (Wingfield et al. 2016), to better understand their biology.

Huntiella species are most commonly found in tropical and sub-tropical regions of the world (Van Wyk et al. 2004, 2006, 2011; Kamgan Nkuekam et al. 2012; De Errasti et al. 2015; Mbenoun et al. 2014, 2016; Liu et al. 2018). Twenty-nine species are currently recognised in the genus (Liu et al. 2018). These fungi are grouped in three well-supported genealogical lineages that correspond to geographic centres, where they appear to have radiated (Mbenoun et al. 2016; Liu et al. 2018). These include species in an African Clade known only from Africa, an Asian Clade distributed across Asia and an Indo-Pacific Clade found in Australia and Pacific Islands and some parts of Asia. However, the diversity of *Huntiella* in most regions, including especially Europe, North and South America, is largely unexplored.

The objective of this study was to identify two fungal isolates collected from *Platanus orientalis* L. in Greece and four isolates from *Colophospermum mopane* (Benth.) J. Léonard and *Senegalia nigrescens* (Oliv.) P. Hurter in South Africa. These fungi displayed typical culture characteristics of *Huntiella* spp., including rapid growth on agar medium, white fluffy mycelia when young, as well as the production of fruity aroma. Identification was accomplished, based on morphology and multigene phylogenies for the ITS, BT1 and TEF-1α gene regions. Furthermore, we considered the mating biology of these isolates in order to complement our taxonomic studies.

Materials and methods

Fungal isolations

Three South African *Huntiella* isolates were collected from fresh wounds of *Colophospermum mopane* in Kruger National Park in April 2009 and another one of the South African isolates was obtained from a broken branch of a *Senegalia nigrescens* tree damaged by elephants in Kruger National Park in June 2010. The isolates from Greece were obtained from the stump of a *Platanus orientalis* tree that was cut about two months before sampling, in a natural forest along the banks of the Spercheios River in Phthiotis Regional Unit during November 2018. Isolation from wood samples was performed using a trapping technique originally described by Grosclaude et al. (1988). This is a standard diagnostic protocol for the isolation of *Ceratocystis platani* (Walter) Engelbrecht & Harrington using freshly-cut twigs of *P. orientalis* as bait (OEPP/EPPO 2014).

Isolates from Greece were made by transferring ascospore masses from the tips of the ascomata on the surface of *Platanus* twig baits, formed on infected wood surface, to 2% malt extract agar (MEA: 20 g Biolab malt extract, 20 g Difco agar, 1 litre water), using a sterile needle under a dissection microscope (Carl Zeiss Co. Ltd., Oberkochen, Germany). The South African isolate was obtained by transferring mycelial strands from infected wood on to MEA. Primary isolations were incubated

for 3–7 d at 25 °C. From these isolations, purified cultures from single hyphal tips were prepared for morphological characterisation, phylogenetic analyses and mating-type studies. All purified isolates were deposited in the culture collection (CMW) of the Forestry and Agricultural Biotechnology Institute (FABI), University of Pretoria, South Africa and the living culture collection (PPRI) of the South African National Collection of Fungi (NCF), Roodeplaat, Pretoria, South Africa. The dried-down type specimens were deposited in the National Collection of Fungi (PREM), Roodeplaat, Pretoria, South Africa.

DNA extraction, PCR and sequencing

All the isolates obtained in this study were used for DNA sequence-based characterisation. Total genomic DNA was extracted from the mycelium of isolates grown on 2% MEA for 3–4 d at 25 °C, using Prepman Ultra Sample Preparation Reagent (Thermo Fisher Scientific, Waltham, MA, USA) following the manufacturer's protocols. Three gene regions were amplified for sequencing and phylogenetic analyses. These included the Internal Transcribed Spacer (ITS) regions 1 and 2, including the 5.8S rRNA, a partial β-tubulin 1 gene (BT1) and a partial Translation Elongation factor-1α gene (TEF-1α), amplified using the set of primers as described by Liu et al. (2018).

A total volume of 25 µl PCR reaction mixture contained 1 µl of DNA template, 0.5 µl (10 pM) of each primer (Forward and Reverse), 5 µl MyTaq PCR buffer (Bioline GmbH, Germany) and 0.3 µl of MyTaq DNA Polymerase (Bioline GmbH, Germany). The PCR reactions were conducted using an Applied Biosystems ProFlex PCR System (Thermo Fisher Scientific, Waltham, MA, USA). The PCR programme for amplification of the ITS, BT1 and TEF1-α gene regions was as follows: an initial denaturation step at 95 °C for 5 min followed by 35 cycles of 30 s at 95 °C, 45 s at 56 °C and 60 s at 72 °C and a final extension step at 72 °C for 10 min. Amplified fragments were purified using ExoSAP-IT™ PCR Product Cleanup Reagent (Thermo Fisher Scientific, Waltham, MA, USA) to remove excess primers and dNTPs. Amplicons were sequenced in both directions using an ABI PRISM™ 3100 DNA sequencer (Applied Biosystems, USA) at the Sequencing Facility of the Faculty of Natural and Agricultural Sciences, University of Pretoria, Pretoria, South Africa.

Multi-gene phylogenetic analyses

The programme Geneious v. 7.0 was used to edit and assemble raw sequence reads into contigs (Kearse et al. 2012). Sequence data for representative type isolates of all described *Huntiella* spp. (except *H. decorticans*) were downloaded from GenBank (http://www.ncbi.nlm.nih.gov). The sequences were aligned using MAFFT v. 7 with an online FFT-NS-i strategy (https://mafft.cbrc.jp/alignment/server/; Katoh and Standley 2013)

and confirmed visually. Sequences for the novel species discovered in this study were deposited in GenBank.

Single gene sequence datasets of the ITS, BT1 and TEF-1α and the combined dataset of the three gene regions were analysed using Maximum Likelihood (ML), Maximum Parsimony (MP) and Bayesian Inference (BI). The appropriate substitution model for each dataset was obtained using the software package jModeltest v. 2.1.5 (Posada 2008). The ML phylogenetic analyses were conducted using PhyML v. 3.0 (Guindon and Gascuel 2003). Confidence levels for the nodes were determined using 1000 bootstrap replicates. MP analyses were performed using PAUP v. 4.0b10 (Swofford 2003). Gaps were treated as a fifth character. BI analyses were conducted using MrBayes v. 3.2.6 (Ronquist et al. 2012) on the CIPRES Science Gateway v. 3.3. Four Markov Chain Monte Carlo (MCMC) chains were run from a random starting tree for five million generations and trees were sampled every 100 generations. Twenty-five percent of the trees sampled were discarded as burn-in and the remaining trees were used to construct 50% majority rule consensus trees. *Ceratocystis cercfabiensis* (isolate CMW 43029) was used as the outgroup taxon for all the phylogenetic analyses. The resulting trees were visualised using MEGA v. 7.

Microscopy, growth study and mating-type assignment

Morphological features were studied on the isolates grown on 2% MEA. The fruiting structures were initially mounted in water and this was later replaced with 85% lactic acid and in which measurements were made and images captured. Nikon microscopes (Eclipse N*i*, SMZ 18, Nikon, Tokyo, Japan) mounted with a camera (Nikon DS Ri-2) were used for all observations. Fifty measurements of each relevant microscopic structure were made when available and these are presented as minimum–maximum and average ± standard deviation.

A study of growth in culture was conducted at temperatures from 5–35 °C at 5 °C intervals on the 90 mm Petri dishes containing 2% MEA. A mycelial plug (5 mm diam.) taken from an actively-growing colony was placed at the centres of Petri dishes. Four replicates per isolate were used to study growth rate and the experiment was repeated once. Colony diameters were assessed by taking two measurements perpendicular to each other for all isolates daily and growth rates were calculated. Colony characteristics were described on the same medium used for the growth studies and colours were assessed using the colour charts of Rayner (1970).

The mating type (MAT) of the studied *Huntiella* spp. was determined, based on the results of the mating type PCR reactions (Wilson et al. 2015). Primers, to see which of the MAT genes, Oman_111_F and Oman_111_R were thus used to amplify a 335 bp fragment of the MAT1-1-1 gene and Om_Mo_121_F and Om_Mo_121_R to amplify a 572 bp fragment of the MAT1-2-1 gene, as described by Wilson et al. (2015).

Results

Fungal isolations

Six isolates resembling *Huntiella* spp. were included in this study. Two isolates had ascomata with long necks, conical spines on the ascomatal bases and hat-shaped ascospores and four isolates had only thielaviopsis-like asexual state (Van Wyk et al. 1991). Four isolates were collected from *Colophospermum mopane* and *Senegalia nigrescens* in the Kruger National Park of South Africa and two isolates were from *Platanus orientalis* in Greece. Ascomata resembling *Huntiella* spp. were observed on twig baits from *P. orientalis* samples from Greece and two isolates were obtained in pure culture. All isolates obtained in this study have been preserved in the culture collections described above (Table 1).

Multi-gene phylogenetic analyses

All six isolates, included in this study, were successfully sequenced at all three selected gene regions for phylogenetic analyses, resulting in DNA sequence data of approximately 614, 574 and 830 bp for the ITS, BT1 and TEF-1α gene regions, respectively. These newly-generated sequences were deposited in GenBank (Table 1). Comparisons with reference sequences of previously-described *Huntiella* spp. produced a concatenated sequence alignment which was deposited in TreeBASE (no. 26341).

The three tree topologies resulting from ML, MP and BI were concordant and showed similar phylogenetic relationships amongst taxa (Fig. 1, Suppl. materials 1–3: Figs S1–S3). Based on the phylogenetic analyses of the BT1 (Suppl. materil 2, Fig. S2), TEF-1α (Suppl. material 3: Fig. S3) and the combined gene regions (Fig. 1), the six isolates clustered in two well-supported clades, clearly separated from each other and from previously described *Huntiella* spp. The ITS tree (Suppl. material 1: Fig. S1) provided a poor resolution to separate the species. All the isolates grouped in the African Clade of *Huntiella* spp. (Fig. 1).

Taxonomy

Huntiella hellenica **F.F. Liu. Marinc. & M.J. Wingf., sp. nov.**
MycoBank No: 835637
Fig. 2

Etymology. The name refers to the country, Greece where this fungus was collected.

Mating strategy. Homothallic, with sexually complementary isolates having both the MAT1-1-1 and MAT1-2-1 genes.

Sexual state. *Ascomata* produced in 2% MEA in a week, perithecial; *ascomatal bases* mostly embedded in thick or loose mycelial mat, globose to ellipsoidal or obpyriform, pale brown when young, becoming dark brown with age, 173–377 μm long (avg. 238.8 μm),

Table 1. List of *Huntiella* species included in this study.

Species[a]	CMW No.[b]	Other No.[b]	GenBank accession No.[c]			Hosts (or substrate)	Origin	Reference
			ITS	BT1	TEF-1α			
Ceratocystis cercfabiensis	CMW 43029	CERC 2170; CBS 139654	KP727592	KP727618	KP727643	*Eucalyptus* sp.	China	Liu et al. 2015
Huntiella ani	CMW 44684	CERC 2827; CBS 143283	MH118602	MH118635	MH118668	*Eucalyptus* sp.	China	Liu et al. 2018
H. ani	CMW 44686	CERC 2829; CBS 143282	MH118603	MH118636	MH118669	*Eucalyptus* sp.	China	Liu et al. 2018
H. bellula	CMW 49312	CERC 2854; CBS 143286	MH118607	MH118640	MH118673	*Eucalyptus* sp.	China	Liu et al. 2018
H. bellula	CMW 49314	CERC 2862; CBS 143285	MH118610	MH118643	MH118676	*Eucalyptus* sp.	China	Liu et al. 2018
H. bhutanensis	CMW 8242	CBS 112907	AY528951	AY528956	AY528961	*Picea spinulosa*	Bhutan	Van Wyk et al. 2004
H. bhutanensis	CMW 8217	CBS 114289	AY528957	AY528962	AY528952	*P. spinulosa*	Bhutan	Van Wyk et al. 2004
H. ceramica	CMW 15245	CBS 122299	EU245022	EU244994	EU244926	*Eucalyptus grandis*	Malawi	Heath et al. 2009
H. ceramica	CMW 15248	CBS 122300	EU245024	EU244996	EU244928	*E. grandis*	Malawi	Heath et al. 2009
H. chinaeucensis	CMW 24658	CBS 127185	JQ862729	JQ862717	JQ862741	*Eucalyptus* sp.	China	Chen et al. 2013
H. chinaeucensis	CMW 24661	CBS 127186	JQ862731	JQ862719	JQ862743	*Eucalyptus* sp.	China	Chen et al. 2013
H. chlamydoformis	CMW 36932	CBS 131674	KF769087	KF769109	KF769098	*Theobroma cacao*	Cameroon	Mbenoun et al. 2016
H. chlamydoformis	CMW 37102	CBS 131675	KF769088	KF769110	KF769099	*Terminalia superba*	Cameroon	Mbenoun et al. 2016
H. confusa	CMW 43452	CERC 2158; CBS 143577	MH118583	MH118616	MH118649	*Acacia confusa*	China	Liu et al. 2018
H. confusa	CMW 43453	CERC 2162; CBS 143288	MH118584	MH118617	MH118650	*A. confusa*	China	Liu et al. 2018
H. cryptoformis	CMW 36826	CBS 131277	KC691462	KC691486	KC691510	*Terminalia sericea*	South Africa	Mbenoun et al. 2014
H. cryptoformis	CMW 36828	CBS 131279	KC691464	KC691488	KC691512	*Ziziphus mucronata*	South Africa	Mbenoun et al. 2014
H. decipiens	CMW 25918	CBS 129735	HQ203218	HQ203235	HQ236437	*E. cloeziana*	South Africa	Kamgan Nkuekam et al. 2013
H. decipiens	CMW 25914	CBS 129737	HQ203219	HQ203236	HQ236438	*E. maculata*	South Africa	Kamgan Nkuekam et al. 2013
H. eucalypti	CMW 44692	CERC 2840; CBS 143291	MH118605	MH118638	MH118671	*Eucalyptus* sp.	China	Liu et al. 2018
H. eucalypti	CMW 44693	CERC 2841; CBS 143290	MH118606	MH118639	MH118672	*Eucalyptus* sp.	China	Liu et al. 2018

Species[a]	CMW No.[b]	Other No.[b]	GenBank accession No.[c]			Hosts (or substrate)	Origin	Reference
			ITS	BT1	TEF-1α			
H. fabiensis	CMW 49307	CERC 2753; CBS 143294	MH118596	MH118629	MH118662	*Eucalyptus* sp.	China	Liu et al. 2018
H. fabiensis	CMW 49309	CERC 2763; CBS143292	MH118599	MH118632	MH118665	*Eucalyptus* sp.	China	Liu et al. 2018
H. fecunda	CMW 49302	CERC 2449; CBS 143296	MH118586	MH118619	MH118652	*Eucalyptus* sp.	China	Liu et al. 2018
H. fecunda	CMW 49303	CERC 2451a; CBS 143295	MH118587	MH118620	MH118653	*Eucalyptus* sp.	China	Liu et al. 2018
H. glaber	CMW 43436	CERC 2132; CBS 143298	MH118580	MH118613	MH118646	*E. exserta*	China	Liu et al. 2018
H. glaber	CMW 49299	CERC 2133; CBS 143297	MH118581	MH118614	MH118647	*E. exserta*	China	Liu et al. 2018
H. hellenica	**CMW 54800**	**PPRI 27982**	**MT524073**	**MT513125**	**MT513131**	***Platanus orientalis***	**Greece**	**Present study**
H. hellenica	**CMW 54801**	**PPRI 27983**	**MT524072**	**MT513124**	**MT513130**	***P. orientalis***	**Greece**	**Present study**
H. inaequabilis	CMW 44372	CERC 2740; CBS 143300	MH118590	MH118623	MH118656	*Eucalyptus* sp.	China	Liu et al. 2018
H. inaequabilis	CMW 49306	CERC 2749; CBS 143299	MH118595	MH118628	MH118661	*Eucalyptus* sp.	China	Liu et al. 2018
H. inquinana	CMW 21106		EU588587	EU588666	EU588674	*Acacia mangium*	Indonesia	Tarigan et al. 2010
H. inquinana	CMW 21107	CBS 124009	EU588588	EU588667	EU588675	*A. mangium*	Indonesia	Tarigan et al. 2010
H. krugeri	**CMW 36849**	**CBS 131676 PPRI 27952**	**MT524068**	**MT513120**	**MT513126**	***A. nigrescens***	**South Africa**	**Present study**
H. krugeri	**CMW 55933**		**MT524069**	**MT513121**	**MT513127**	***Colophospermum mopane***	**South Africa**	**Present study**
H. krugeri	**CMW 55934**		**MT524070**	**MT513122**	**MT513128**	***C. mopane***	**South Africa**	**Present study**
H. krugeri	**CMW 55935**		**MT524071**	**MT513123**	**MT513129**	***C. mopane***	**South Africa**	**Present study**
H. meiensis	CMW 44374	CERC 2742; CBS 143302	MH118591	MH118624	MH118657	*Eucalyptus* sp.	China	Liu et al. 2018
H. meiensis	CMW 44376	CERC 2746; CBS 143301	MH118594	MH118627	MH118660	*Eucalyptus* sp.	China	Liu et al. 2018
H. microbasis	CMW 21117	CBS 124013	EU588593	EU588672	EU588680	*A. mangium*	Indonesia	Tarigan et al. 2010
H. microbasis	CMW 21115	CBS 124015	EU588592	EU588671	EU588679	*A. mangium*	Indonesia	Tarigan et al. 2010
H. moniliformis	CMW 9590	CBS 116452	AY431101	AY528985	AY529006	*E. grandis*	South Africa	Van Wyk et al. 2006

Species[a]	CMW No.[b]	Other No.[b]	GenBank accession No.[c]			Hosts (or substrate)	Origin	Reference
			ITS	BT1	TEF-1α			
H. moniliformis	CMW 4114	CBS 118151	AY528997	AY528986	AY529007	*Shizolobium parahyba*	Ecuador	Van Wyk et al. 2006
H. moniliformopsis	CMW 9986	CBS 109441	AY528998	AY528987	AY529008	*E. obliqua*	Australia	Yuan & Mohammed 2002
H. moniliformopsis	CMW 10214	CBS 115792	AY528999	AY528988	AY529009	*E. sieberi*	Australia	Yuan & Mohammed 2002
H. oblonga	CMW 23803	CBS 122291	EU245019	EU244991	EU244951	*A. mearnsii*	South Africa	Heath et al. 2009
H. oblonga	CMW 23802		EU245020	EU244992	EU244952	*A. mearnsii*	South Africa	Heath et al. 2009
H. omanensis	CMW 11048	CBS 115787	DQ074742	DQ074732	DQ074737	*Mangifera indica*	Oman	Al-subhi et al. 2006
H. omanensis	CMW 3800	CBS 117839	DQ074743	DQ074733	DQ074738	*M. indica*	Oman	Al-subhi et al. 2006
H. pycnanthi	CMW 36916	CBS 131672	KF769096	KF769118	KF769107	*The. cacao*	Cameroon	Mbenoun et al. 2016
H. pycnanthi	CMW 36910		KF769095	KF769117	KF769106	*The. cacao*	Cameroon	Mbenoun et al. 2016
H. salinaria	CMW 25911	CBS 129733	HQ203213	HQ203230	HQ236432	*E. maculata*	South Africa	Kamgan Nkuekam et al. 2013
H. salinaria	CMW 30703	CBS 129734	HQ203214	HQ203231	HQ236433	*E. saligna*	South Africa	Kamgan Nkuekam et al. 2013
H. savannae	CMW 17300	CBS 121151	EF408551	EF408565	EF408572	*A. nigrescens*	South Africa	Kamgan Nkuekam et al. 2008
H. savannae	CMW 17297		EF408552	EF408566	EF408573	*Combretum zeyheri*	South Africa	Kamgan Nkuekam et al. 2008
H. sublaevis	CMW 22449	CBS 122517	FJ151431	FJ151465	FJ151487	*Terminalia ivorensis*	Ecuador	Van Wyk et al. 2011
H. sublaevis	CMW 22444	CBS 122518	FJ151430	FJ151464	FJ151486	*T. ivorensis*	Ecuador	Van Wyk et al. 2011
H. sumatrana	CMW 21109	CBS 124011	EU588589	EU588668	EU588676	*A. mangium*	Indonesia	Tarigan et al. 2010
H. sumatrana	CMW 21111	CBS 124012	EU588590	EU588669	EU588677	*A. mangium*	Indonesia	Tarigan et al. 2010
H. tribiliformis	CMW 13011	CBS 115867	AY528991	AY529001	AY529012	*Pinus merkusii*	Indonesia	Van Wyk et al. 2006
H. tribiliformis	CMW 13012	CBS 118242	AY528992	AY529002	AY529013	*P. merkusii*	Indonesia	Van Wyk et al. 2006
H. tyalla	CMW 28917		HM071899	HM071909	HQ236448	*E. grandis*	Australia	Kamgan Nkuekam et al. 2012
H. tyalla	CMW 28920		HM071896	HM071910	HQ236449	*E. grandis*	Australia	Kamgan Nkuekam et al. 2012

[a] Species indicated in bold are newly described in this study.

[b] CBS = Westerdijk Fungal Biodiversity Institute, Utrecht, the Netherlands; CERC = Culture collection of China Eucalypt Research Centre (CERC), Chinese Academy of Forestry (CAF), ZhanJiang, GuangDong Province, China; CMW = Culture collection of the Forestry and Agricultural Biotechnology Institute (FABI), University of Pretoria, Pretoria, South Africa; PPRI = The living culture collection (PPRI) of the South African National Collection of Fungi (NCF), Roodeplaat, Pretoria, South Africa.

[c] GenBank accession numbers indicated in bold are generated in this study.

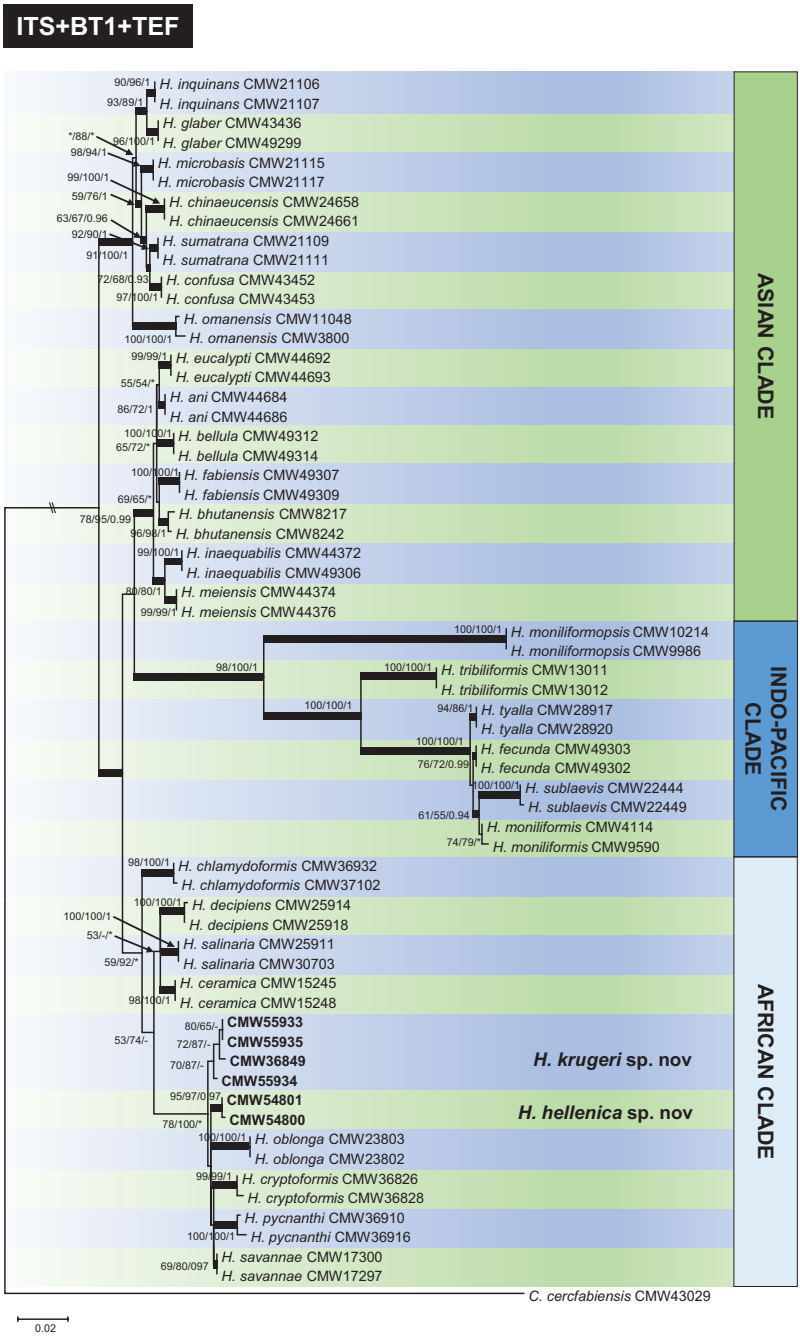

Figure 1. ML tree of *Huntiella* species generated from the combined DNA sequence data of ITS, BT1 and TEF-1α DNA. Sequences generated from this study are printed in bold type. Bold branches indicate posterior probabilities values ≥ 0.9. Bootstrap values and posterior probabilities values are presented above branches as ML/MP/BI. Bootstrap value < 50% or probabilities values < 0.9 are marked with *. Nodes lacking the support value are marked with -. *Ceratocystis cercfabiensis* (CMW 43029) represents the outgroup.

157–493 µm wide (avg. 218.2 µm), ornamented with spine-like structures, dark brown, conical, 12–29 µm long, 4–9 µm wide at base becoming attenuated; *ostiolar necks* upright, straight, occasionally situated at off-centre of base, darker than base when young, 344–616 µm long (avg. 515.5 µm), 34–60 µm wide (avg. 46.6 µm) at base, gradually tapering towards apex; *ostiolar hyphae* hyaline, straight to divergent, 15–39 µm long, 1–3 µm wide, tapering towards apex. *Asci* evanescent. *Ascospores* hyaline, subglobose, aseptate, covered with sheath giving a hat-like feature in side view, 4–5.5 × 3–4.5 µm (5 ± 0.23 × 4 ± 0.28 µm) excluding sheath.

Asexual state. Thielaviopsis-like *Conidiophores* macronematous, simple or branched; when branched radiating from basal cell once, often reduced to conidiogenous cells. *Conidiogenus cells* endoblastic, hyaline, varying from lageniform to cylindrical depending spore shape; in case of thick barrel-shaped conidia, apex often becoming wider than base. *Conidia* hyaline, 1-celled, in two recognisable shapes; majority ellipsoidal to barrel-shaped (side swollen, ends round), typical fat barrel-shaped 5–8 × 4.5–7.5 µm (5.9 ± 0.61 × 5.3 ± 0.55 µm), width of some barrel-shaped ranging 2.5–4 µm wide; rectangular-shaped (side straight, ends truncated), not commonly found, 5–9 × 1–3 µm (6.9 ± 1.18 × 2.3 ± 0.38 µm). *Aleurioconidia* not observed.

Culture characteristics. Cultures on 2% MEA in dark in 8 d showing circular growth with even edge, mycelium flat, superficial, medium dense and texture becoming pelt-like with age, colour above not uniform, salmon (11f') to ochreous (15b') with inner half irregularly umber (13m), below ochreous (15b') with inner half irregularly umber (13i') at centre. Optimum growth temperatures at 30 °C at 9.6 mm/d, followed by at 25 °C (7.6 mm/d), 35 °C (7.2 mm/d), 20 °C (4.7 mm/d), 15 °C (3.2 mm/d), 10 °C (1.1 mm/d) and 5 °C (0.2 mm/d).

Specimens examined. Greece, Phthiotis, near the village Kastri, occurring on freshly-cut stumps of *Platanus orientalis* in a natural forest along the banks of the Spercheios River, Nov. 2018, P. Tsopelas & N. Soulioti, PREM 62889, holotype (dried culture of CMW 54800), culture ex-holotype CMW 54800 = PPRI 27982, other cultures CMW 54801 = PPRI 27983.

Notes. The sexual state of *H. hellenica* developed at temperatures over 25 °C. Cultures incubated at 20 °C and below produced only the asexual state. *Huntiella hellenica* is closely related to *H. savannae* (Kamgan Nkuekam et al. 2008), *H. pycnanthi* (Mbenoun et al. 2016) and *H. krugeri*. It can, however, be distinguished from these two species by the dimensions of ascomatal necks and barrel-shaped conidia and growth rate. *Huntiella hellenica* produced shorter (average 515.5 µm long) ascomatal necks than *H. savannae* (average 579 µm long) and *H. pycnanthi* (average 673 µm long). *Huntiella hellenica* had larger (average 6.9 × 2.3 µm) barrel-shaped conidia than *H. savannae* (average 4.8 × 3 µm) and *H. pycnanthi* (average 6 × 3 µm). Optimal temperature for growth of *H. hellenica* was 30 °C, similar to *H. savannae* and *H. pycnanthi*, but *H. hellenica* differed from *H. pycnanthi* in growing minimally at 10 °C and below.

Figure 2. Micrographs of *Huntiella hellenica* sp. nov. (ex-holotype CMW 54800 = PPRI 27982) **A** culture grown on 2% MEA at 30 °C (optimum growth temperature) in the dark for 34 d **B, C** colony with ascomatal base embedded in mycelia with ascospore mass at the tip of ostiolar neck **D–F** young ascoma showing development of ostiolar neck and less-pigmented base **G, H** mature ascoma ornamented with spines **I** close-up of ascomatal wall showing spines **J–L** close up of ornament (spin-like) **M, N** Ostiolar hyphae **O** Ascospores **P** Ascospores covered with sheath appearing like a hat **Q, R** Germinating ascospores **S** Lageniform conidiogenous cell **T** Cylindrical-shape conidiogenous cell **U** Conidia in various shapes from diverse barrel-shaped to rectangular-shaped **V** rectangular-shaped conidia **W** chains of conidia. Scale bars: 1 mm (**B, C**); 50 µm (**D–H**); 10 µm (**I–W**).

***Huntiella krugeri* F.F. Liu. Marinc. & M.J. Wingf., sp. nov.**
MycoBank No: 835638
Fig. 3

Etymology. The name refers to the Kruger National Park in South Africa, where this fungus was collected.

Mating strategy. Heterothallic with isolates having either a MAT1-1-1 gene or a MAT1-2-1 gene.

***Sexual state*.** Not observed.

Asexual state. Produced on 2% MEA in 3 weeks. Thielaviopsis-like. *Conidiophores* macronematous, upright, simple or branched in one tier, 29–37 µm in length, often reduced to conidiogenous cells; *Conidiogenous cells* enteroblastic, lageniform, 10–20 µm long, 1.5–3 µm wide, tapering towards apex. *Conidia* hyaline, rectangular-shaped, usually straight, with top-end conidium often club-shaped, 4–11 × 1–2 µm (avg. 6.2 × 1.7 µm). *Aleurioconidia* hyaline, holoblastic, mostly terminal, ellipsoidal to subglobose with an extended tube-like base, club-shaped, 4–7 × 2–3 µm (5.6 ± 0.76 × 2.5 ± 0.24 µm).

Culture characteristics. Cultures on 2% MEA in dark in 8 d showing circular growth with even edge, mycelium superficial, flat, dense, colour above uniformly white, below luteous (19). Optimum growth temperatures were at 30 °C at 9 mm/d, followed by at 25 °C (8.2 mm/d), 35 °C (6.2 mm/d), 20 °C (6 mm/d), 15 °C (3.4 mm/d), 10 °C (0.9 mm/d) and 5 °C (0.3 mm/d).

Specimens examined. South Africa, Mpumalanga, Kruger National Park, Satara rest camp, *Senegalia nigrescens*, June 2010, M. Mbenoun, PREM 62883, holotype (dried culture of CMW 36849), culture ex-holotype CMW 36849 = CBS 131676 = PPRI 27952.

Other cultures. South Africa, Mpumalanga, Kruger National Park, Punda Maria, *Colophospermum mopane*, April 2009, M. Mbenoun, CMW 55933, CMW 55934, CMW 55935.

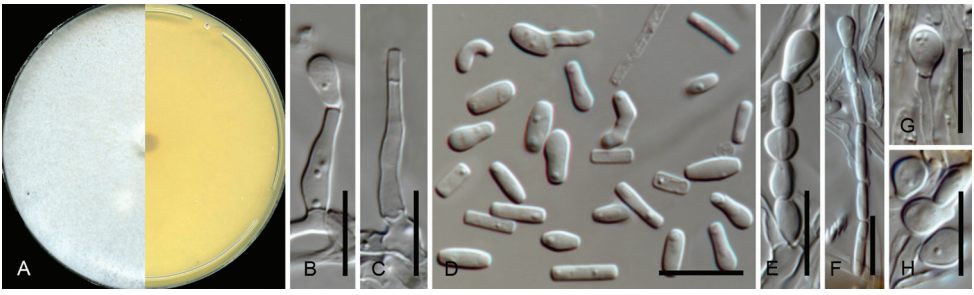

Figure 3. Micrographs of *Huntiella krugeri* sp. nov. (ex-holotype CMW 36849 = CBS 131676 = PPRI 27952). **A** Culture grown on 2% MEA in the dark for 34 d **B, C** Conidiogenous cell **D** Conidia in various shapes **E** Chain of conidia in different shapes **F** Chain of rectangular-shaped conidia with top-end of club-shaped **G, H** Aleurioconidia. Scale bars: 10 µm (**B–H**).

Notes. *Huntiella krugeri* is closely related to *H. hellenica* described in the present study, *H. cryptoformis* (Mbenoun et al. 2014) and *H. savannae* (Kamgan Nkuekam et al. 2008). Due to its heterothallic nature, *H. krugeri* produced only the asexual state in this study. The bacilliform conidia of *H. krugeri* (average 6.2 × 1.7 µm) were longer than those of *H. hellenica* (average 5.9 × 5.3 µm) and *H. cryptoformis* (average 5.5 × 2.5 µm). In addition, *H. krugeri* produced hyaline aleurioconidia, which are absent in other closely-related species in the genus.

Discussion

This study led to the discovery of two novel *Huntiella* species isolated from *Platanus orientalis* in Greece, *Colophospermum mopane* and *Senegalia nigrescens* in the Kruger National Park of South Africa. These two species, provided with the name *H. hellenica* and *H. krugeri*, respectively, were shown to reside in the African Clade of *Huntiella* (Mbenoun et al. 2014; Liu et al. 2018). The identity of *H. hellenica* and *H. krugeri* emerged from a phylogenetic analysis of DNA sequence data for three gene regions (ITS, BT1 and TEF-1α), as well as their distinct morphological characteristics. Mating studies showed that *Huntiella hellenica* and *H. krugeri* were homothallic and heterothallic, respectively. All indications were that these two species are saprobes that grow on the freshly-exposed surfaces of trees.

The stump of *P. orientalis*, from which *H. hellenica* emerged, was sampled approximately two months after tree felling and it was also infected by the pathogen *Ceratocystis platani*, which causes a devastating disease in natural stands of *P. orientalis* in Greece. Colonszation of the stump with *H. hellenica* could have occurred on the freshly-cut surface with a contaminated tool as occurs for *C. platani* (Tsopelas et al. 2017) or was transferred by insect vectors.

The novel species described in this study showed typical characteristics of *Huntiella* spp. They grew rapidly in culture; their mycelium was white when young and turned dark with age. The one species that displayed a sexual state - *H. hellenica*, produced hat-shaped ascospores and had short conical spines on the ascomatal bases. Temperature is known to influence the ability of *Huntiella* spp. to produce a sexual state (Wilson et al. 2015) and this was also true for *H. hellenica*, which did not produce acomata below 25 °C.

Comparison of DNA sequence data for multiple gene regions is essential when seeking to identify species in *Huntiella* (Mbenoun et al. 2014; Liu et al. 2018). The three gene regions, selected for this purpose, have been used in previous studies showing that they can be collectively used to delineate species boundaries in the genus (Van Wyk et al. 2004, 2006, 2011; Kamgan Nkuekam et al. 2012; Mbenoun et al. 2014, 2016; De Errasti et al. 2015; Liu et al. 2018). However, analyses of individual gene regions revealed different levels of resolution, consistent with the results of previous studies on this group of fungi (Mbenoun et al. 2014; Liu et al. 2018). Thus protein coding genes, in this case BT1 and TEF-1α, provided the best resolution for species identification of *Huntiella*, while ITS sequences provided little information or no support.

Primers, developed to identify the mating type idiomorphs in *Huntiella* spp. (Wilson et al. 2015), were effective for this purpose in the present study. The results showed that *H. hellenica* has both mating-type idiomorphs and this explains the presence of sexual structures in all isolates derived from single hyphal tips. In contrast, the isolate of *H. krugeri* contained one mating gene and is clearly a heterothallic species of *Huntiella*, also consistent with the fact that the isolate produced only an asexual state. This result is also consistent with those of Liu et al. (2018) who showed that closely-related *Huntiella* spp. can have different mating strategies. Collectively, *Huntiella* spp. have a remarkable range of mating strategies, including homothallic and heterothallic species, as well as those exhibiting unisexuality (Wilson et al. 2015; Liu et al. 2018). The new species described here will contribute to future studies considering the evolution of mating in *Huntiella*.

The two new species of *Huntiella*, discovered in this study, bring the total number of species in the genus to 31. These are found in many different regions of the world and on a wide variety of woody substrates (Van Wyk et al. 2004, 2006, 2011; Kamgan Nkuekam et al. 2012; De Beer et al. 2014; Mbenoun et al. 2014, 2016; De Errasti et al. 2015; Liu et al. 2018). The renewed interest that these fungi have received during the course of the past decade has revealed unexpected complexity in their ecological interactions (Mbenoun et al. unpublished data), evolutionary history (Mbenoun et al. 2014; Liu et al. 2018) and reproductive biology (Wilson et al. 2015). The description of novel taxa, as reported in this study and the growing accessibility of whole genome sequencing (Wingfield et al. 2016), should enable new avenues of research that will contribute to a considerably better understanding of *Huntiella* species in the future.

Acknowledgements

This study was initiated through the bilateral agreement between the Governments of South Africa and China and supported by The National Key R&D Program of China (China-South Africa Forestry Joint Research Centre Project; project No. 2018YFE0120900), the National Ten-thousand Talents Program (Project No. W03070115) and the GuangDong Top Young Talents Program (Project No. 20171172). We acknowledge members of Tree Protection and Cooperation Programme (TPCP) and the National Research Foundation (NRF), South Africa for financial support.

References

Al-Subhi AM, Al-Adawi AO, Van Wyk M, Deadman ML, Wingfield MJ (2006) *Ceratocystis omanensis*, a new species from diseased mango trees in Oman. Mycological Research 110: 237–245. https://doi.org/10.1016/j.mycres.2005.08.007

Chen SF, Van Wyk M, Roux J, Wingfield MJ, Xie YJ, Zhou XD (2013) Taxonomy and pathogenicity of *Ceratocystis* species on *Eucalyptus* trees in South China, including *C. chinaeucensis* sp. nov. Fungal Diversity 58: 267–279. https://doi.org/10.1007/s13225-012-0214-5

Cristobal BD, Hansen AJ (1962) Un hongo semjante a *Ceratocystis moniliformis* en cacao en Costa Rica. Turrialba 12: 46–47.

Davidson RW (1935) Fungi causing stain in logs and lumber in the southern states, including five new species. Journal of Agricultural Research 50: 789–807.

De Beer ZW, Duong T, Barnes I, Wingfield BD, Wingfield MJ (2014) Redefining *Ceratocystis* and allied genera. Studies in Mycology 79: 187–219. https://doi.org/10.1016/j.simyco.2014.10.001

De Beer ZW, Marincowitz S, Duong TA, Wingfield MJ (2017) *Bretziella*, a new genus to accommodate the oak wilt fungus, *Ceratocystis fagacearum* (Microascales, Ascomycota). MycoKeys 27: 1–19. https://doi.org/10.3897/mycokeys.27.20657

De Errasti A, De Beer ZW, Rajchenberg M, Coetzee MPA, Wingfield MJ, Roux J (2015) *Huntiella decorticans* sp. nov. (Ceratocystidaceae) associated with dying *Nothofagus* in Patagonia. Mycologia 107: 512–521. https://doi.org/10.3852/14-175

Grosclaude C, Olivier R, Pizzuto J-C, Romiti C, Madec S (1988) Détection par piégeage du *Ceratocystis fimbriata* f. *platani*. Application à l'étude de la persistance du parasite dans du bois infecté. European Journal of Forest Pathology 18: 385–390. https://doi.org/10.1111/j.1439-0329.1988.tb00226.x

Guindon S, Gascuel O (2003) A simple, fast, and accurate algorithm to estimate large phylogenies by maximum likelihood. Systematic Biology 52: 696–704. https://doi.org/10.1080/10635150390235520

Harrington TC (2004) CABI crop protection compendium. CABI Publishing. http://www.public. iastate.edu/~tcharrin/cabinfo.html

Heath RN, Wingfield MJ, Wingfield BD, Meke G, Mbaga A, Roux J (2009) *Ceratocystis* species on *Acacia mearnsii* and *Eucalyptus* spp. in eastern and southern Africa including six new species. Fungal Diversity 34: 41–67.

Hedgcock GG (1906) Studies upon some chromogenic fungi which discolor wood. Missouri Botanical Garden Annual Report 17: 59–124. https://doi.org/10.2307/2400089

Kamgan Nkuekam G, Jacobs K, De Beer ZW, Wingfield MJ, Roux J (2008) *Ceratocystis* and *Ophiostoma* species including three new taxa, associated with wounds on native South African trees. Fungal Diversity 29: 37–59.

Kamgan Nkuekam G, Wingfield MJ, Mohammed C, Carnegie AJ, Pegg GS, Roux J (2012) *Ceratocystis* species, including two new species associated with nitidulid beetles, on eucalypts in Australia. Antonie van Leeuwenhoek 101: 217–241. https://doi.org/10.1007/s10482-011-9625-7

Kamgan Nkuekam G, Wingfield MJ, Roux J (2013) *Ceratocystis* species, including two new taxa, from *Eucalyptus* trees in South Africa. Australasian Plant Pathology 42: 283–311. https://doi.org/10.1007/s13313-012-0192-9

Katoh K, Standley DM (2013) MAFFT multiple sequence alignment software version 7: improvements in performance and usability. Molecular Biology and Evolution 30: 772–780. https://doi.org/10.1093/molbev/mst010

Kearse M, Moir R, Wilson A, Stones-Havas S, Cheung M, Sturrock S, Buxton S, Cooper A, Markowitz S, Duran C, Thierer T, Ashton B, Meintjes P, Drummond A (2012) Geneious Basic: an integrated and extendable desktop software platform for the organization and analysis of sequence data. Bioinformatics 28: 1647–1649. https://doi.org/10.1093/bioinformatics/bts199

Kile G (1993) Plant diseases caused by species of *Ceratocystis sensu stricto* and *Chalara*. *Ceratocystis* and *Ophiostoma*: taxonomy, ecology and pathogenicity, 173–183.

Liu FF, Mbenoun M, Barnes I, Roux J, Wingfield MJ, Li GQ, Li JQ, Chen SF (2015) New *Ceratocystis* species from *Eucalyptus* and *Cunninghamia* in South China. Antonie van Leeuwenhoek 107: 1451–1473. https://doi.org/10.1007/s10482-015-0441-3

Liu FF, Li GQ, Roux J, Barnes I, Wilson AM, Wingfield MJ, Chen SF (2018) Nine novel species of *Huntiella* from southern China with three distinct mating strategies and variable levels of pathogenicity. Mycologia 110: 1145–1171. https://doi.org/10.1080/00275514.2018.1515450

Mayers CG, McNew DL, Harrington TC, Roeper RA, Fraedrich SW, Biedermann PH, Castrillo LA, Reed SE (2015) Three genera in the Ceratocystidaceae are the respective symbionts of three independent lineages of ambrosia beetles with large, complex mycangia. Fungal Biology 119: 1075–1092. https://doi.org/10.1016/j.funbio.2015.08.002

Mayers CG, Harrington TC, Masuya H, Jordal BH, McNew DL, Shih H-H, Roets F, Kietzka GJ (2020) Patterns of coevolution between ambrosia beetle mycangia and the Ceratocystidaceae, with five new fungal genera and seven new species. Persoonia 44: 41–66. https://doi.org/10.3767/persoonia.2020.44.02

Mbenoun M, Wingfield MJ, Begoude Boyogueno AD, Wingfield BD, Roux J (2014) Molecular phylogenetic analyses reveal three new *Ceratocystis* species and provide evidence for geographic differentiation of the genus in Africa. Mycological Progress 13: 219–240. https://doi.org/10.1007/s11557-013-0907-5

Mbenoun M, Wingfield MJ, Begoude Boyogueno AD, Nsouga AF, Petchayo TS, ten Hoopen GM, Mfegue CV, Dibog L, Nyassé S, Wingfield BD, Roux J (2016) Diversity and pathogenicity of the Ceratocystidaceae associated with cacao agroforests in Cameroon. Plant Pathology 65: 64–78. https://doi.org/10.1111/ppa.12400

Mbenoun M, Garnas JR, Wingfield MJ, Begoude Boyogueno AD, Roux J (2017) Metacommunity analyses of Ceratocystidaceae fungi across heterogeneous African savanna landscapes. Fungal Ecology 28: 76–85. https://doi.org/10.1016/j.funeco.2016.09.007

Moreau C (1952) Coexistence des formes *Thielaviopsis* et Graphium chez une souche de *Ceratocystis* major (van Beyma) nov. comb. Remarques sur les variations des *Ceratocystis*. Revue de Mycologie (Supplément Colonial No. 1) 12: 17–25.

Nel WJ, Duong TA, Wingfield BD, Wingfield MJ, De Beer ZW (2018) A new genus and species for the globally important, multi-host root pathogen *Thielaviopsis basicola*. Plant Pathology 67: 871–882. https://doi.org/10.1111/ppa.12803

OEPP/EPPO (2014) PM 7/98 (2) Specific requirements for laboratories preparing accreditation for a plant pest diagnostic activity. European and Mediterranean Plant Protection Organization Bulletin – OEPP/EPPO Bullettin 44: 117–147. https://doi.org/10.1111/epp.12118

Posada D (2008) jModelTest: phylogenetic model averaging. Molecular Biology and Evolution 25: 1253–1256. https://doi.org/10.1093/molbev/msn083

Rayner RW (1970) A mycological colour chart. Commonwealth Mycological Institute Kew, Surrey and British Mycological Society.

Ronquist F, Teslenko M, van der Mark P, Ayres DL, Darling A, Höhna S, Larget B, Liu L, Suchard MA, Huelsenbeck JP (2012) MrBayes 3.2: efficient Bayesian phylogenetic inference and model choice across a large model space. Systematic Biology 61: 539–542. https://doi.org/10.1093/sysbio/sys029

Roux J, Wingfield MJ (2009) *Ceratocystis* species: emerging pathogens of non-native plantation *Eucalyptus* and *Acacia* species. Southern Forests: a Journal of Forest Science 71: 115–120. https://doi.org/10.2989/SF.2009.71.2.5.820

Swofford DL (2003) PAUP*. Phylogenetic Analysis Using Parsimony (*and other methods). Version 4. Sunderland, MA, USA: Sinauer Associates.

Tarigan M, Van Wyk M, Roux J, Tjahjono B, Wingfield MJ (2010) Three new *Ceratocystis* spp. in the *Ceratocystis moniliformis* complex from wounds on *Acacia mangium* and *A. crassicarpa*. Mycoscience 51: 53–67. https://doi.org/10.1007/S10267-009-0003-5

Tsopelas P, Santini A, Wingfield MJ, De Beer ZW (2017) Canker stain: a lethal disease destroying iconic plane trees. Plant Disease 101: 645–658. https://doi.org/10.1094/PDIS-09-16-1235-FE

Van Wyk M, Roux J, Barnes I, Wingfield BD, Chhetri DB, Kirisits T, Wingfield MJ (2004) *Ceratocystis bhutanensis* sp. nov., associated with the bark beetle *Ips schmutzenhoferi* on *Picea spinulosa* in Bhutan. Studies in Mycology 50: 365–379.

Van Wyk M, Roux J, Barnes I, Wingfield BD, Wingfield MJ (2006) Molecular phylogeny of the *Ceratocystis moniliformis* complex and description of *C. tribilliformis* sp. nov. Fungal Diversity 21: 181–201.

Van Wyk M, Wingfield BD, Wingfield MJ (2011) Four new *Ceratocystis* spp. associated with wounds on *Eucalyptus*, *Schizolobium* and *Terminalia* trees in Ecuador. Fungal Diversity 46: 111–131. https://doi.org/10.1007/s13225-010-0051-3

Van Wyk PWJ, Wingfield MJ, Van Wyk PS (1991) Ascospore development in *Ceratocystis moniliformis*. Mycological Research 95: 96–103. https://doi.org/10.1016/S0953-7562(09)81365-8

Von Schrenk H (1903) The "bluing" and the "red-hot" of the western yellow pine, with special reference to the Black Hills Forest Reserve. U.S. Department of Agriculture. Bureau of Plant Industry Bulletin 36: 1–46. https://doi.org/10.5962/bhl.title.65090

Wilson AM, Godlonton T, Van der Nest MA, Wilken PM, Wingfield MJ, Wingfield BD (2015) Unisexual reproduction in *Huntiella moniliformis*. Fungal Genetics and Biology 80: 1–9. https://doi.org/10.1016/j.fgb.2015.04.008

Wingfield BD, Van Wyk M, Roos H, Wingfield M (2013) *Ceratocystis*: emerging evidence for discrete generic boundaries. In. The ophiostomatoid fungi: expanding frontiers, 57–64.

Wingfield BD, Duong TA, Hammerbacher A, van der Nest MA, Wilson A, Chang R, de Beer ZW, Steenkamp ET, Wilken PM, Naidoo K, Wingfield MJ (2016) IMA Genome-F 7 Draft genome sequences for *Ceratocystis fagacearum*, *C. harringtonii*, *Grosmannia penicillata*, and *Huntiella bhutanensis*. IMA Fungus 7: 317–323. https://doi.org/10.5598/imafungus.2016.07.02.11

Yuan ZQ, Mohammed C (2002) *Ceratocystis moniliformopsis* sp. nov., an early colonizer of *Eucalyptus obliqua* logs in Tasmania, Australia. Australian Systematic Botany 15: 125–133. https://doi.org/10.1071/SB00024

Supplementary material 1

Figure S1. ML tree of *Huntiella* species generated from the ITS DNA sequence data
Authors: FeiFei Liu, Seonju Marincowitz, ShuaiFei Chen, Michael Mbenoun, Panaghiotis Tsopelas, Nikoleta Soulioti, Michael J. Wingfield
Data type: phylogenetic tree
Explanation note: Sequences generated from this study are printed in bold type. Bold branches indicate posterior probabilities values ≥ 0.9. Bootstrap values and posterior probabilities value are presented above branches as ML/MP/BI. Bootstrap value < 50% or probabilities values < 0.9 are marked with *. Nodes lacking the support value are marked with -. *Ceratocystis cercfabiensis* (CMW 43029) represents the outgroup.

Link: https://doi.org/10.3897/mycokeys.69.53205.suppl1

Supplementary material 2

Figure S2. ML tree of *Huntiella* species generated from the BT1 DNA sequence data
Authors: FeiFei Liu, Seonju Marincowitz, ShuaiFei Chen, Michael Mbenoun, Panaghiotis Tsopelas, Nikoleta Soulioti, Michael J. Wingfield
Data type: phylogenetic tree
Explanation note: Sequences generated from this study are printed in bold type. Bold branches indicate posterior probabilities values ≥ 0.9. Bootstrap values and posterior probabilities values are presented above branches as ML/MP/BI. Bootstrap value < 50% or probabilities values < 0.9 are marked with *. Nodes lacking the support value are marked with -. *Ceratocystis cercfabiensis* (CMW 43029) represents the outgroup.

Link: https://doi.org/10.3897/mycokeys.69.53205.suppl2

Supplementary material 3

Figure S3. ML tree of *Huntiella* species generated from the TEF-1α DNA sequence data

Authors: FeiFei Liu, Seonju Marincowitz, ShuaiFei Chen, Michael Mbenoun, Panaghiotis Tsopelas, Nikoleta Soulioti, Michael J. Wingfield

Data type: phylogenetic tree

Explanation note: Sequences generated from this study are printed in bold type. Bold branches indicate posterior probabilities values ≥ 0.9. Bootstrap values and posterior probabilities values are presented above branches as ML/MP/BI. Bootstrap value < 50% or probabilities values < 0.9 are marked with *. Nodes lacking the support value are marked with -. *Ceratocystis cercfabiensis* (CMW 43029) represents the outgroup.

Link: https://doi.org/10.3897/mycokeys.69.53205.suppl3

MycoKeys 69: 53–69 (2020)
doi: 10.3897/mycokeys.69.51652
http://mycokeys.pensoft.net

RESEARCH ARTICLE

A peer-reviewed open-access journal
MycoKeys
Launched to accelerate biodiversity research

Two new species of *Perenniporia* (Polyporales, Basidiomycota)

Chao-Ge Wang[1], Shi-Liang Liu[2], Fang Wu[1]

1 *School of Ecology and Nature Conservation, Beijing Forestry University, Beijing 100083, China* **2** *State Key Laboratory of Mycology, Institute of Microbiology, Chinese Academy of Sciences, Beijing 100101, China*

Corresponding author: Fang Wu (fangwubjfu2014@yahoo.com)

Academic editor: Bao-Kai Cui | Received 2 March 2020 | Accepted 27 May 2020 | Published 10 July 2020

Citation: Wang C-G, Liu S-L, Wu F (2020) Two new species of *Perenniporia* (Polyporales, Basidiomycota). MycoKeys 69: 53–69. https://doi.org/10.3897/mycokeys.69.51652

Abstract

Two new species of *Perenniporia*, *P. pseudotephropora* **sp. nov.** and *P. subcorticola* **sp. nov.**, are introduced respectively from Brazil and China based on morphological characteristics and molecular data. *Perenniporia pseudotephropora* is characterised by perennial, pileate basidiocarps with distinctly stratified tubes, grey pores, tissues becoming dark in KOH, a dimitic hyphal system with slightly dextrinoid arboriform skeletal hyphae and broadly ellipsoid to subglobose, truncate, weakly dextrinoid, cyanophilous basidiospores, measuring 4.9–5.2 × 4–4.8 µm. *Perenniporia subcorticola* is characterised by resupinate basidiocarps, yellow pores with thick dissepiments, tissues becoming dark in KOH, flexuous skeletal hyphae, ellipsoid, truncate and slightly dextrinoid basidiospores, measuring 4.2–5 × 3.5–4.2 µm. The morphologically-similar species and phylogenetically closely-related species to the two new species are discussed.

Keywords

phylogeny, polypore, taxonomy, wood-decaying fungi

Introduction

Perenniporia Murrill (Polyporales, Basidiomycetes) is typified by *Polyporus unitus* Pers. (Decock and Stalpers 2006). Species in the genus are important, not only for the wood-decaying, but also for their potential application in both biomedical engineering and biodegradation (Younes et al. 2007; Dai et al. 2009; Zhao et al. 2013; Si et al. 2016). *Perenniporia* is characterised by mostly perennial, resupinate to pileate ba-

sidiocarps, a dimitic to trimitic hyphal system with generative hyphae bearing clamp connections, cyanophilous and variably dextrinoid skeletal hyphae or skeletal-binding hyphae in most species and ellipsoid, to subglobose, truncate or not, thick-walled, variably dextrinoid and cyanophilous basidiospores. All *Perenniporia* species cause a white rot (Ryvarden and Gilbertson 1994; Decock and Ryvarden 1999; Cui et al. 2019).

Extensive studies on the genus have been carried out during the last 20 years showing a high species diversity and nowadays, 120 taxa have been found (e.g. Hattori and Lee 1999; Decock 2001a, b; Decock et al. 2001; Dai et al. 2002; Decock and Stalpers 2006; Cui et al. 2007; Xiong et al. 2008; Cui and Zhao 2012; Zhao and Cui 2012; Zhao et al. 2013; Decock and Ryvarden 2015; Jang et al. 2015; Decock 2016; Viacheslav and Ryvarden 2016; Huang et al. 2017; Ji et al. 2017; Liu et al. 2017; Shen et al. 2018; Cui et al. 2019; Zhao and Ma 2019).

According to the phylogenetic analysis, based on ITS and nuclear ribosomal partial LSU DNA sequences, Robledo et al. (2009) demonstrated the fundamental phylogeny of *Perenniporia* s.l., combined with such characteristics as a diversity of the vegetative hyphae and basidiospores morphology. In their study, *Perenniporia* s.s. and *Perenniporia* s.l. were scattered into distinct clades, which is also supported by different morphological traits. Zhao et al. (2013) divided *Perenniporia* s.l. into seven clades, based on ITS and nLSU DNA phylogenetic inferences, each of these seven clades being distinguished by a specific combination of morphological characteristics that supported recognition at the genus level. Some genera, having similar morphological characteristics to *Perenniporia*, such as *Amylosporia* B.K. Cui et al., *Murinicarpus* B.K. Cui & Y.C. Dai, *Vanderbylia* D.A. Reid, *Truncospora* Pilát and *Hornodermoporus* Teixeira, were also proved to form distinct lineages in DNA-based phylogenetic analyses (Cui et al. 2019). Besides, several new species were proved to belong to *Perenniporia*, based on morphological characteristics and phylogenetic evidence, which improved the understanding of the phylogenetic structure of *Perenniporia* (Jang et al. 2015; Huang et al. 2017; Ji et al. 2017; Liu et al. 2017; Zhao and Ma 2019).

During a study of wood-inhabiting polypore from Brazil and China, two unknown species of *Perenniporia* were distinguished by both morphology and molecular data. In this study, the two species are described and illustrated.

Materials and methods

Morphological studies

The studied specimens are deposited in the herbaria of the Institute of Microbiology, Beijing Forestry University (**BJFC**) and Universidade Federal de Pernambuco (**URM**). Morphological descriptions are based on field notes and herbarium specimens. Microscopic analyses follow Zhao and Cui (2013). In the description: KOH = 5% potassium hydroxide, IKI = Melzer's reagent, IKI– = neither amyloid nor dextrinoid, CB = Cotton Blue, CB+ = cyanophilous in Cotton Blue, CB– = acyanophilous, L = arithmetic

average of all spore length, W = arithmetic average of all spore width, Q = L/W ratios, n = number of spores/measured from given number of specimens. Colour terms are cited from Anonymous (1969) and Petersen (1996).

Molecular studies and phylogenetic analysis

A CTAB rapid plant genome extraction kit-DN14 (Aidlab Biotechnologies Co., Ltd, Beijing) was used to obtain PCR products from dried specimens, according to the manufacturer's instructions with some modifications (Shen et al. 2019; Sun et al. 2020). Two DNA gene fragments, ITS and nrLSU were amplified using the primer pairs ITS5/ITS4 (White et al. 1990) and LR0R/LR7 (http://www.biology.duke.edu/fungi/mycolab/primers.htm). The PCR procedures for ITS and nLSU followed Zhao et al. (2013) in the phylogenetic analyses. DNA sequencing was performed at Beijing Genomics Institute and the newly-generated sequences were deposited in the GenBank database. Sequences generated for this study were aligned with additional sequences downloaded from GenBank, using BioEdit (Hall 1999) and ClustalX (Thompson et al. 1997).

In the study, nuclear ribosomal RNA genes were used to determine the phylogenetic position of the new species. Sequence alignment was deposited at TreeBase (submission ID 26254). Sequences of *Donkioporia expansa* (Desm.) Kotl. and Pouzar and *Pyrofomes demidoffii* (Lév.) Kotl. and Pouzar, obtained from GenBank, were used as outgroups (Zhao et al. 2013).

Phylogenetic analyses, used in this study, followed the approach of Han et al. (2016) and Zhu et al. (2019). Maximum parsimony (MP) and Maximum Likelihood (ML) analyses were conducted for the datasets of ITS and nLSU sequences. The best-fit evolutionary model was selected by hierarchical likelihood ratio tests (hLRT) and Akaike Information Criterion (AIC) in MrModeltest 2.2 (Nylander 2004) after scoring 24 models of evolution by PAUP* version 4.0b10 (Swofford 2002).

The MP topology and bootstrap values (MP-BS) obtained from 1000 replicates were performed using PAUP* version 4.0b10 (Swofford 2002). All characters were equally weighted and gaps were treated as missing. Trees were inferred using the heuristic search option with TBR branch swapping and 1000 random sequence additions. Max-trees were set to 5,000, branches of zero length were collapsed and all parsimonious trees were saved. Descriptive tree statistics tree length (TL), consistency index (CI), retention index (RI), rescaled consistency index (RC) and homoplasy index (HI) were calculated for each Maximum Parsimonious Tree (MPT) generated. Sequences were also analysed using Maximum Likelihood (ML) with RAxML-HPC2 through the CIPRES Science Gateway (www.phylo.org; Miller et al. 2009). Branch support (BT) for ML analysis was determined by 1000 bootstrap replicates.

Bayesian phylogenetic inference and Bayesian posterior probabilities (BPP) were performed with MrBayes 3.1.2 (Ronquist and Huelsenbeck 2003). Four Markov chains were run for 4,650,000 generations until the split deviation frequency value was less than 0.01 and trees were sampled every 100 generations. The first 25% of the

sampled trees were discarded as burn-in and the remaining ones were used to reconstruct a majority rule consensus and calculate Bayesian posterior probabilities (BPP) of the clades.

Branches that received bootstrap support for maximum likelihood (ML), maximum parsimony (MP) and Bayesian posterior probabilities (BPP) ≥ 75% (ML-BS), 75% (MP-BT) and 0.95 (BPP) were considered as significantly supported, respectively.

Results

Phylogeny results

The combined ITS and nLSU dataset contained 101 sequences from 101 specimens referring to 59 taxa in this study. They were downloaded from GenBank and the sequences about *Perenniporia corticola*, *P. pseudotephropora* and *P. subcorticola* are new (Table 1). The dataset had an aligned length of 2089 characters in the dataset, of which, 1400 characters are constant, 181 are variable and parsimony-uninformative and 508 are parsimony informative. Maximum Parsimony analysis yielded one equally-parsimonious tree (TL = 2627, CI = 0.389, RI = 0.711, RC = 0.277, HI = 0.611) and a strict consensus tree of these trees is shown in Fig. 1. Best model applied in the Bayesian analysis: GTR+I+G, lset nst = 6, rates = invgamma; prset statefreqpr = dirichlet (1, 1, 1, 1). Bayesian analysis resulted in a same topology with an average standard deviation of split frequencies = 0.009950.

From the phylogenetic tree (Fig. 1), *P. pseudotephropora* and *P. subcorticola* were absorbed in the genus *Perenniporia*. Moreover, *P. subcorticola* formed a direct lineage with a high approval rating (98/99/1.00) and *P. pseudotephropora* produced an independent lineage.

Taxonomy

Perenniporia pseudotephropora **Chao G. Wang & F. Wu, sp. nov.**
MycoBank No: 835122
Figs 2, 3

Diagnosis. The very thick dissepiments (thicker than pore diameter), tissues becoming pale olivaceous to dark in KOH, flexuous and arboriform skeletal hyphae, ellipsoid to globose, truncate and slightly dextrinoid basidiospores measuring 4.9–5.2 × 4–4.8 μm highlight the species in *Perenniporia*.

Holotype. Brazil. Manaus, Parque Municipal Cachoeira das Orqideas, on rotten angiosperm wood, 12. V. 2017, Y.C. Dai 17383 (BJFC024919).

Etymology. *Pseudotephropora* (Lat.): referring to the species similar to *Perenniporia tephropora*.

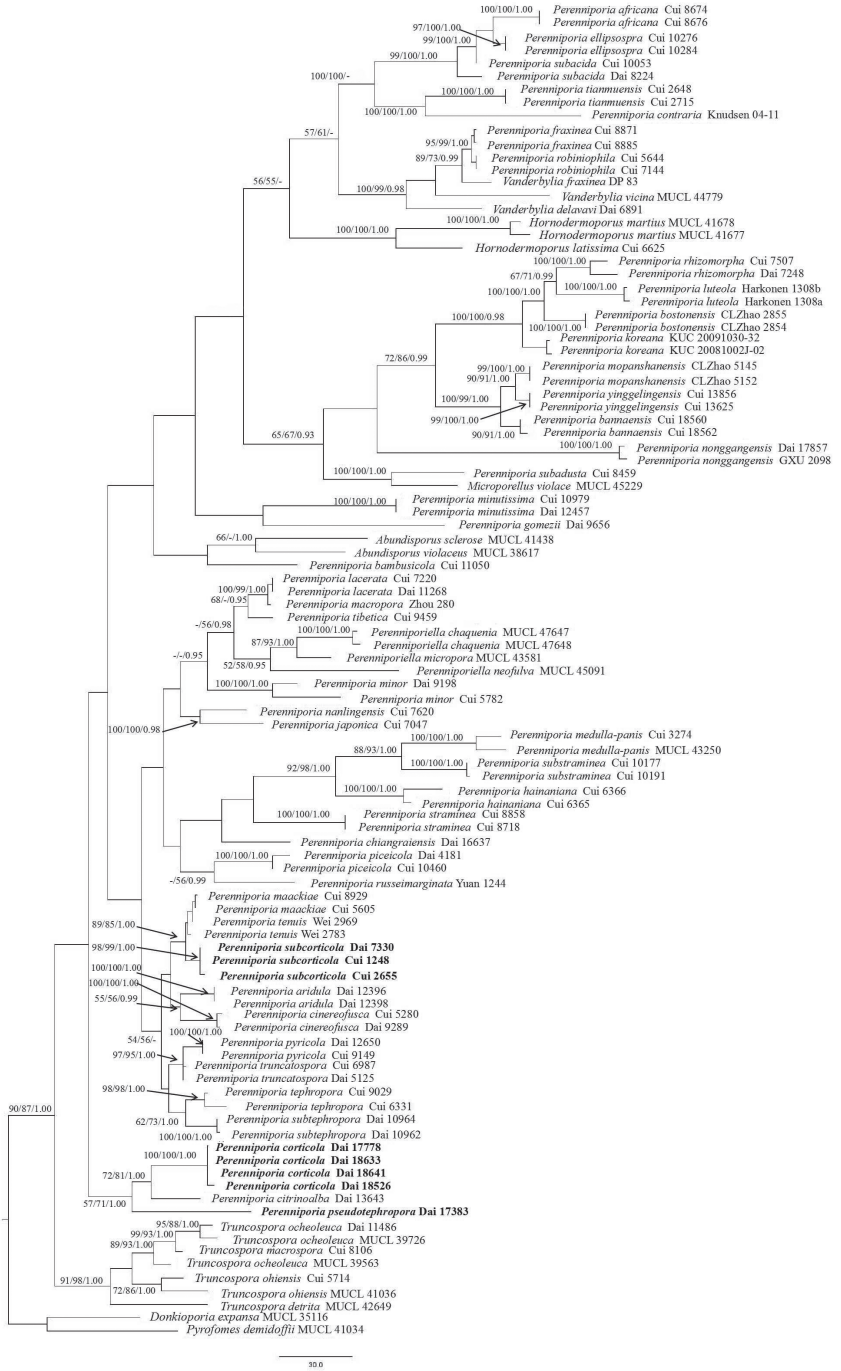

Figure 1. Phylogeny of *Perenniporia* and related species generated by maximum parsimony analysis, based on combined ITS and nLSU sequences. Bootstrap supports for Maximum Likelihood (ML), Maximum parsimony (MP) and Bayesian posterior probabilities (BPP) are not lower than: 50% (ML-BS), 50% (MP-BT) and 0.90 (BPP) on the branches.

Table 1. Information for the sequences used in this study.

Species	Sample namber	ITS	nLSU
Abundisporus sclerosetosus	MUCL 41438	FJ411101	FJ393868
A. violaceus	MUCL 38617	FJ411100	FJ393867
Donkioporia expansa	MUCL 35116	FJ411104	FJ393872
Hornodermoporus latissima	Cui 6625	HQ876604	JF706340
H. martius	MUCL 41678	FJ411093	FJ393860
	MUCL 41677	FJ411092	FJ393859
Microporellus violaceo-cinerascens	MUCL 45229	FJ411106	FJ393874
Perenniporia africana	Cui 8674	KF018119	KF018128
P. africana	Cui 8676	KF018120	KF018129
P. aridula	Dai 12396	JQ001854	JQ001846
	Dai 12398	JQ001855	JQ001847
P. corticola	**Dai 17778**	**MT117219**	**MT117224**
	Dai 18526	**MT117216**	**MT117221**
	Dai 18641	**MT117218**	**MT117223**
	Dai 18633	**MT117217**	**MT117222**
P. bambusicola	Cui 11050	KX900668	KX900719
P. bannaensis	Cui 8560	JQ291727	JQ291729
	Cui 8562	JQ291728	JQ291730
P. bostonensis	CL Zhao 2855	MG491285	MG491288
	CL Zhao 2854	MG491284	MG491287
P. chiangraiensis	Dai 16637	KY475566	–
P. cinereofusca	Dai 9289	KF568893	KF568895
	Cui 5280	KF568892	KF568894
P. subcorticola	**Cui 2655**	**HQ654093**	**HQ848483**
	Dai 7330	**HQ654094**	**HQ654108**
	Cui 1248	**HQ848472**	**HQ848482**
P. ellipsospora	Cui 10276	KF018124	KF018132
	Cui 10284	JQ861739	KF018133
P.fraxinea	Cui 8871	JF706329	JF706345
P. fraxinea	Cui 8885	HQ876611	JF706344
P. gomezii	Dai 9656	KX900672	KX900722
P. hainaniana	Cui 6366	JQ861745	JQ861761
	Cui 6365	JQ861744	JQ861760
P. japonica	Cui 7047	HQ654097	HQ654111
P. koreana	KUC 20091030-32	KJ156313	KJ156305
	KUC 20081002J-02	KJ156310	KJ156302
P. lacerata	Cui 7220	JX141448	JX141458
	Dai 11268	JX141449	JX141459
P. luteola	Harkonen 1308a	JX141456	JX141466
	Harkonen 1308b	JX141457	JX141467
P. macropora	Zhou 280	JQ861748	JQ861764
P. maackiae	Cui 8929	HQ654102	JF706338
	Cui 5605	JN048760	JN048780
P. medulla-panis	MUCL 43250	FJ411087	FJ393875
	Cui 3274	JN112792	JN112793
P. minor	Dai 9198	KF495005	KF495016
	Cui 5782	HQ883475	HQ654115
P. minutissima	Cui 10979	KF495003	KF495013
	Dai 12457	KF495004	KF495014
P. mopanshanensis	CL Zhao 5145	MH784912	MH784916
	CL Zhao 5152	MH784913	MH784917
P. nanlingensis	Cui 7620	HQ848477	HQ848486

Species	Sample namber	ITS	nLSU
P. nonggangensis	Dai 17857	MT232521	MT232515
	GXU 2098	KT894732	KT894733
P. piceicola	Cui 10460	JQ861742	JQ861758
	Dai 4181	JF706328	JF706336
P. pseudotephropora	**Dai 17383**	**MT117215**	**MT117220**
P. pyricola	Dai 10265	JN048761	JN048781
	Cui 9149	JN048762	JN048782
P. rhizomorpha	Dai 7248	JF706330	JF706348
	Cui 7507	HQ654107	HQ654117
P. robiniophila	Cui 7144	HQ876608	JF706341
	Cui 5644	HQ876609	JF706342
P. russeimarginata	Yuan 1244	JQ861750	JQ861766
P. straminea	Cui 8858	HQ654104	JF706334
	Cui 8718	HQ876600	JF706335
P. subacida	Cui 10053	KF495006	KF495017
	Dai 8224	HQ876605	JF713024
P. subadusta	Cui 8459	HQ876606	HQ654113
P. substraminea	Cui 10177	JQ001852	JQ001844
	Cui 10191	JQ001853	JQ001845
P. subtephropora	Dai 10964	JQ861753	JQ861769
	Dai 10962	JQ861752	JQ861768
P. tenuis	Wei 2969	JQ001859	JQ001849
	Wei 2783	JQ001858	JQ001848
P. tephropora	Cui 9029	HQ876601	JF706339
	Cui 6331	HQ848473	HQ848484
P. tibetica	Cui 9459	JF706327	JF706333
P. tianmuensis	Cui 2648	JX141453	JX141463
	Cui 2715	JX141454	JX141464
P. truncatospora	Cui 6987	JN048778	HQ654112
	Dai 5125	HQ654098	HQ848481
P. yinggelingensis	Cui 13856	MH427957	MH427965
	Cui 13625	MH427960	MH427967
Perenniporiella chaquenia	MUCL 47647	FJ411083	FJ393855
P. chaquenia	MUCL 47648	FJ411084	FJ393856
P. micropora	MUCL 43581	FJ411086	FJ393858
P. neofulva	MUCL 45091	FJ411080	FJ393852
Pyrofomes demidoffii	MUCL 41034	FJ411105	FJ393873
Truncospora detrita	MUCL 42649	FJ411099	FJ393866
T. macrospora	Cui 8106	JX941573	JX941596
T. ochroleuca	MUCL 39563	FJ411097	FJ393864
	MUCL 39726	FJ411098	FJ393865
	Dai 11486	HQ654105	JF706349
T. ohiensis	MUCL 41036	FJ411096	FJ393863
	Cui 5714	HQ654103	HQ654116
Vanderbylia delavavi	Dai 6891	JQ861738	KF495019
V. fraxinea	DP 83	AM269789	AM269853
V. vicina	MUCL 44779	FJ411095	FJ393862

Basidiocarps. Perennial, resupinate or effused-reflexed to pileate, without odour or taste when fresh, becoming hard corky when dry. Pilei applanate, semicircular to fan-shaped, projecting up to 1 cm, 3.5 cm wide and about 1 cm thick at base. Pile-

Figure 2. Basidiocarps of *Perenniporia pseudotephropora* (Holotype, Y.C. Dai 17383). Scale bar: 1 cm. Photo by Fang Wu.

al surface pinkish-buff, grey to greyish-brown, smooth. Pore surface greyish to pale brown; pores tiny, round, 8–9 per mm; dissepiments thick, thicker than pore diameter, entire. Context thin, fawn to brown, corky, up to 0.5 mm thick. Tubes buff to brown, darker than pore surface, distinctly stratified, hard corky, up to 9.5 mm long.

Hyphal structure. Hyphal system dimitic; generative hyphae bearing clamp connections; skeletal hyphae arboriform branched, slightly dextrinoid, CB+; tissues becoming pale olivaceous to dark in KOH.

Context. Generative hyphae infrequent, hyaline, thin-walled, bearing clamp connections, 1.6–2.2 μm in diam.; skeletal hyphae dominant, thick-walled with a wide lumen, hyaline to pale brown, frequently arboriform branched, flexuous, interwoven, 1.5–2.8 μm.

Tubes. Generative hyphae infrequent, hyaline, thin-walled, bearing clamp connections, 1.5–2 μm in diam.; skeletal hyphae dominant, thick-walled with a wide lumen, hyaline to pale brown, frequently arboriform branched, flexuous, interwoven, 1.5–3 μm in diam. Cystidia absent, cystidioles present, clavate or fusoid, hyaline, thin-walled, 11–12.5 × 3–4 μm; basidia barrel- to pear-shaped, with four sterigmata and a basal clamp connection, 12.3–13.7 × 6.2–7.5 μm; basidioles in shape similar to basidia, but smaller.

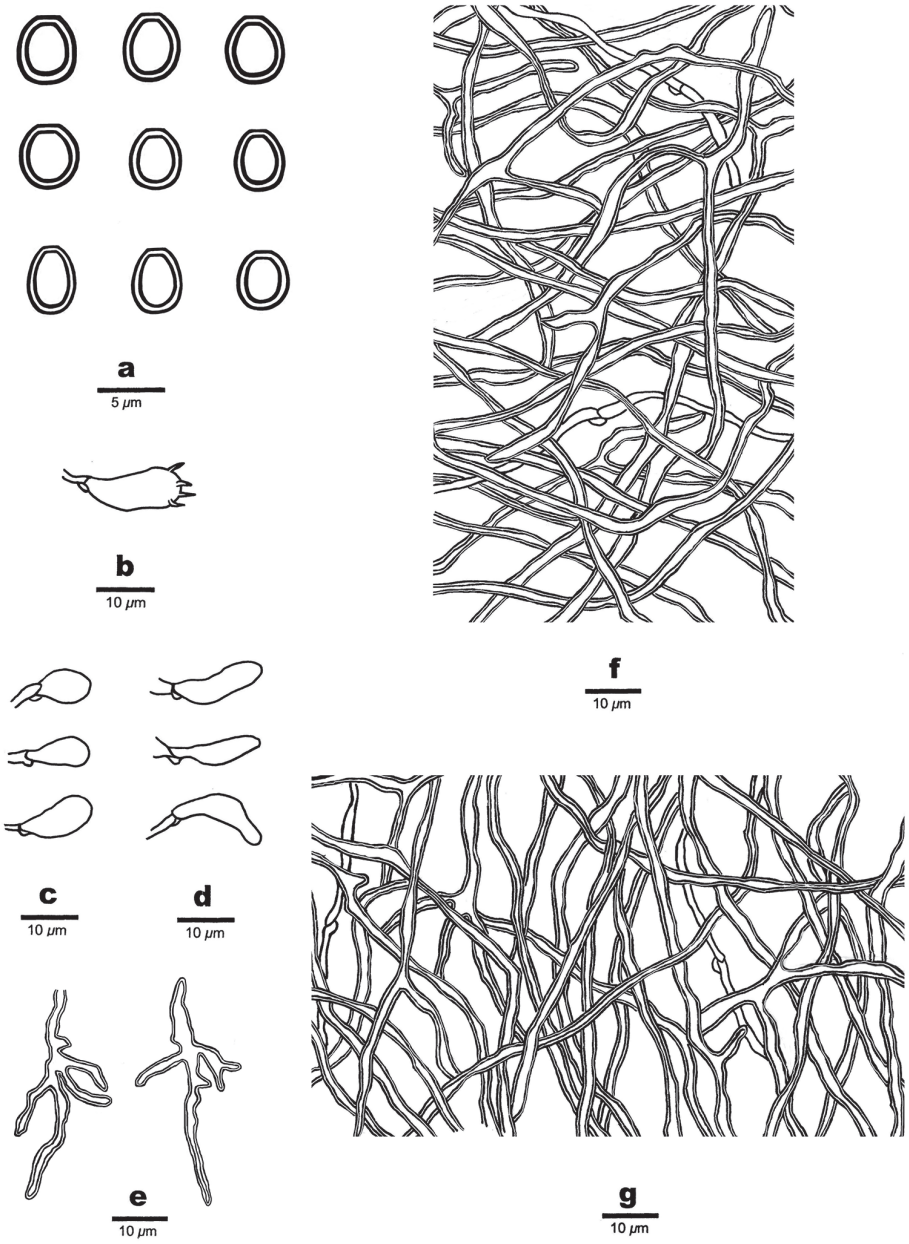

Figure 3. Microscopic structures of *Perenniporia pseudotephropora* (Holotype, Dai17383) **a** basidiospores **b** A basidium **c** basidioles **d** cystidioles **e** arboriform skeletal hyphae **f** hyphae from trama **g** hyphae from context.

Spores. Basidiospores broadly ellipsoid to subglobose, hyaline to pale brown, truncate, thick-walled, smooth, slightly dextrinoid, CB+, (4.5–)4.9–5.2(–5.3) × 4–4.8(–5) μm, L = 5.02 μm, W = 4.22 μm, Q = 1.19 (n = 30/1).

Perenniporia subcorticola **Chao G. Wang & F. Wu, sp. nov.**
MycoBank No: 835519
Figs 4, 5

Diagnosis. *Perenniporia subcorticola* is characterised by resupinate basidiocarps, yellow pores with thick dissepiments, tissues becoming dark in KOH, flexuous skeletal hyphae, ellipsoid, truncate and slightly dextrinoid basidiospores measuring 4.2–5 × 3.5–4.2 μm.

Holotype. China. Fujian Province, Wuyishan Nature Reserve, on rotten wood of *Pinus*, 21.X.2005, Y.C. Dai 7330 (BJFC001421).

Etymology. *Subcorticola* (Lat.): referring to the species similar to *Perenniporia corticola*.

Basidiocarps. Perennial, resupinate, soft corky and without odour or taste when fresh, becoming corky when dry, up to 10 cm long, 5 cm wide, 3.5 mm thick at centre. Pore surface yellow when fresh, becoming buff-yellow to curry-yellow when dry; margin narrow, thinning out; pores tiny, round, 7–8 per mm; dissepiments thick, entire. Subiculum thin, cream, up to 2 mm thick. Tubes concolorous with pore surface, up to 1.5 mm long.

Hyphal structure. Hyphal system dimitic; generative hyphae with clamp connections; skeletal hyphae weakly dextrinoid, CB+; tissues darkening in KOH.

Subiculum. Generative hyphae infrequent, hyaline, thin-walled, occasionally branched, 2–3 μm in diam.; skeletal hyphae dominant, thick-walled with a wide lumen, frequently branched, interwoven, 2–3.5 μm in diam.

Figure 4. A basidiocarp of *Perenniporia subcorticola* (from Dai 3257). Scale bar: 1 cm. Photo by Yu-Cheng Dai.

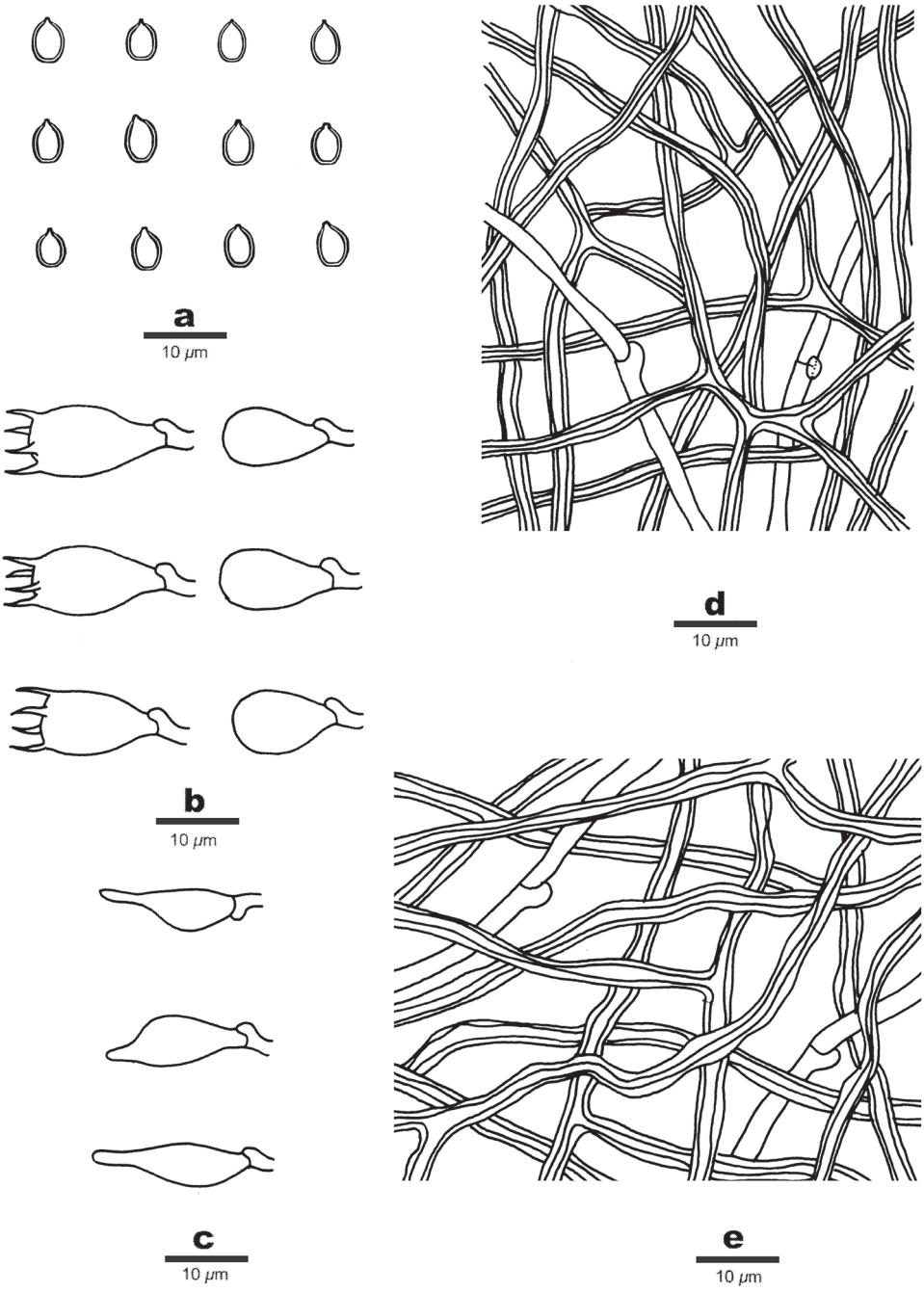

Figure 5. Microscopic structures of *Perenniporia subcorticola* (Holotype, Dai 7330) **a** basidiospores **b** basidia and basidioles **c** cystidioles **d** hyphae from trama **e** hyphae from subiculum.

Tubes. Generative hyphae infrequent, hyaline, thin-walled, occasionally branched, 2–3μm in diam.; skeletal hyphae dominant, thick-walled with a wide lumen, frequently branched, interwoven, 1.8–3 μm in diam. Cystidia absent, fusoid cystidioles present, hyaline, thin-walled, 14–18 × 4.5–7.5 μm; basidia barrel-shaped, with four sterigmata and a basal clamp connection, 13–16 × 6.5–9 μm; basidioles dominant, mostly pear-shaped to capitate, slightly smaller than basidia.

Spores. Basidiospores ellipsoid, truncate, hyaline, thick-walled, smooth, dextrinoid, CB+, (4–)4.2–5(–5.5) × (3–)3.5–4.2(–4.7) μm, L = 4.66 μm, W = 3.91 μm, Q = 1.16–1.23 (n = 60/2).

Additional specimens (paratypes) examined. China. Hunan Province, Liuyang, Daweishan Forest Park, fallen angiosperm trunk, 21.XII.2000, Dai 3257 (BJFC009205); Zhejiang Province, Tianmushan Nature Reserve, on fallen angiosperm branch, 10.X.2005, Cui 2655 (BJFC001422).

Perenniporia corticola **(Corner) Decock, Mycologia 93: 776 (2001)**
Fig. 6

Note. *Perenniporia corticola* and *P. dipterocarpicola* Hattori & S.S. Lee were described from Malaysia (Corner 1989; Hattori and Lee 1999). Decock (2001a) restudied the types of the two taxa and treated *P. dipterocarpicola* as a synonym of *P. corticola*. *Perenniporia corticola* grows on *Dipterocarpus* in lowland forests of Southeast Asia (Decock 2001a; Hattori and Lee 1999) and was not phylogenetically analysed. In this study, *P. corticola* is closely related to *P. citrinoalba* and *P. pseudotephropora.* However, *P. citrinoalba* has larger basidiospores, 5.5–6 ×4.7–5.2 μm (Cui et al. 2019); while basidiospores are 4.6–5(–5.1) × 3.5–4(–4.1) μm in *P. corticola* (4.4–5 × 3.4–4 μm from the type, Decock 2001a). *Perenniporia pseudotephropora* differs from *P. corticola* by resupinate or effused-reflexed to pileate basidiocarps with greyish to pale brown pores, absence of dendrohyphidia and larger basidiospores (4.9–5.2 × 4–4.8 μm vs. 4.6–5 × 3.5–4 μm).

Specimens examined. Malaysia. Selangor, Kota Damansara, Community Forest Reserve, on angiosperm stump, 17. IV. 2018, Y.C. Dai 18641 (BJFC026929), Y.C. Dai 18633 (BJFC026921); Taman Botani Negara Shah Alam, on rotten angiosperm wood, 12. IV. 2018, Y.C. Dai 18526 (BJFC026815), Singapore. Singapore Botanical Garden, on rotten angiosperm wood, 17. VII. 2017, Y.C. Dai 17778 (BJFC025310).

Discussion

Perenniporia pseudotephropora is somehow related to *P. corticola* and *P. citrinoalba* B.K. Cui, C.L. Zhao & Y.C. Dai in our phylogeny (Fig. 1). However, the latter two species have completely resupinate basidiocarps with white to yellow pores. *Perenniporia corticola* has smaller basidiospores, 4.6–5 × 3.5–4 μm, while *P. citrinoalba* has larger basidiospores, 5.5–6 × 4.7–5.2 (Cui et al. 2019) vs. 4.9–5.2 × 4–4.8 μm in *P. pseudotephropora*.

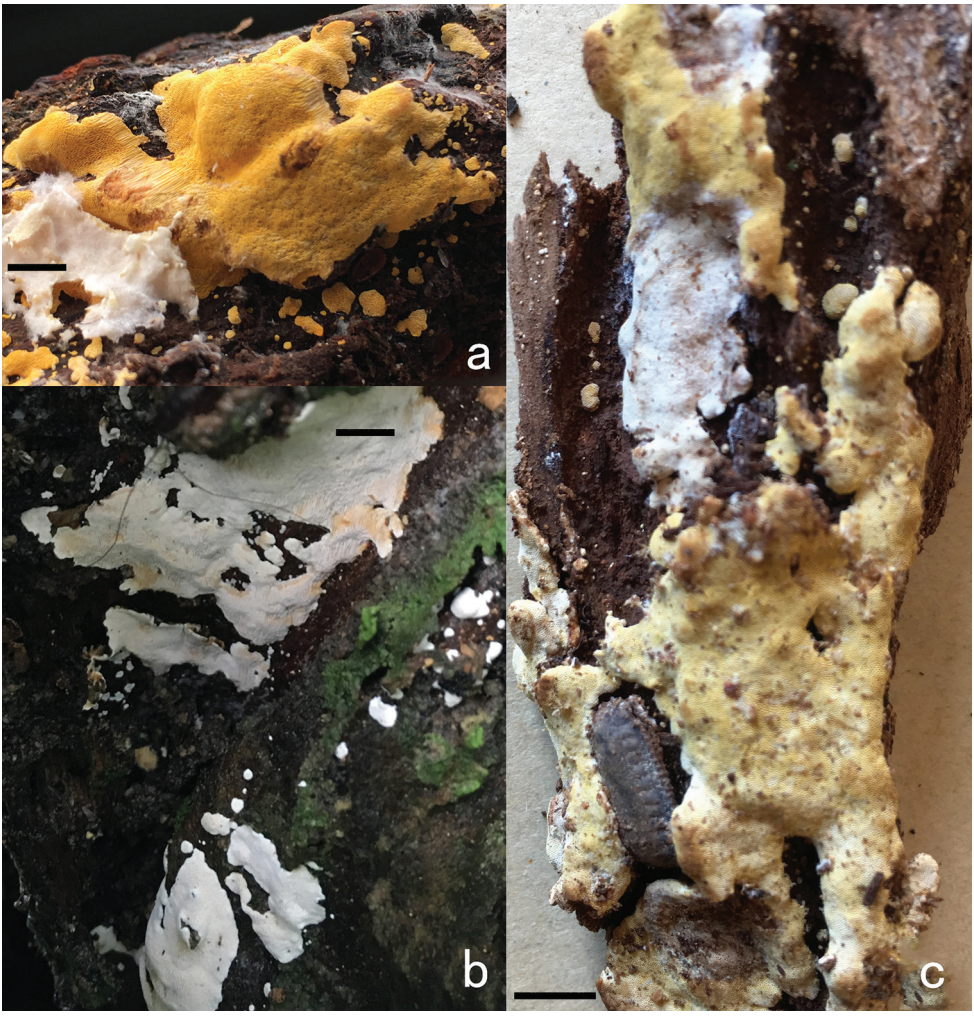

Figure 6. Basidiocarps of *Perenniporia corticola* **a** Dai 18641 **b** Dai 18633 **c** Dai 17778. Scale bars: 1 cm. Photos by Yu-Cheng Dai.

Perenniporia tephropora (Mont.) Ryvarden is similar to *P. pseudotephropora* in having perennial, resupinate to pileate basidiocarps with grey or greyish to pale brown pore surface, tissues becoming pale olivaceous to dark in KOH and broadly ellipsoid, truncate, dextrinoid basidiospores (Ryvarden and Johansen 1980; Corner 1989). However, *P. tephropora* has larger pores (4–6 per mm, Ryvarden and Johansen 1980). In addition, the two species are phylogenetically distantly related.

Phylogenetically, *Perenniporia subcorticola* is related to *P. maackiae* (Bondartsev & Ljub.) Parmasto and *P. tenuis* (Schwein.) Ryvarden (Fig. 1) and all these three species have yellow pores. However, *P. maackiae* has effused-reflexed basidiocarps, strongly dextrinoid skeketal hyphae, ellipsoid basidiospores measuring 5–6.5 × 3.5–4.5 µm and grows exclusively on *Maackia* (Dai et al. 2002); while *P. subcorticola*

has completely resupinate basidiocarps, weakly dextrinoid skeketal hyphae, basidiospores measuring 4.2–5 × 3.5–4.2 μm and grows on a different tree. *Perenniporia tenuis* is different from *P. subcorticola* by larger pores (3–5 per mm), distinct dextrinoid skeketal hyphae and slightly larger basidiospores measuring 5.5–6.5 × 4.5–5.5 μm (Dai et al. 2002).

Macromorphologically, *Perenniporia subcorticola* is similar to *P. corticola* by its yellow pores and almost the same size of basidiospores and that is the reason why the specimens of *P. subcorticola* were previously treated as *P.* cf. *subcorticola* (Dai et al. 2002). However, *P. corticola* has arboriform branched skeletal hyphae and dendrohyphidia at dissepiments and it is a tropical species usually growing on the wood of Dipterocarpaceae (Decock 2001a); while *P. subcorticola* lacks arboriform branched skeletal hyphae and dendrohyphidia and it seems to be a warm temperate species growing on both gymnosperm and angiosperm wood.

Perenniporia xantha Decock & Ryvarden and *P. subcorticola* have yellow hymenophore and almost the same size of pores and basidiospores, but *P. xantha* has arboriform skeletal hyphae, lacks cystidioles and its basidiospores are weakly dextrinoid (Decock and Ryvarden 1999); while *P. subcorticola* lacks arboriform skeletal hyphae, has cystidioles and its basidiospores are distinctly dextrinoid.

Acknowledgements

We express our gratitude to Prof. Yu-Cheng Dai (BJFC, China) who allowed us to study his specimens. The research is supported by the National Natural Science Foundation of China (Project No. 31701978).

References

Anonymous (1969) Flora of British Fungi. Colour Identification Chart. Her Majesty's Stationery Office, London.

Corner EJH (1989) Ad Polyporaceas 5. Beihefte zur Nova Hedwigia 96: 1–218.

Cui BK, Dai YC, Decock C (2007) A new species of *Perenniporia* (Basidiomycota, Aphyllophorales) from eastern China. Mycotaxon 99: 175–180.

Cui BK, Li HJ, Ji X, Zhou JL, Song J, Si J, Yang ZL, Dai YC (2019) Species diversity, taxonomy and phylogeny of Polyporaceae (Basidiomycota) in China. Fungal Diversity 97: 137–302. https://doi.org/10.1007/s13225-019-00427-4

Cui BK, Zhao CL (2012) Morphological and molecular evidence for a new species of *Perenniporia* (Basidiomycota) from Tibet, southwestern China. Mycoscience 53: 365–372. https://doi.org/10.1007/S10267-011-0180-X

Dai YC, Niemelä T (1995) Changbai wood-rotting fungi 4. Some species described by A.S. Bondartsev and L.V. Lyubarsky from the Russian Far East. Annales Botanici Fennici 32: 211–226.

Dai YC, Niemelä T, Kinnunen J (2002) The polypore genera *Abundisporus* and *Perenniporia* (Basidiomycota) in China, with notes on *Haploporus*. Annales Botanici Fennici 39: 169–182.

Dai YC, Yang ZL, Cui BK, Yu CJ, Zhou LW (2009) Species diversity and utilization of medicinal mushrooms and fungi in China (Review). International Journal of Medicinal Mushrooms 11: 287–302. https://doi.org/10.1615/IntJMedMushr.v11.i3.80

Decock C (2001a) Studies in Perenniporia. Some Southeast Asian taxa revisited. Mycologia 93: 774–795. https://doi.org/10.1080/00275514.2001.12063210

Decock C (2001b) Studies in *Perenniporia*: African taxa I. *Perenniporia dendrohyphidia* and *Perenniporia subdendrohyphia*. Systematics and Geography of Plants 71: 45–51. https://doi.org/10.2307/3668752

Decock C (2016) The Neotropical *Perenniporia* s. l. (Basidiomycota): *Perenniporia nouraguensis* sp. nov. and a note on *Perenniporia sinuosa*, from the rainforest in French Guiana. Plant Ecology and Evolution 149: 233–240. https://doi.org/10.5091/plecevo.2016.1188

Decock C, Ryvarden L (1999) Studies in neotropical polypores. Some coloured resupinate *Perenniporia* species. Mycological Research 103: 1138–1144. https://doi.org/10.2307/3761384

Decock C, Ryvarden L (2015) Studies in *Perenniporia* s.l. African taxa 9: *Perenniporia vanhullii* sp. nov. from open woodlands. Synopsis Fungorum 33: 43–49.

Decock C, Sara HF, Ryvarden L (2001) Studies in *Perenniporia*. *Perenniporia contraria* and its presumed taxonomic synonym *Fomes subannosus*. Mycologia 93: 196–204. https://doi.org/10.2307/3761616

Decock C, Stalpers J (2006) Studies in *Perenniporia*: *Polyporus unitus*, *Boletus medulla-panis*, the nomenclature of *Perenniporia*, *Poria* and *Physisporus*, and a note on European *Perenniporia* with a resupinate basidiome. Taxon 53: 759–778. https://doi.org/10.2307/25065650

Hall TA (1999) BioEdit: a user-friendly biological sequence alignment editor and analysis program for Windows 95/98/NT. Nucleic Acids Symposium Series 41: 95–98.

Han ML, Chen YY, Shen LL, Song J, Vlasák J, Dai YC, Cui BK (2016) Taxonomy and phylogeny of the brown-rot fungi: *Fomitopsis* and its related genera. Fungal Diversity 80: 343–373. https://doi.org/10.1007/s13225-016-0364-y

Hattori T, Lee SS (1999) Two new species of *Perenniporia* described from a lowland rainforest of Malaysia. Mycologia 91: 525–531. https://doi.org/10.2307/3761354

Huang FC, Liu B, Wu H, Shao YY, Qin PS, Li JF (2017) Two new species of aphyllophoroid fungi (Basidiomycota) from southern China. Mycosphere 8: 1270–1282. https://doi.org/10.5943/mycosphere/8/6/12

Jang Y, Jang S, Lim YW (2015) *Perenniporia koreana*, a new wood-rotting basidiomycete from South Korea. Mycotaxon 130: 173–179. https://doi.org/10.5248/130.173

Ji XH, Thawthong A, Wu F (2017) A new species of *Perenniporia* (Polyporales, Basidiomycota) from Thailand. Mycosphere 8: 1102–1107. https://doi.org/10.5943/mycosphere/8/8/10

Liu WL, Xu T, Shen S, Liu XF, Sun Y, Zhao XL (2017) *Perenniporia puerensis* sp. nov. from southern China. Mycotaxon 132: 867–874. https://doi.org/10.5248/132.867

Miller MA, Holder MT, Vos R, Midford PE, Liebowitz T, Chan L, Hoover P, Warnow T (2009) The CIPRES Portals. CIPRES URL: http://www.phylo.org/sub_sections/portal [Archived by WebCite(r) at http://www.webcitation.org/5imQlJeQa]

Nylander JAA (2004) MrModeltest v2. Program distributed by the author. Evolutionary Biology Centre, Uppsala University.

Petersen JH (1996) The Danish Mycological Society's colour-chart. Foreningen til Svampekundskabens Fremme, Greve.

Robledo GL, Amalfi M, Castillo G, Rajchenberg M, Decock C (2009) *Perenniporiella chaquenia* sp. nov. and further notes on *Perenniporiella* and its relationships with *Perenniporia* (Poriales, Basidiomycota). Mycologia 101: 657–673. https://doi.org/10.5248/132.867

Ronquist F, Huelsenbeck JP (2003) MRBAYES 3: Bayesian phylogenetic inference under mixed models. Bioinformatics 19: 1572–1574. https://doi.org/10.1093/bioinformatics/btg180

Ryvarden L (1988) Two new polypores from Burundi in Africa. Mycotaxon 31: 407–409.

Ryvarden L, Gilbertson RL (1994) European polypores 2. Synopsis Fungorum 7: 394–743.

Ryvarden L, Johansen I (1980) A preliminary polypore flora of East Africa. Fungiflora, Oslo.

Shen S, Xu TM, Karakehian J, Zhao CL (2018) Morphological and molecular identification of a new species of *Perenniporia* (Polyporales, Basidiomycota) in North America. Phytotaxa 351: 63–71. https://doi.org/10.11646/phytotaxa.351.1.5

Shen LL, Wang M, Zhou JL, Xing JH, Cui BK, Dai YC (2019) Taxonomy and phylogeny of *Postia*. Multi-gene phylogeny and taxonomy of the brown-rot fungi: *Postia* (Polyporales, Basidiomycota) and related genera. Persoonia 42:101–126. https://doi.org/10.3767/persoonia.2019.42.05

Si J, Cui BK, Yuan Y, Dai YC (2016) Biosorption performances of raw and chemically modified biomasses from *Perenniporia subacida* for heterocycle dye Neutral Red. Desalination and Water Treatment 57: 8454–8469. https://doi.org/10.1080/19443994.2015.1025439

Sun YF, Costa-Rezende DH, Xing JH, Zhou JL, Zhang B, Gibertoni TB, Gates G, Glen M, Dai YC, Cui BK (2020) Multi-gene phylogeny and taxonomy of *Amauroderma* s.lat. (Ganodermataceae). Persoonia 44: 206–239. https://doi.org/10.3767/persoonia.2020.44.08

Swofford DL (2002) PAUP*: phylogenetic analysis using parsimony (*and other methods), version 4.0b10. Sinauer Associates, Sunderland. https://doi.org/10.1002/0471650129.dob0522

Thompson JD, Gibson TJ, Plewniak F, Jeanmougin F, Higgins DG (1997) The Clustal_X windows interface: flexible strategies for multiple sequence alignment aided by quality analysis tools. Nucleic Acids Research 25: 4876–4882. https://doi.org/10.1093/nar/25.24.4876

Viacheslav S, Ryvarden L (2016) Some basidiomycetes (Aphyllophorales) from Mexico. Synopsis Fungorum 35: 34–42.

White TJ, Bruns T, Lee S, Taylor J (1990) Amplification and direct sequencing of fungal ribosomal RNA genes for phylogenetics. In: Innis MA, Gefand DH, Sninsky JJ, White JT (Eds) PCR Protocols: A Guide to Methods and Applications. Academic Press, San Diego, 315–322. https://doi.org/10.1016/B978-0-12-372180-8.50042-1

Xiong HX, Dai YC, Cui BK (2008) *Perenniporia minor* (Basidiomycota, Polyporales), a new polypore from China. Mycotaxon 105: 59–64.

Younes SB, Mechichi T, Sayadi S (2007) Purification and characterization of the laccase secreted by the white rot fungus *Perenniporia tephropora* and its role in the decolourization of synthetic dyes. Journal of Applied Microbiology 102: 1033–1042. https://doi.org/10.1111/j.1365-2672.2006.03152.x

Zhao CL, Cui BK (2012) A new species of *Perenniporia* (Polyporales, Basidiomycota) described from southern China based on morphological and molecular characters. Mycological Progress 11: 555–560. https://doi.org/10.1007/s11557-011-0770-1

Zhao CL, Cui BK (2013) Morphological and molecular identification of four new resupinate species of *Perenniporia* (Polyporales) from southern China. Mycologia 105: 945–958. https://doi.org/10.3852/12-201

Zhao CL, Cui BK, Dai YC (2013) New species and phylogeny of *Perenniporia* based on morphological and molecular characters. Fungal Diversity 58: 47–60. https://doi.org/10.1007/s13225-012-0177-6

Zhao CL, Ma X (2019) *Perenniporia mopanshanensis* sp. nov. from China. Mycotaxon 134: 125–137. https://doi.org/10.5248/134.125

Zhu L, Song J, Zhou JL, Si J, Cui BK (2019) Species diversity, phylogeny, divergence time and biogeography of the genus *Sanghuangporus* (Basidiomycota). Frontiers in Microbiology 10: 812. https://doi.org/10.3389/fmicb.2019.00812

MycoKeys 69: 71–89 (2020)
doi: 10.3897/mycokeys.69.54012
http://mycokeys.pensoft.net

RESEARCH ARTICLE

A peer-reviewed open-access journal
MycoKeys
Launched to accelerate biodiversity research

Tree inhabiting gnomoniaceous species from China, with *Cryphogonomonia* gen. nov. proposed

Qin Yang[1,2*], Ning Jiang[2*], Cheng-Ming Tian[2]

1 *Forestry Biotechnology Hunan Key Laboratories, Central South University of Forestry and Technology, Changsha 410004, China* **2** *The Key Laboratory for Silviculture and Conservation of the Ministry of Education, Beijing Forestry University, Beijing 100083, China*

Corresponding author: Cheng-Ming Tian (chengmt@bjfu.edu.cn)

Academic editor: Andrew Miller | Received 10 May 2020 | Accepted 11 June 2020 | Published 10 July 2020

Citation: Yang Q, Jiang N, Tian C-M (2020) Tree inhabiting gnomoniaceous species from China, with *Cryphogonomonia* gen. nov. proposed. MycoKeys 69: 71–89. https://doi.org/10.3897/mycokeys.69.54012

Abstract

Species of Gnomoniaceae are commonly associated with leaf spot diseases of a wide range of plant hosts worldwide. During our investigation of fungi associated with tree diseases in China, several gnomoniaceous isolates were recovered from symptomatic branches and leaves on different woody plants in the Fagaceae, Pinaceae, and Salicaceae families. These isolates were studied by applying a polyphasic approach including morphological, cultural data, and phylogenetic analyses of partial ITS, LSU, *tef1*, *rpb2* and *tub2* gene sequences. As a result, three species were identified with characters fitting into the family Gnomoniaceae. One of these species is described herein as *Cryphognomonia pini* **gen. et sp. nov.**, characterized by developed pseudostromata and ascospores with obvious hyaline sheath; *Gnomoniopsis xunwuensis* **sp. nov.** is illustrated showing sympodially branched conidiophore, oval or fusiform conidia; and one known species, *Plagiostoma populinum*. The current study improves the understanding of gnomoniaceous species causing diebacks and leaf spot on ecological and economic forest trees.

Keywords

forest trees, Gnomoniaceae, new genus, phylogeny, systematics

Introduction

The Gnomoniaceae (Diaporthales, Sordariomycetes, Ascomycota) is a family of perithecial ascomycetes that occur as endophytes, pathogens, or saprobes on growing and over-

* Contributed equally as the first authors.

wintered leaves of hardwood trees, shrubs, and herbaceous plants (Walker 2012). Many species in the Gnomoniaceae cause serious tree diseases such as cherry leaf scorch (*Apiognomonia erythrostoma* (Pers.) Höhn.), oak dieback (*A. errabunda* (Roberge) Höhn), sycamore canker (*A. veneta* (Sacc. & Speg.) Höhn), and chestnut dieback (*Gnomoniopsis daii* Tian & Jiang) (Sogonov et al. 2008; Walker et al. 2010; Jiang et al. 2019).

The sexual morph of Gnomoniaceae is characterized by ascomata that are generally immersed, solitary or aggregated in an undeveloped stroma (Rossman et al. 2007; Sogonov et al. 2008). The perithecia are dark brown to black and pseudoparenchymatous with central, eccentric, or lateral necks (Rossman et al. 2007; Sogonov et al. 2008). Asci usually have an inconspicuous or distinct apical ring. Ascospores are generally small, hyaline, uniseptate. The asexual morph is characterized by acervular or pycnidial, phialidic, with non-septate conidia (Monod 1983).

The generic concepts of Gnomoniaceae were recently revised based on a survey of leaf-inhabiting diaporthalean fungi (Sogonov et al. 2008). Phylogenetic analyses of molecular markers is the primary methodology for systematic studies of the Gnomoniaceae, however, host specificity and morphology can also be useful for species identification. Recent phylogenetic studies have shown that species of Gnomoniaceae often have a narrow host range associating with a single host genus or species (Mejía et al. 2008, 2011a, b, 2012; Sogonov et al. 2008; Walker et al. 2010, 2012, 2013). For example, *Cryptosporella* is a well-defined genus which was frequently limited to a single host species, especially in the host family Betulaceae, except for *C. wehmeyeriana* on *Tilia* spp. and type species *C. hypodermia* on *Ulmus* spp. (Mejía et al. 2008, 2011b).

Several fungal species of Gnomoniaceae, *Cryptosporella platyphylla* from *Betula platyphylla*, *Flavignomonia rhoigena* from *Rhus chinensis*, *Gnomoniopsis daii* and *Ophiognomonia castaneae* from *Castanea mollissima*, have been reported from China (Fan et al. 2016; Gong et al. 2017; Jiang and Tian 2019; Jiang et al. 2019). In the present study, tree inhabiting gnomoniaceous species, mainly on cankered branches and leaves, were surveyed in China. The aim of the present study was to identify these fungi via morphology and multi-locus phylogeny based on modern taxonomic concepts.

Materials and methods

Isolates

Fresh specimens of Gnomoniaceae-related fungi were collected from branches and leaves of hosts in Beijing, Jiangxi and Shaanxi provinces (Tables 1–3). Isolates from host material were obtained by removing a mucoid spores mass from perithecia and pycnidia-like conidiomata, spreading the suspension on the surface of 1.8% potato dextrose agar (PDA), and incubating at 25 °C for up to 24 h. Single germinating conidia/ascospore was removed and plated on to fresh PDA plates. Specimens are deposited in the Museum of the Beijing Forestry University (**BJFC**). Axenic cultures are maintained in the China Forestry Culture Collection Centre (**CFCC**).

Morphological analysis

Morphological observations of the asexual/sexual morph in the natural environment were based on features of the conidiomata or ascomata on infected plant tissues and micromorphology, supplemented by cultural characteristics. Ascomata and conidiomata from tree barks were sectioned by hand, using a double-edged blade and structures were observed under a dissecting microscope. The gross morphology of conidiomata or ascomata was recorded using a Leica stereomicroscope (M205 FA). Fungal structures were mounted in clear lactic acid and micromorphological characteristics were examined using a Leica compound microscope (DM 2500) with differential interference contrast (DIC) optics. Thirty measurements of each structure were determined for each collection. Colony characters and pigment production on PDA were noted after 10 d. Colony colors were described according to Rayner (1970).

DNA extraction, PCR amplification and sequencing

Total genomic DNA was extracted from fresh mycelium grown on PDA using a cetyltrimethylammonium bromide (CTAB) method (Doyle and Doyle 1990). PCR amplifications were performed in a DNA Engine Peltier Thermal Cycler (PTC-200; Bio-Rad Laboratories, Hercules, CA, USA). The primer sets ITS1 and ITS4 (White et al. 1990) were used to amplify the ITS region. The primer sets LR0R and LR7 (Vilgalys and Hester 1990; Vilgalys and Sun 1994) were used to amplify the nuclear ribosomal large subunit (LSU) region. The primer sets EF1-728F (Carbone and Kohn 1999) and EF1-1567R (Rehner 2001) were used to amplify a partial fragment of the translation elongation factor 1-α gene (*tef1-α*). The primer sets RPB2-5F and fRPB2-7cR (Liu et al. 1999) were used to amplify the partial RNA polymerase II subunit (*rpb2*) region. The primer sets T1 (O'Donnell and Cigelnik 1997) and Bt2b (Glass and Donaldson 1995) were used to amplify the beta-tubulin gene (*tub2*). The PCR conditions were: an initial denaturation step of 5 min at 94 °C followed by 35 cycles of 30 sec at 94 °C, 50 sec at 48 °C (ITS, LSU) or 54 °C (*tef-1α*) or 55 °C (*rpb2*, *tub2*) and 1 min at 72 °C, and a final elongation step of 7 min at 72 °C. PCR amplification products were assayed via electrophoresis in 2% agarose gels. DNA sequencing was performed using an ABI PRISM 3730XL DNA Analyser with a BigDye Terminater Kit v.3.1 (Inv-itrogen, USA) at the Shanghai Invitrogen Biological Technology Company Limited (Beijing, China).

Phylogenetic analyses

The quality of our amplified nucleotide sequences was checked and combined by SeqMan v.7.1.0 and reference sequences were retrieved from the National Center for Biotechnology Information (NCBI), based on Mejía et al. (2011a), Senanayake et al. (2018), Jiang and Tian (2019), and Jiang et al. (2019), supplemented by sequences

Table 1. Strains and GenBank accession numbers used in the phylogenetic analyses of Gnomoniaceae.

Species	Strains	Genbank accession number			
		ITS	LSU	*tef1*	*rpb2*
Alnecium auctum	CBS 124263	KF570154	KF570154	KF570200	KF570170
Ambarignomonia petiolorum	CBS 116866	EU199193	AY818963	NA	EU199151
	CBS 121227	EU254748	EU255070	EU221898	EU219307
Amphiporthe tiliae	CBS 119289	EU199178	EU199122	NA	EU199137
Anisogramma anomala	529478	EU683064	EU683066	NA	NA
Anisogramma virgultorum	529479	EU683062	EU683065	NA	NA
Apiognomonia errabunda	AR 2813	DQ313525	NG027592	DQ313565	DQ862014
Apiognomonia veneta	MFLUCC 16-1193	MF190114	MF190056	NA	NA
Apioplagiostoma populi	858501	KP637024	NA	NA	NA
Asteroma alneum	CBS 109840	EU167609	EU167609	NA	NA
Asteroma sp.	Masuya 8Ah9-1	NA	AB669035	NA	NA
Cryphognomonia pini	**CFCC 53020**	**MK432672**	**MK429915**	**MK578144**	**MK578100**
	CFCC 53021	**MK432673**	**MK429916**	**MK578145**	**MK578101**
Cryptosporella hypodermia	CBS 116866	EU199181	AF408346	NA	EU199140
Discula destructiva	MD 254	AF429741	AF429721	AF429732	NA
Ditopella biseptata	MFLU 15-2661	MF190147	MF190091	NA	MF377616
Ditopella ditopa	CBS 109748	DQ323526	EU199126	NA	EU199145
Ditopellopsis sp.	CBS 121471	EU254763	EU255088	EU221936	EU219254
Flavignomonia rhoigena	CFCC 53118	MK432674	MK429917	NA	MK578102
	CFCC 53119	MK432675	MK429918	NA	MK578103
	CFCC 53120	MK432676	MK429919	NA	MK578104
Gnomonia gnomon	CBS 199.53	DQ491518	AF408361	EU221885	EU219295
	CBS 829.79	AY818957	AY818964	EU221905	NA
Gnomoniopsis alderdunensis	CBS 125680	GU320825	NA	NA	NA
Gnomoniopsis chamaemori	CBS 803.79	EU254808	EU255107	NA	NA
Gnomoniopsis racemula	AR 3892	EU254841	EU255122	EU221889	EU219241
Mamianiella coryli	BPI 877578	EU254862	NA	NA	NA
Marsupiomyces quercina	MFLUCC 13-0664	MF190116	MF190061	NA	NA
Marsupiomyces epidermoidea	MFLU 15-2921	NA	MF190058	NA	NA
Melanconis marginalis	CBS 109744	EU199197	AF408373	EU221991	EU219301
Neognomoniopsis quercina	CBS 145575	MK876399	MK876440	NA	NA
Occultocarpon ailaoshanense	LCM 524.01	JF779849	JF779853	NA	JF779856
	LCM 522.01	JF779848	JF779852	JF779862	JF779857
Ophiognomonia melanostyla	LCM 389.01	JF779850	JF779854	NA	JF779858
Ophiognomonia vasiljevae	AR 4298	EU254977	EU255162	EU221999	EU219331
Plagiostoma aesculi	AR 3640	EU254994	EU255164	NA	EU219269
Linospora capreae	CBS 372.69	NA	AF277143	NA	NA
Pleuroceras oregonense	AR 4333	EU255060	EU255196	EU221931	EU219313
Pleuroceras pleurostylum	CBS 906.79	EU255061	EU255197	EU221962	EU219311
Phragmoporthe conformis	AR 3632	NA	AF408377	NA	NA
Valsalnicola oxystoma	AR 5137	JX519561	NA	NA	NA
	AR 4833	JX519559	JX519563	NA	NA
Sirococcus tsugae	AR 4010	EF512478	EU255207	EU221928	EU219289
	CBS 119626	EU199203	EU199136	EF512534	EU199159
Tenuignomonia styracis	BPI 89278	NA	LC379288	LC379282	LC379294

Note: NA, not applicable. Strains in this study are marked in bold.

of *Tenuignomonia styracis* and *Neognomoniopsis quercina* from Crous et al. (2019) and Minoshima et al. (2019). Sequences were aligned using MAFFT v. 6 (Katoh and Toh 2010) and manually corrected using Bioedit 7.0.9.0 (Hall 1999).

Table 2. Strains and GenBank accession numbers used in the phylogenetic analyses of *Gnomoniopsis*.

Species	Strain	Genbank accession number		
		ITS	*tef1*	*tub2*
Apiognomonia veneta	CBS 342.86	DQ313531	DQ318036	EU219235
Gnomoniopsis alderdunensis	CBS 125679	GU320826	GU320813	GU320788
	CBS 125680	GU320825	GU320801	GU320787
	CBS 125681	GU320827	GU320802	GU320789
Gnomoniopsis chamaemori	CBS 804.79	GU320817	GU320809	GU320777
Gnomoniopsis chinensis	CFCC 52286	MG866032	MH545370	MH545366
	CFCC 52287	MG866033	MH545371	MH545367
	CFCC 52288	MG866034	MH545372	MH545368
	CFCC 52289	MG866035	MH545373	MH545369
Gnomoniopsis clavulata	CBS 121255	EU254818	GU320807	EU219211
Gnomoniopsis comari	CBS 806.79	EU254821	GU320810	EU219156
	CBS 807.79	EU254822	GU320814	GU320779
	CBS 809.79	EU254823	GU320794	GU320778
Gnomoniopsis daii	CFCC 54043	MN598671	MN605519	MN605517
	CMF002B	MN598672	MN605520	MN605518
Gnomoniopsis fructicola	CBS 121226	EU254824	GU320792	EU219144
	CBS 208.34	EU254826	GU320808	EU219149
	CBS 125671	GU320816	GU320793	GU320776
Gnomoniopsis guttulata	MS 0312	EU254812	NA	NA
Gnomoniopsis idaeicola	CBS 125672	GU320823	GU320797	GU320781
	CBS 125673	GU320824	GU320798	GU320782
	CBS 125674	GU320820	GU320796	GU320780
	CBS 125675	GU320822	GU320799	GU320783
	CBS 125676	GU320821	GU320811	GU320784
Gnomoniopsis macounii	CBS 121468	EU254762	GU320804	EU219126
Gnomoniopsis occulta	CBS 125677	GU320828	GU320812	GU320785
	CBS 125678	GU320829	GU320800	GU320786
Gnomoniopsis paraclavulata	CBS 123202	GU320830	GU320815	GU320775
Gnomoniopsis racemula	CBS 121469	EU254841	GU320803	EU219125
Gnomoniopsis sanguisorbae	CBS 858.79	GU320818	GU320805	GU320790
Gnomoniopsis smithogilvyi	CBS 130190	JQ910642	KR072534	JQ910639
	CBS 130189	JQ910644	KR072535	JQ910641
	CBS 130188	JQ910643	KR072536	JQ910640
	MUT 401	HM142946	KR072537	KR072532
	MUT 411	HM142948	KR072538	KR072533
Gnomoniopsis tormentillae	CBS 904.79	EU254856	GU320795	EU219165
Gnomoniopsis xunwuensis	**CFCC 53115**	**MK432667**	**MK578067**	**MK578141**
	CFCC 53116	**MK432668**	**MK578068**	**MK578142**
	CFCC 53117	**MK432669**	**MK578069**	**MK578143**
Plagiostoma euphorbiae	CBS 340.78	DQ323532	GU354016	GU367034

Note: NA, not applicable. Strains in this study are marked in bold.

The phylogenetical analyses were conducted using Maximum Parsimony (MP), Maximum Likelihood (ML) and Bayesian inference (BI). MP was performed with PAUP v. 4.0b10 (Swofford 2003) using tree-bisection-reconnection (TBR) as the branch-swapping algorithm. Other calculated parsimony scores were tree length (TL), consistency index (CI), retention index (RI), and rescaled consistency (RC). ML was performed with RAxML (Stamatakis 2006) as implemented in raxmlGUI 1.3 (Silvestro

Table 3. Strains and GenBank accession numbers used in the phylogenetic analyses of *Gnomoniopsis*.

Species	Strain	Genbank accession number		
		ITS	*tef1*	*tub2*
Apiognomonia errabunda	AR 4182	DQ313543	KJ509937	KJ509947
Plagiostoma aceris-palmati	CBS 137265	KJ509959	KJ509938	KJ509949
Plagiostoma aesculi	CBS 121905	EU254994	GU367022	GU354005
Plagiostoma amygdalinae	CBS 791.79	EU254995	GU367030	GU354012
Plagiostoma apiculatum	CBS 109775	DQ323529	GU367008	GU353990
	CBS 126126	GU367066	GU367009	GU353991
Plagiostoma barriae	LCM 601.01	GU367054	GU366997	GU353980
	LCM 484.01	GU367053	GU366995	GU353979
Plagiostoma convexum	CBS 123206	EU255047	EU219112	GU353994
Plagiostoma devexum	CBS 123201	EU255001	GU367027	GU354010
Plagiostoma dilatatum	LCM 403.02	GU367069	GU367012	GU353995
	CBS 124976	GU367070	GU367014	GU353996
Plagiostoma euphorbiaceum	CBS 816.79	EU255003	EU219158	GU354013
Plagiostoma euphorbiae	CBS 340.78	DQ323532	GU367034	GU354016
	CBS 817.79	KJ509960	GU367028	KJ509950
Plagiostoma exstocollum	CBS 127662	GU367046	GU366988	GU353972
	LCM 422.01	GU367043	GU366989	GU353969
Plagiostoma fraxini	CBS 121258	EU255008	KJ509939	KJ509951
	CBS 109498	AY455810	GU367033	GU354015
Plagiostoma geranii	CBS 824.79	EU255009	GU367032	GU354014
Plagiostoma imperceptibile	LCM 456.01	GU367059	GU367002	GU353984
Plagiostoma jonesii	MFLUCC 16–1189	MF190159	NA	MF377589
Plagiostoma mejianum	CBS 137266	KJ509961	KJ509940	KJ509952
Plagiostoma oregonense	CBS 126124	GU367073	GU367016	GU353999
Plagiostoma ovalisporum	CBS 124977	GU367072	GU367015	GU353998
Plagiostoma petiolophilum	AR 3821	EU255039	GU367025	GU354008
	CBS 126123	GU367078	GU367023	GU354006
Plagiostoma populinum	**CFCC 53016**	**MK432677**	**MK578070**	**MK578146**
	CFCC 53017	**MK432678**	**MK578071**	**MK578147**
Plagiostoma populinum	CBS 174.58	GU367074	GU367017	GU354000
	CBS 144.57	GU367075	GU367018	GU354001
Plagiostoma pulchellum	CBS 170.69	EU255043	KJ509941	GU353989
	CBS 126653	GU367063	GU367006	GU353987
Plagiostoma rhododendri	CBS 847.79	EU255044	GU367026	GU354009
Plagiostoma robergeanum	CBS 121472	EU255046	GU367029	GU354011
Plagiostoma rubrosporum	CBS 137267	KJ509962	KJ509942	KJ509953
Plagiostoma salicellum	CBS 126121	GU367037	GU366977	GU353961
	CBS 121466	EU254996	GU366978	GU353962
Plagiostoma salicicola	MFLUCC 13–0656	MF190161	NA	NA
Plagiostoma samuelsii	CBS 125668	GU367051	GU366993	GU353977
	LCM 596.01	GU367052	GU366994	GU353978
Plagiostoma triseptatum	CBS 137268	KJ509963	KJ509943	KJ509954
Plagiostoma tsukubense	CBS 137269	KJ509964	KJ509944	KJ509955
	CBS 137270	KJ509965	KJ509945	KJ509956
Plagiostoma versatile	CBS 124978	GU367038	GU366979	GU393963
	LCM 598.01	GU367040	GU366981	GU393965
Plagiostoma yunnanense	LCM 513.02	GU367036	GU366976	GU353960
	CBS 124979	GU367035	GU366975	GU353959

Note: NA, not applicable. Strains in this study are marked in bold.

and Michalak 2012), using the ML + rapid bootstrap setting and the GTRGAMMA substitution model with 1000 bootstrap replicates. BI was performed using a Markov Chain Monte Carlo (MCMC) algorithm in MrBayes v. 3.0b4 (Ronquist and Huelsenbeck 2003). Two MCMC chains, started from random trees for 1,000,000 generations and trees, were sampled every 100th generation, resulting in a total of 10,000 trees. The first 25% of trees were discarded as burn-in of each analysis. Branches with significant Bayesian Posterior Probabilities (BPP) were estimated in the remaining 7500 trees. Phylogenetic trees were viewed with FigTree v.1.4.3 (Rambaut 2016) and processed by Adobe Illustrator CS5. Alignment and trees were deposited in TreeBASE (submission ID: S26271). The nucleotide sequence data of the new taxa have been deposited in GenBank (Tables 1–3).

Results

Phylogenetic analyses

The first sequences dataset for the ITS, LSU, *tef1*, and *rpb2* was analyzed to focus on Gnomoniaceae. The alignment included 45 taxa, including the outgroup sequences of *Melanconis marginalis* (Table 1). The aligned four-locus datasets included 3388 characters. Of these, 2180 characters were constant, 198 variable characters were parsimony-uninformative and 1010 characters were parsimony informative. The heuristic search using maximum parsimony (MP) generated 4 parsimonious trees (TL = 3241, CI = 0.539, RI = 0.672, RC = 0.362), from which one was selected (Fig. 1). In the phylogenetic tree, two strains form a well-supported clade (MP/ML/BI=100/100/1) sister to the species *Flavignomonia rhoigena* from *Rhus chinensis*.

The second dataset with ITS, *tef1* and *tub2* sequences were analyzed in combination to infer the interspecific relationships within *Gnomoniopsis*. The alignment included 36 taxa, including the outgroup sequences of *Apiognomonia veneta* and *Plagiostoma euphorbiae* (Table 2). The aligned three-locus datasets included 2481 characters. Of these, 1443 characters were constant, 186 variable characters were par-simony-uninformative and 852 characters were parsimony informative. The heuristic search using maximum parsimony (MP) generated one parsimonious tree (TL = 2644, CI = 0.620, RI = 0.781, RC = 0.485), which is shown in Fig. 2. In the phylogenetic tree, three strains form a well-supported clade (MP/ML/BI=100/100/1) that does not include any previously described species.

The third dataset with ITS, *tef1* and *tub2* sequences were analyzed in combination to infer the interspecific relationships within *Plagiostoma*. The alignment included 48 taxa, including the outgroup sequences of *Apiognomonia errabunda* (Table 3). The aligned three-locus datasets included 2311 characters. Of these, 1556 characters were constant, 204 variable characters were parsimony-uninformative and 551

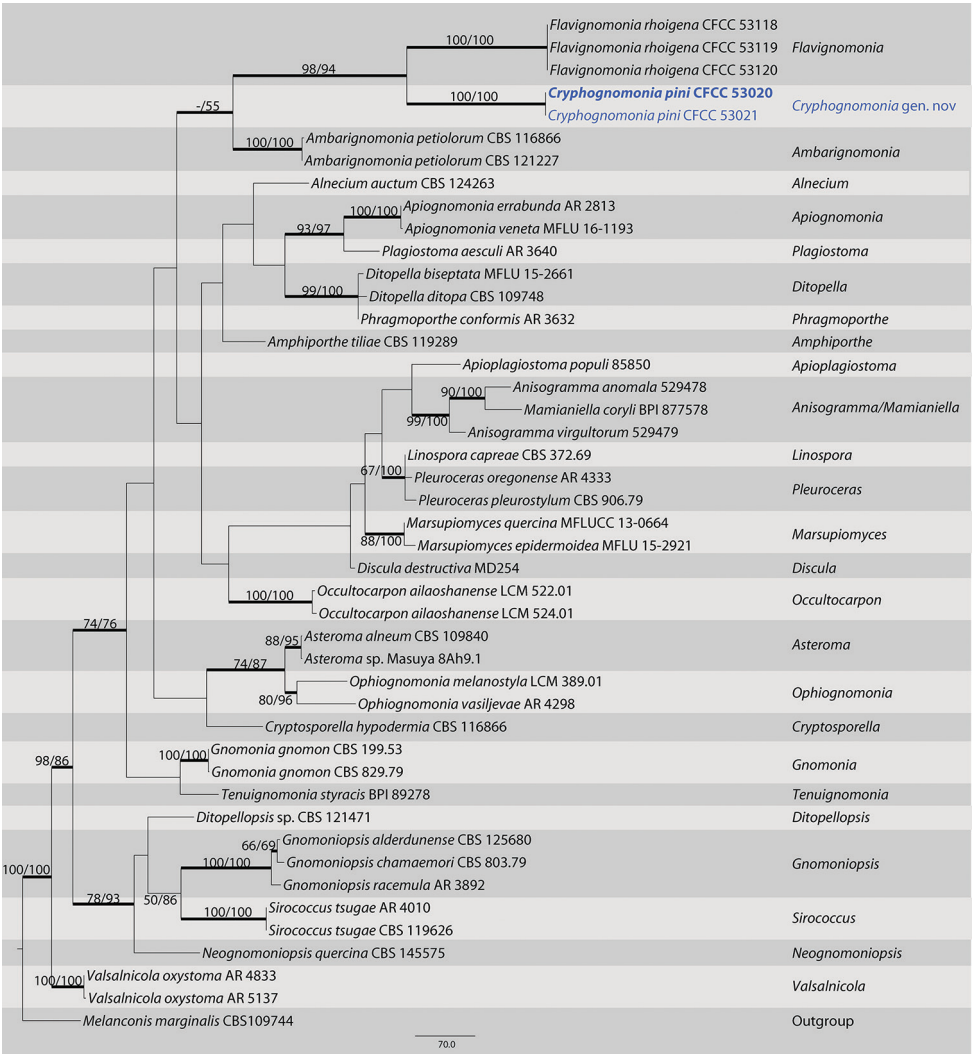

Figure 1. Maximum parsimony phylogram of Gnomoniaceae based on a combined matrix of ITS, LSU, *tef1* and *rpb2* genes. The MP and ML bootstrap support values above 50% are shown at the first and second position, respectively. Thickened branches represent posterior probabilities above 0.90 from BI. Scale bar: 80 nucleotide substitutions. Strains in this study are in blue and ex-type strains are in blod.

characters were parsimony informative. The heuristic search using maximum parsimony (MP) generated 6 parsimonious trees (TL = 1462, CI = 0.685, RI = 0.779, RC = 0.534), from which one was selected (Fig. 3). In the phylogenetic tree, four strains from this study group in a well-supported clade with *Plagiostoma populinum*. The topologies resulting from MP, ML and BI analyses of the concatenated dataset were congruent.

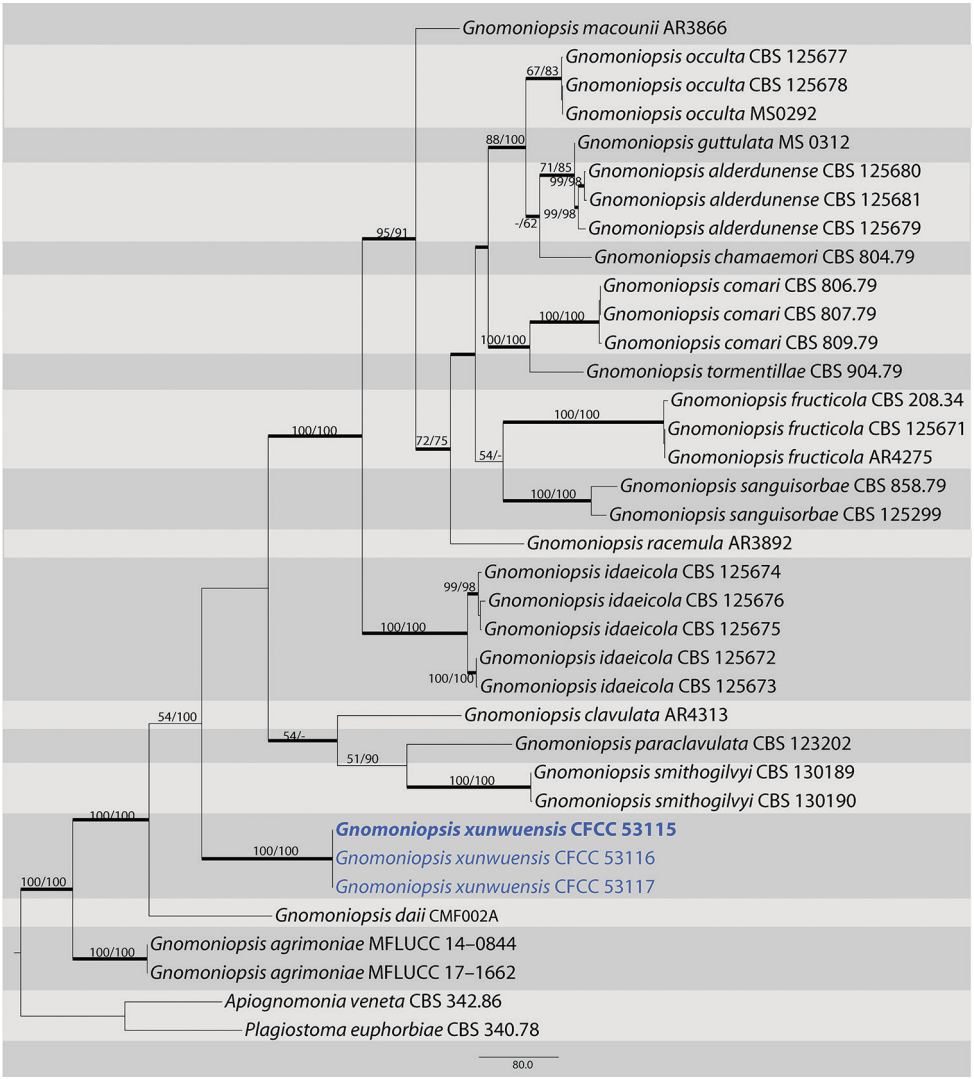

Figure 2. Maximum parsimony phylogram of *Gnomoniosis* based on a combined matrix of ITS, *tef1-α* and *tub2* genes. The MP and ML bootstrap support values above 50% are shown at the first and second position, respectively. Thickened branches represent posterior probabilities above 0.90 from BI. Scale bar: 80 nucleotide substitutions. Strains in this study are in blue and ex-type strains are in blod.

Taxonomy

Cryphognomonia **C.M. Tian & N. Jiang, gen. nov.**
MycoBank No: 829509

Etymology. *Crypho* + *gnomonia*, referring to the cryptic stromata on hosts.

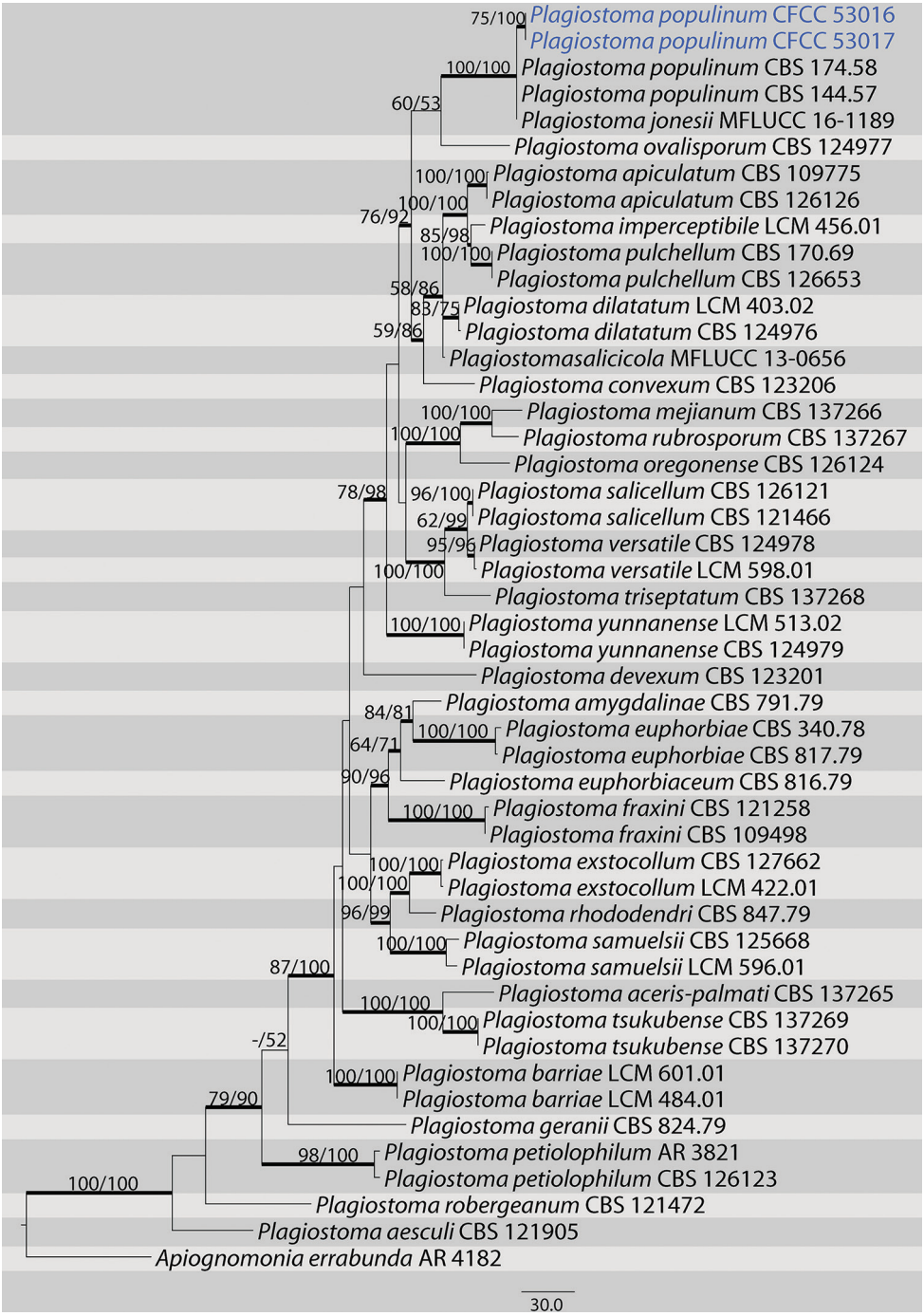

Figure 3. Maximum parsimony phylogram of *Plagiostoma* based on a combined matrix of ITS, *tef1-α* and *tub2* genes. The MP and ML bootstrap support values above 50% are shown at the first and second position, respectively. Thickened branches represent posterior probabilities above 0.90 from BI. Scale bar: 30 nucleotide substitutions. Strains in this study are in blue.

Type species. *Cryphognomonia pini* C.M. Tian & N. Jiang

Description. ***Pseudostromata*** erumpent, causing a pustulate bark surface. ***Central column*** yellowish to brownish. ***Stromatic zones*** lacking. ***Perithecia*** conspicuous, flask-shaped to spherical, umber to fuscous black, regularly scattered. ***Paraphyses*** deliquescent. ***Asci*** fusoid, 8-spored, biseriate, with an apical ring. ***Ascospores*** hyaline, clavate to cylindrical, smooth, multi-guttulate, symmetrical to asymmetrical, straight to slightly curved, bicellular, with a median septum distinctly constricted, with distinct hyaline sheath. ***Asexual morph*:** not observed.

Notes. *Cryphognomonia* was classified as a new genus in Gnomoniaceae throughout molecular data and the characteristics of sexual morph. Morphologically, *Cryphognomonia* can be distinguished from the other genera by pseudostromata and ascospores with obvious hyaline sheath.

Cryphognomonia pini **C.M. Tian & N. Jiang, sp. nov.**
MycoBank No: 829510
Figure 4

Diagnosis. *Cryphognomonia pini* differs from its closest phylogenetic neighbor, *F. rhoigena*, in ITS, LSU, *tef1* and *rpb2* loci based on the alignments deposited in TreeBASE.

Etymology. Named after the genus of the host plant from which the holotype was collected, *Pinus*.

Description. ***Pseudostromata*** erumpent, causing a pustulate bark surface, 650–1200 μm diam., containing up to 12 perithecia. ***Central column*** yellowish to brownish. ***Stromatic zones*** lacking. *Perithecia* conspicuous, flask-shaped to spherical, umber to fuscous black, regularly scattered, 350–600 μm diam. ***Paraphyses*** deliquescent. ***Asci*** fusoid, 8-spored, biseriate, with an apical ring, (60–)65–80(–90) × (21–)22–31(–35) μm. ***Ascospores*** hyaline, clavate to cylindrical, smooth, multi-guttulate, symmetrical to asymmetrical, straight to slightly curved, bicellular, with a median septum distinctly constricted, with distinct hyaline sheath, (15.5–)18–25(–27) × (8.5–)9.5–11.5(–12) μm. ***Asexual morph*:** not observed.

Culture characters. Cultures incubated on PDA at 25 °C in the dark, initially pale white, becoming olive-green after 3 wk. The colonies are flat, with regular margins; texture initially uniform, becoming compact after 1 month.

Specimens examined. China. Shaanxi Province: Ankang City, Huoditang forest farm, 33°26'7"N, 108°26'48"E, on branches of *Pinus armandii*, 8 June 2018, *N. Jiang* & *C.M. Tian* (holotype BJFC-S1725; ex-type living culture: CFCC 53020); 33°26'7"N, 108°26'48"E, on branches of *Pinus armandii*, 8 June 2018, *N. Jiang* & *C.M. Tian* (BJFC-S1726; living culture: CFCC 53021).

Notes. *Cryphognomonia pini* is the type species of *Cryphognomonia*, and occurs on *Pinus armandii* in China. Morphologically, *Cryphognomonia pini* is characterized based on bicellular ascospores with obvious hyaline sheath. In the phylogenetic tree, this species is most closely related to *F. rhoigena* (Fig. 1). However, *Cryphognomonia pini* can be

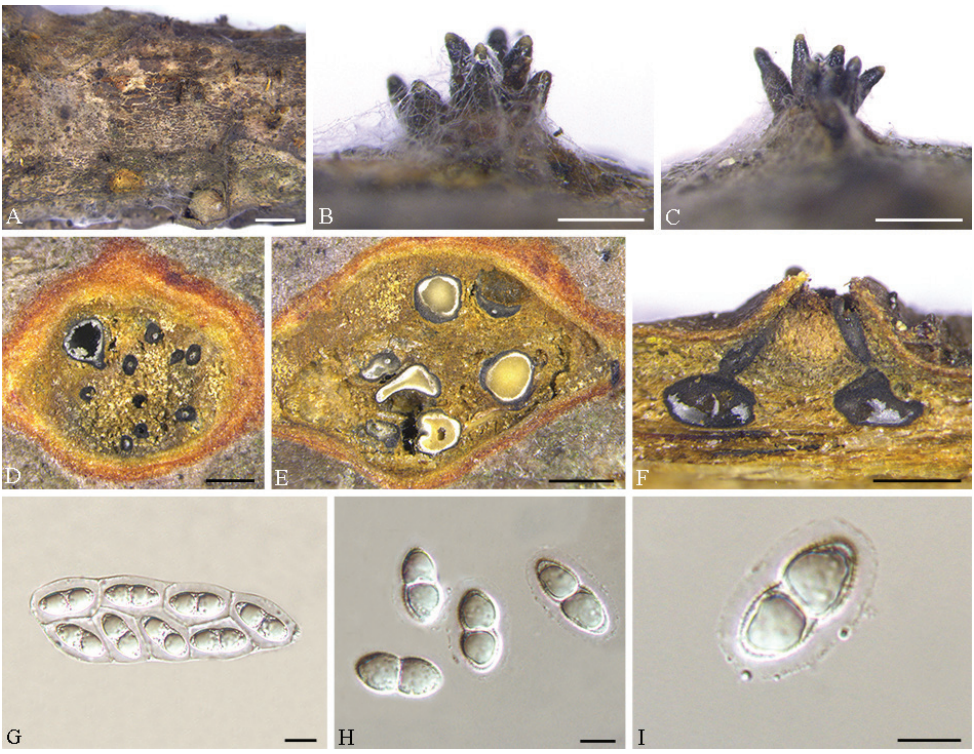

Figure 4. *Cryphognomonia pini* on *Pinus armandii* (BJFC-S1725) **A–C** habit of ascomata on twigs **D, E** transverse section of ascomata **F** longitudinal section through ascomata **G** asci **H, I** ascospores. Scale bars: 2 mm (**A**); 500 μm (**B–F**); 10 μm (**G–I**).

distinguished from *F. rhoigena* based on ITS, LSU, *tef1* and *rpb2* loci (73/512 in ITS, 4/775 in LSU, 186/437 in *tef1* and 90/1064 in *rpb2*).

Gnomoniopsis xunwuensis **C.M. Tian & Q. Yang, sp. nov.**
MycoBank No: 829529
Figure 5

Diagnosis. *Gnomoniopsis xunwuensis* differs from its closest phylogenetic neighbor, *G. daii*, in ITS, *tef1* and *tub2* loci based on the alignments deposited in TreeBASE.

Etymology. Named after the County (Xunwu), where the species was first collected.

Description. On PDA: ***Conidiomata*** pycnidial, (115–)130–210(–250) μm diam., globose, solitary to gregarious, or occasionally coalescing, deeply embedded in the medium, erumpent, brown to dark black. White to cream conidial drops exuding from the ostioles. ***Conidiophores*** (40–)43–58(–60.5) × 2–2.5(–3) μm, cylindrical, hyaline, phialidic, branched or sympodially branched, straight or slightly curved. ***Conidia*** oval or fusiform, straight to slightly curved, hyaline, multiguttules, (14–)16.5–20 × 4–5.5 μm.

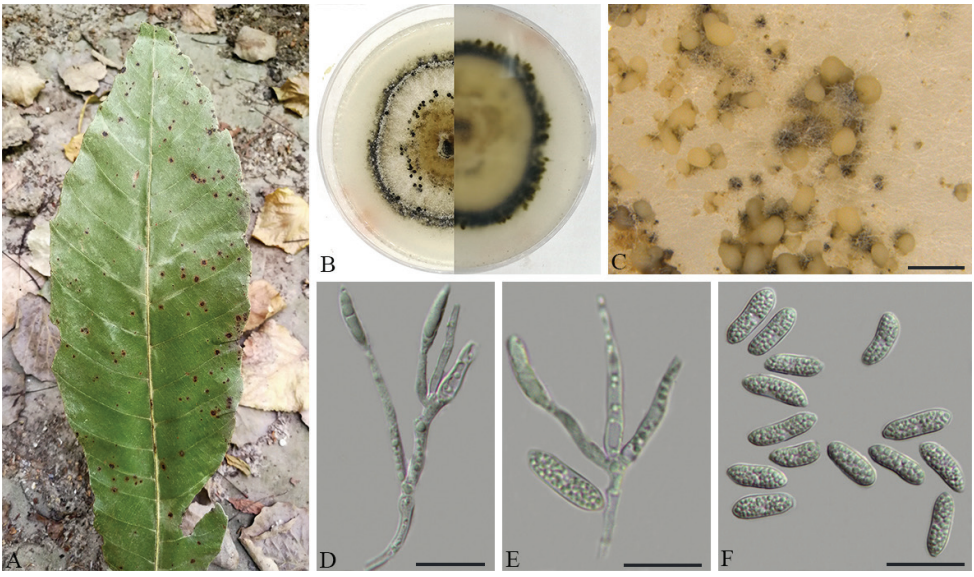

Figure 5. *Gnomoniopsis xunwuensis* on *Castanopsis fissa* (BJFC-S1688) **A** symptoms on leaves of host plant **B** the colony on PDA **C** conidiomata on PDA **D, E** conidiophores attached with condia **F** conidia. Scale bars: 500 μm (**C**); 20 μm (**D–F**).

Culture characters. Cultures incubated on PDA at 25 °C in the dark. Colony originally compact and flat with white aerial mycelium, then developing pale brown aerial mycelium at the center and blackish green mycelium at the marginal area, zonate with 2 well defined zones with regular edge; conidiomata dense, regularly distributed over agar surface.

Specimens examined. China. Jiangxi Province: Ganzhou City, Xunwu County, 24°40'50"N, 115°34'37"E, on leaves of *Castanopsis fissa*, 12 May 2018, *Q. Yang*, *Y. Liu* & *Y.M. Liang* (holotype BJFC-S1688; ex-type living culture: CFCC 53115); 24°52'20"N, 115°35'25"E, on leaves of *Castanopsis fissa*, 12 May 2018, *Q. Yang*, *Y. Liu* & *Y.M. Liang* (BJFC-S1689; living culture: CFCC 53116 and CFCC 53117).

Notes. *Gnomoniopsis xunwuensis* is associated with leaf spot of *Castanopsis fissa*, representing the first report from this host in China. It is characterized by sympodially branched conidiophore and oval or fusiform conidia. Morphologically, *G. xunwuensis* differs from *G. daii* in having bigger conidia (16.5–20 × 4–5.5 vs. 5.5–7 × 2–3.5 μm) (Jiang and Tian 2019). The phylogenetic inferences indicated this species as an individual well-supported clade (MP/ML/BI=100/100/1) in the genus *Gnomoniopsis* (Fig. 2).

***Plagiostoma populinum* (Fuckel) L.C. Mejía. Stud. Mycol. 68: 225. 2011.**
Figure 6

Description. See Butin (1958)

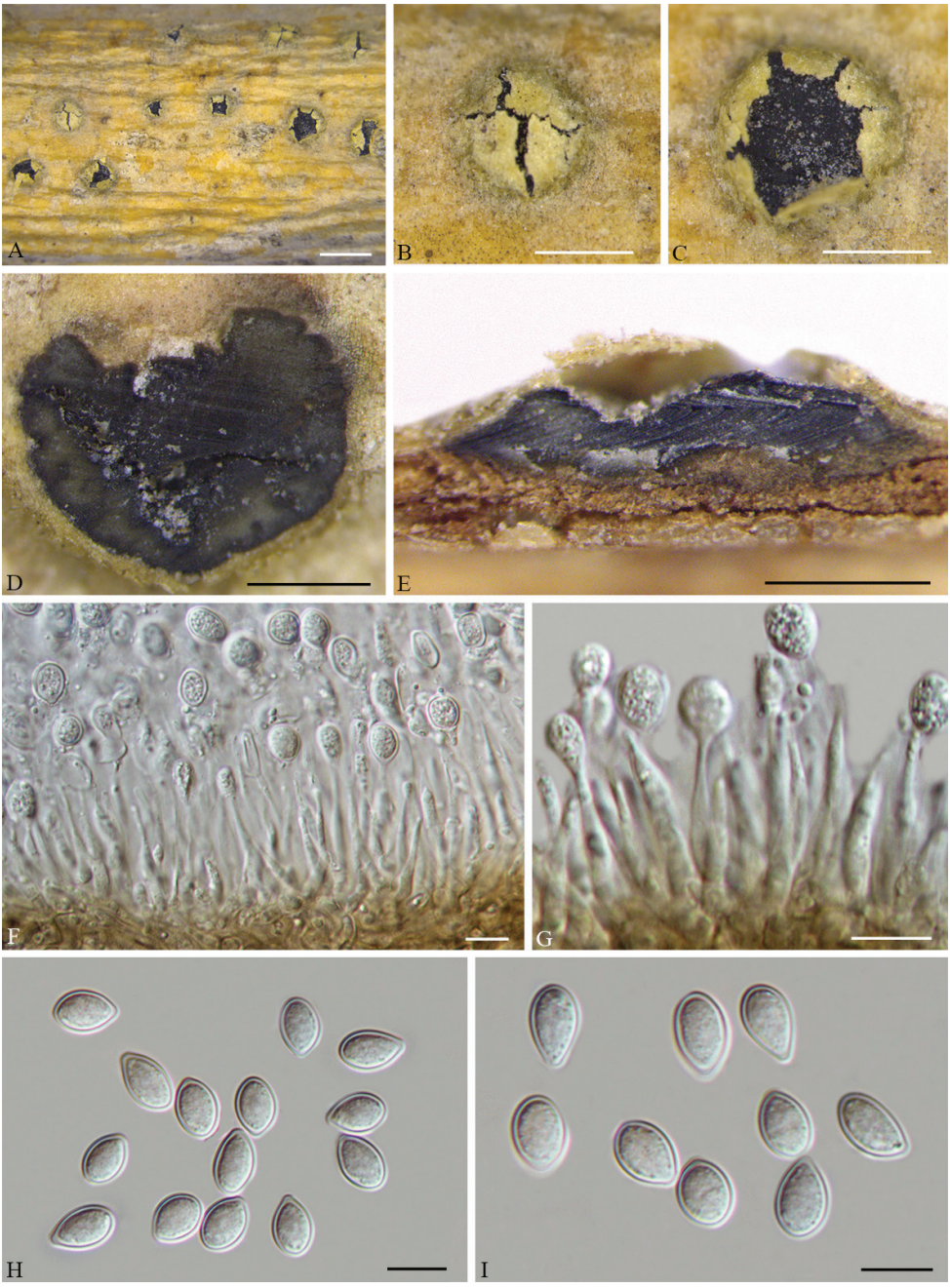

Figure 6. *Plagiostoma populinum* on *Populus tomentosa* (BJFC-S1724) **A–C** habit of conidiomata on twigs **D** transverse section through conidiomata **E** longitudinal section through conidiomata **F, G** conidiogenous cells attached with conidia **H, I** condia. Scale bars: 2 mm (**A**); 1 mm (**B, C**); 500 μm (**D, E**); 10 μm (**F–I**).

Specimens examined. China. Beijing: Haidian district, 40°31'55"N, 116°20'24"E, on branches of *Populus tomentosa*, 12 November 2017, *N. Jiang* (BJFC-S1724; living culture: CFCC 53016 and CFCC 53017).

Notes. *Plagiostoma populinum* is a common plant pathogenic fungus causing poplar canker in China. The current identification follows previous descriptions and records (Butin 1958). In the present study, two isolates (CFCC 53016 and CFCC 53017) from symptomatic branches of *Populus tomentosa* were congruent with *P. populinum* based on morphology and DNA sequences data (Fig. 3). We therefore describe *P. populinum* as a known species for this clade.

Discussion

In this study, three gnomoniaceous species were identified based on morphological and molecular phylogenetic analyses. As a result, *Cryphognomonia* typified with *C. pini* is proposed as a new genus in Gnomoniaceae for its distinct phylogenic position and distinctive sexual morphs. Also, *Gnomoniopsis xunwuensis* strains were successfully isolated from leaf spot of *Castanopsis fissa*, and were identified as a new species in *Gnomoniopsis*, which was typified by *Gnomoniopsis chamaemori* having pycnidia with hyaline, oval, one-celled conidia (Walker et al. 2010).

The type species of *Cryphognomonia*, *C. pini*, is unique through its developed pseudostromata and ascospores with distinct hyaline sheath. In the molecular phylogeny, *C. pini* is closely related to species of *F. rhoigena*. *Flavignomonia rhoigena* is characterized by the formation of synnemata and no sexual morph is known for this species (Jiang et al. 2019). However, *C. pini* can be easily distinguished from *F. rhoigena* based on ITS, LSU, *tef1* and *rpb2* loci. Therefore, the unique morphology in combination with an isolated phylogenetic position within Gnomoniaceae warrant the establishment of a new genus.

Most species of *Gnomoniopsis* show host preference or potentially limited host specificity to genera in the Fagaceae, Onagraceae and Rosaceae (Sogonov et al. 2008). In the present study, isolates were collected from leaf spot of *Castanopsis fissa*, and described as a novel pathogen depending on its asexual state, *G. xunwuensis*. Four taxa, *G. clavulata*, *G. daii*, *G. paraclavulata*, and *G. smithogilvyi*, have been found on Fagaceae host plants. However, *Gnomoniopsis xunwuensis* can be easily distinguished from the four species in conidial size (16.5–20 × 4–5.5 μm in *G. xunwuensis* vs. 5.0–8.0 × 2.0–4.0 μm in *G. clavulata* vs. 5.0–8.0 × 2.0–3.5 μm in *G. daii* vs. 6.0–9.5 × 2.0–3.5 μm in *G. paraclavulata* vs. 4.9–9.8 × 2.9–4.9 μm in *G. smithogilvyi*), as well as supported by molecular data (Walker et al. 2010; Crous et al. 2012; Visentin et al. 2012).

Plagiostoma populinum is regarded as the pathogen responsible for poplar canker. Butin (1958) presented a full description with illustrations of this species as *Cryptodiaporthe populea.* Mejía et al. (2011a) treated *C. populea* as a synonym of *P. populinum*

based on analyses of cultural and DNA sequence data. In this paper, *P. populinum* forms a highly supported monophyletic group (Fig. 3) characterized by having conidia with obvious hyaline sheath. It is the first time that we have been able to provide detailed morphological diagrams in China.

Acknowledgements

This study is financed by the Research Foundation of Education Bureau of Hunan Province, China (Project No.: 19B608), the introduction of talent research start-up fund project of CSUFT (Project No.: 2019YJ025) and National Natural Science Foundation of China (Project No.: 31670647). We are grateful to Chungen Piao, Minwei Guo (China Forestry Culture Collection Center (CFCC), Chinese Academy of Forestry, Beijing.

References

Butin H (1958) Über die auf *Salix* und *Populus* vorkommenden Arten der Gattung *Cryptodiaporthe* Petrak. Phytopathologische Zeitschrift 32: 399–415. https://doi.org/10.1111/j.1439-0434.1958.tb01783.x

Carbone I, Kohn LM (1999) A method for designing primer sets for speciation studies in filamentous ascomycetes. Mycologia 3: 553–556. https://doi.org/10.1080/00275514.1999.12061051

Crous PW, Carnegie AJ, Wingfield MJ, Sharma R, Mughini G, Noordeloos ME, Santini A, Shouche YS, Bezerra JDP, Dima B, Guarnaccia V, Imrefi I, Jurjević Ž, Knapp DG, Kovács GM, Magistà D, Perrone G, Rämä T, Rebriev YA, Shivas RG, Singh SM, Souza-Motta CM, Thangavel R, Adhapure NN, Alexandrova AV, Alfenas AC, Alfenas RF, Alvarado P, Alves AL, Andrade DA, Andrade JP, Barbosa RN, Barili A, Barnes CW, Baseia IG, Bellanger J-M, Berlanas C, Bessette AE, Bessette AR, Biketova AYu, Bomfim FS, Brandrud TE, Bransgrove K, Brito ACQ, Cano-Lira JF, Cantillo T, Cavalcanti AD, Cheewangkoon R, Chikowski RS, Conforto C, Cordeiro TRL, Craine JD, Cruz R, Damm U, de Oliveira RJV, de Souza JT, de Souza HG, Dearnaley JDW, Dimitrov RA, Dovana F, Erhard A, Esteve-Raventós F, Félix CR, Ferisin G, Fernandes RA, Ferreira RJ, Ferro LO, Figueiredo CN, Frank JL, Freire KTLS, García D, Gené J, Gęsiorska A, Gibertoni TB, Gondra RAG, Gouliamova DE, Gramaje D, Guard F, Gusmão LFP, Haitook S, Hirooka Y, Houbraken J, Hubka V, Inamdar A, Iturriaga T, Iturrieta-González I, Jadan M, Jiang N, Justo A, Kachalkin AV, Kapitonov VI, Karadelev M, Karakehian J, Kasuya T, Kautmanová I, Kruse J, Kušan I, Kuznetsova TA, Landell MF, Larsson K-H, Lee HB, Lima DX, Lira CRS, Machado AR, Madrid H, Magalhães OMC, Majerova H, Malysheva EF, Mapperson RR, Marbach PAS, Martín MP, Martín-Sanz A, Matočec N, McTaggart AR, Mello JF, Melo RFR, Me&353;ič A, Michereff SJ, Miller AN, Minoshima A, Molinero-Ruiz L, Morozova OV, Mosoh D, Nabe M, Naik R, Nara K, Nascimento SS, Neves RP, Olariaga I, Oliveira RL, Oliveira TGL, Ono T, Ordoñez ME, de M Ottoni A, Paiva LM, Pancorbo F, Pant B,

Pawłowska J, Peterson SW, Raudabaugh DB, Rodríguez-Andrade E, Rubio E, Rusevska K, Santiago ALCMA, Santos ACS, Santos C, Sazanova NA, Shah S, Sharma J, Silva BDB, Siquier JL, Sonawane MS, Stchigel AM, Svetasheva T, Tamakeaw N, Telleria MT, Tiago PV, Tian CM, Tkalčec Z, Tomashevskaya MA, Truong HH, Vecherskii MV, Visagie CM, Vizzini A, Yilmaz N, Zmitrovich IV, Zvyagina EA, Boekhout T, Kehlet T, Læssøe T, Groenewald JZ (2019) Fungal Planet description sheets: 868–950. Persoonia 42: 291–473. https://doi.org/10.3767/persoonia.2019.42.11

Crous PW, Summerell BA, Shivas RG, Burgess TI, Decock CA, Dreyer LL, Granke LL, Guest DI, Hardy GESTJ, Hausbeck MK, Hüberli D, Jung T, Koukol O, Lennox CL, Liew ECY, Lombard L, McTaggart AR, Pryke JS, Roets F, Saude C, Shuttleworth LA, Stukely MJC, Vánky K, Webster BJ, Windstam ST, Groenewald JZ (2012) Fungal Planet description sheets: 107–127. Persoonia 28: 138–182. https://doi.org/10.3767/003158512X652633

Doyle JJ, Doyle JL (1990) Isolation of plant DNA from fresh tissue. Focus 12: 13–15. https://doi.org/10.2307/2419362

Fan XL, Du Z, Hyde KD, Liang YM, Pan YP, Tian CM (2016) *Cryptosporella platyphylla*, a new species associated with *Betula platyphylla* in China. Phytotaxa 253: 285–292. https://doi.org/10.11646/phytotaxa.253.4.4

Glass NL, Donaldson GC (1995) Development of primer sets designed for use with the PCR to amplify conserved genes from filamentous ascomycetes. Applied and Environmental Microbiology 61: 1323–1330. https://doi.org/10.1128/AEM.61.4.1323-1330.1995

Gong S, Zhang X, Jiang S, Chen C, Ma HB, Nie Y (2017) A new species of *Ophiognomonia* from Northern China inhabiting the lesions of chestnut leaves infected with *Diaporthe eres*. Mycological progress 16: 83–91. https://doi.org/10.1007/s11557-016-1255-z

Guindon S, Dufayard JF, Lefort V, Anisimova M, Hordijk W, Gascuel O (2010) New algorithms and methods to estimate maximum-likelihood phylogenies: assessing the performance of PhyML 3.0. Systematic Biology 59: 307–321. https://doi.org/10.1093/sysbio/syq010

Hall T (1999) BioEdit: a user-friendly biological sequence alignment editor and analysis program for Windows 95/98/NT. Nucleic Acids Symposium Series 41: 95–98.

Jiang N, Tian CM (2019) An Emerging Pathogen from Rotted Chestnut in China: *Gnomoniopsis daii* sp. nov. Forests 10: 1016. https://doi.org/10.3390/f10111016

Jiang N, Yang Q, Liang YM, Tian CM (2019) Taxonomy of two synnematal fungal species from *Rhus chinensis*, with *Flavignomonia* gen. nov. described. MycoKeys 60: 17–29. https://doi.org/10.3897/mycokeys.60.46395

Katoh K, Toh H (2010) Parallelization of the MAFFT multiple sequence alignment program. Bioinformatics 26: 1899–1900. https://doi.org/10.1093/bioinformatics/btq224

Liu YJ, Whelen S, Hall BD (1999) Phylogenetic relationships among ascomycetes: evidence from an RNA polymerse II subunit. Molecular Biology and Evolution 16: 1799–1808. https://doi.org/10.1093/oxfordjournals.molbev.a026092

Mejía LC, Castlebury LA, Rossman AY, Sogonov MV, White JF (2008) Phylogenetic placement and taxonomic review of the genus *Cryptosporella* and its synonyms *Ophiovalsa* and *Winterella* (Gnomoniaceae, Diaporthales). Mycological Research 112: 23–35. https://doi.org/10.1016/j.mycres.2007.03.021

Mejía LC, Castlebury LA, Rossman AY, Sogonov MV, White JF (2011a) A systematic account of the genus *Plagiostoma* (Gnomoniaceae, Diaporthales) based on morphology, host-associations, and a four-gene phylogeny. Studies in Mycology 68: 211–235. https://doi.org/10.3114/sim.2011.68.10

Mejía LC, Rossman AY, Castlebury LA, White JF (2011b) New species, phylogeny, host-associations and geographic distribution of genus *Cryptosporella* (Gnomoniaceae, Diaporthales). Mycologia 103: 379–399. https://doi.org/10.3852/10-134

Mejía LC, Rossman AY, Castlebury LA, Yang ZL, White JF (2012) *Occultocarpon*, a new monotypic genus of Gnomoniaceae on *Alnus nepalensis* from China. Fungal Diversity 52: 99–105. https://doi.org/10.1007/s13225-011-0108-y

Minoshima A, Walker DM, Takemoto S, Hosoya T, Walker AK, Ishikawa S, Hirooka Y (2019) Pathogenicity and taxonomy of *Tenuignomonia styracis* gen. et sp. nov., a new monotypic genus of Gnomoniaceae on *Styrax obassia* in Japan. Mycoscience 60: 31–39. https://doi.org/10.1016/j.myc.2018.08.001

Monod M (1983) Monographie taxonomique des Gnomoniaceae (Ascomycétes de l'ordre des Diaporthales I). Beihefte zur Sydowia 9: 1–315.

O'Donnell K, Cigelnik E (1997) Two divergent intragenomic rDNA ITS2 types within a monophyletic lineage of the fungus Fusarium are nonorthologous. Molecular Phylogenetics and Evolution 7: 103–116. https://doi.org/10.1006/mpev.1996.0376

Rambaut A (2016) FigTree, version 1.4.3. University of Edinburgh, Edinburgh.

Rayner RW (1970) A mycological colour chart. Commonwealth Mycological Institute, Kew.

Rehner SA (2001) EF1 alpha primers. http//ocid.nacse.org/research/deephyphae/EF1primer.pdf

Ronquist F, Huelsenbeck JP (2003) MrBayes 3: Bayesian phylogenetic inference under mixed models. Bioinformatics 19: 1572–1574. https://doi.org/10.1093/bioinformatics/btg180

Rossman AY, Farr DF, Castlebury LA (2007) A review of the phylogeny and biology of the Diaporthales. Mycoscience 48: 135–144. https://doi.org/10.1007/S10267-007-0347-7

Senanayake IC, Jeewon R, Chomnunti P, Wanasinghe DN, Norphanphoun C, Karunarathna A, Pem D, Perera RH, Camporesi E, McKenzie EHC, Hyde KD, Karunarathna SC (2018) Taxonomic circumscription of Diaporthales based on multigene phylogeny and morphology. Fungal Diversity 93: 241–443. https://doi.org/10.1007/s13225-018-0410-z

Silvestro D, Michalak I (2012) raxmlGUI: a graphical front-end for RAxML. Organisms Diversity and Evolution 12: 335–337. https://doi.org/10.1007/s13127-011-0056-0

Sogonov MV, Castlebury LA, Rossman AY, Mejía LC, White JF (2008) Leaf-inhabiting genera of the Gnomoniaceae, Diaporthales. Studies in Mycology 62: 1–77. https://doi.org/10.3114/sim.2008.62.01

Stamatakis E (2006) RAxML-VI-HPC: maximum likelihood-based phylogenetic analyses with thousands of taxa and mixed models. Bioinformatics 22: 2688–2690. https://doi.org/10.1093/bioinformatics/btl446

Swofford DL (2003) PAUP*: Phylogenetic Analyses Using Parsimony (*and other methods). Version 4.0b10. Sinauer Associates, Sunderland.

Vilgalys R, Hester M (1990) Rapid genetic identification and mapping of enzymatically amplified ribosomal DNA from several Cryptococcus species. Journal of Bacteriology 172: 4238–4246. https://doi.org/10.1128/JB.172.8.4238-4246.1990

Vilgalys R, Sun BL (1994) Ancient and recent patterns of geographic speciation in the oyster mushroom Pleurotus revealed by phylogenetic analysis of ribosomal DNA sequences. Proceedings of the National Academy of Science USA 91: 4599–4603. https://doi.org/10.1073/pnas.91.10.4599

Visentin I, Gentile S, Valentino D, Gonthier P, Cardinale F (2012) *Gnomoniopsis castanea* sp. nov. (Gnomoniaceae, Diaporthales) as the causal agent of nut rot in sweet chestnu. Journal of Plant Pathology 94: 411–419.

Walker DM (2012) Taxonomy, systematics, ecology, and evolutionary biology of the Gnomoniaceae (Diaporthales), with emphasis on *Gnomoniopsis* and *Ophiognomonia*. Rutgers The State University of New Jersey-New Brunswick.

Walker DM, Castlebury LA, Rossman AY, Mejía LC, White JF (2012) Phylogeny and taxonomy of *Ophiognomonia* (Gnomoniaceae, Diaporthales), including twenty-five new species in this highly diverse genus. Fungal Diversity 57: 85–147. https://doi.org/10.1007/s13225-012-0200-y

Walker DM, Castlebury LA, Rossman AY, Sogonov MV, White JF (2010) Systematics of genus *Gnomoniopsis* (Gnomoniaceae, Diaporthales) based on a three gene phylogeny, host associations and morphology. Mycologia 102: 1479–1496. https://doi.org/10.3852/10-002

Walker DM, Castlebury LA, Rossman AY, Struwe L (2013) Host conservatism or host specialization? Patterns of fungal diversification are influenced by host plant specificity in *Ophiognomonia* (Gnomoniaceae: Diaporthales). Biological Journal of the Linnean Society 111: 1–16. https://doi.org/10.1111/bij.12189

White TJ, Bruns T, Lee S, Taylor JM (1990) Amplification and direct sequencing of fungal ribosomal RNA genes for phylogenetics. PCR Protocols: A Guide to Methods and Applications 18: 315–322. https://doi.org/10.1016/B978-0-12-372180-8.50042-1

MycoKeys 69: 91–109 (2020)
doi: 10.3897/mycokeys.69.49437
http://mycokeys.pensoft.net

RESEARCH ARTICLE

A peer-reviewed open-access journal
MycoKeys
Launched to accelerate biodiversity research

Three new species of *Cortinarius* subgenus *Telamonia* (Cortinariaceae, Agaricales) from China

Meng-Le Xie[1,2], Tie-Zheng Wei[3], Yong-Ping Fu[2], Dan Li[2], Liang-Liang Qi[4], Peng-Jie Xing[2], Guo-Hui Cheng[5,2], Rui-Qing Ji[2], Yu Li[2,1]

1 *Life Science College, Northeast Normal University, Changchun 130024, China* **2** *Engineering Research Center of Edible and Medicinal Fungi, Ministry of Education, Jilin Agricultural University, Changchun 130118, China* **3** *State Key Laboratory of Mycology, Institute of Microbiology, Chinese Academy of Sciences, Beijing 100101, China* **4** *Microbiology Research Institute, Guangxi Academy of Agriculture Sciences, Nanning, 530007, China* **5** *College of Plant Protection, Shenyang Agricultural University, Shenyang 110866, China*

Corresponding authors: Rui-Qing Ji (jiruiqingjrq@126.com), Yu Li (yuli966@126.com)

Academic editor: O. Raspé | Received 16 December 2019 | Accepted 23 June 2020 | Published 14 July 2020

Citation: Xie M-L, Wei T-Z, Fu Y-P, Li D, Qi L-L, Xing P-J, Cheng G-H, Ji R-Q, Li Y (2020) Three new species of *Cortinarius* subgenus *Telamonia* (Cortinariaceae, Agaricales) from China. MycoKeys 69: 91–109. https://doi.org/10.3897/mycokeys.69.49437

Abstract

Cortinarius is an important ectomycorrhizal genus that forms a symbiotic relationship with certain trees, shrubs and herbs. Recently, we began studying *Cortinarius* in China and here we describe three new species of *Cortinarius* subg. *Telamonia* based on morphological and ecological characteristics, together with phylogenetic analyses. *Cortinarius laccariphyllus* **sp. nov.** (section *Colymbadini*) is associated with broadleaf trees, with strongly hygrophanous basidiomata, special *Laccaria*-like lamellae and white and extremely sparse universal veil. *Cortinarius neotorvus* **sp. nov.** (section *Telamonia*) is associated with broadleaf trees and is easily confused with *C. torvus*, but can be distinguished by the colour of the fresh basidiomes and the stipe usually somewhat tapering towards the base. *Cortinarius subfuscoperonatus* **sp. nov.** (section *Fuscoperonati*) is associated with coniferous trees, with subglobose to broadly ellipsoid spores and is closely related to *C. fuscoperonatus*. A key to the new species and similar species in sections *Colymbadini*, *Telamonia* and *Fuscoperonati* is provided.

Keywords

Ectomycorrhizal fungi, morphology, phylogeny, taxonomy

Introduction

Cortinarius (Pers.) Gray is one of the most species-rich agaric genera, with reportedly more than 2250 species worldwide (He et al. 2019). While most of the *Cortinarius* species were described from Europe and North America, there are also some species described from Oceania (e.g. Bougher and Hilton 1989; Soop 2005; Gasparini and Soop 2008), South America (e.g. Valenzuela and Esteve-Raventos 1994; Garnica et al. 2003; San-Fabian et al. 2018) and Asia (e.g. Miyauchi 2001; Peintner et al. 2003; Xie et al. 2019). It was assumed that more than 900 species occur in northern European countries, based on phylogenetic studies (Niskanen et al. 2012). At least 500 *Cortinarius* species were reported in North America (Bessette et al. 1997). Only 229 *Cortinarius* species have been reported in China (Teng 1963; Tai 1979; Shao and Xiang 1997; Wei and Yao 2013; Li et al. 2015; Xie 2018; Xie et al. 2019; Cheng et al. 2019; Wei and Liu 2019). Recently, many new species have been described, based on the phylogenetic analyses, together with morphological and ecological data (e.g. Bojantchev and Davis 2011; Wei and Yao 2013; Harrower et al. 2015; Brandrud et al. 2018a). Many studies showed that nrDNA ITS barcodes are typically effective in distinguishing *Cortinarius* species (e.g. Liimatainen et al. 2014; Garnica et al. 2016; Schmidt-Stohn et al. 2017; Brandrud et al. 2018b).

Previously, phylogenetic studies of *Cortinarius* have shown that many traditional infrageneric groups are artificial (Høiland & Holst-Jensen 2000; Garnica et al. 2003; Garnica et al. 2005; Niskanen 2008; Harrower et al. 2011), based on ITS+LSU datasets or only ITS datasets. *Cortinarius* subg. *Telamonia* (Fr.) Trog sensu lato was a traditional subgenus, based on moist to dry, strongly to weakly hygrophanous and often brown coloured pileus (Brandrud et al. 1989; Bidaud et al. 1994). Some species in traditional subgenus *Telamonia* sensu lato were classified into other subgenera and several new sections in subgenus *Telamonia* sensu stricto, based on phylogenetic studies (Niskanen et al. 2015; Soop et al. 2019). Sections *Colymbadini* Melot, *Fuscoperonati* Liimat. & Niskanen and *Telamonia* (Fr.) Gillot & Lucand, all belonging to subgenus *Telamonia* sensu stricto, are included in this paper.

The diverse ecosystems in China provide a conducive environment for the growth of *Cortinarius* species. Research, dedicated to the phylogeny and taxonomy of Chinese *Cortinarius*, was initiated in recent years. During field trips in the past years, many specimens of *Cortinarius* were collected from China. However, only two new *Cortinarius* species have been described and reported, based on Chinese specimens until now (Wei and Yao 2013; Xie et al. 2019). There are still many species that have never been reported according to the phylogenetic analyses, based on our materials. Further efforts are necessary to describe these species and reveal the species diversity of *Cortinarius* in China. In this study, three new species of the subgenus *Telamonia* sensu stricto were described, based on morphological and ecological characteristics, as well as phylogenetic analyses. An identification key to the new species and similar species in sections *Colymbadini*, *Telamonia* and *Fuscoperonati* is provided.

Materials and methods

Sampling and morphological studies

We collected specimens from northeast China and northwest China, two important floristic areas of China. Fresh basidiomata were photographed and noted under daylight in the field, dried in an oven at about 50 °C and deposited in the Herbarium of Mycology, Jilin Agricultural University (HMJAU).

The macroscopic characters were described from fresh basidiomata. Colour codes were taken from Kornerup and Wanscher (1978). The microscopic characters were examined from dried specimens mounted in 5% aqueous potassium hydroxide (KOH) and Melzer's reagent using a Zeiss AX10 light microscope with a high-resolution 100× objective. Twenty to thirty mature basidiospores were measured (excluding apiculus and ornamentation) from each collection. The length/width ratio (Q) was calculated for individual spores. `X and `Q refer to the average value of basidiospores of each specimen. The basidia (ten basidia per collection), sterile cells of lamellar edge (20 sterile cells per collection) and hyphae of the lamellar trama were examined and measured from the pieces of lamellae. The pileipellis structure was studied from radial sections half-way from the pileus centre. Basidiospores, lamellar margin cells of this new species were photographed.

DNA extraction, PCR amplification and sequencing

We extracted the DNA from fresh tissue dried in silica gel by the NuClean PlantGen DNA Kit (CWBIO, China) and amplified the ITS region with primers ITS1F and ITS4 (White et al. 1990; Gardes and Bruns 1993).The PCR amplification progress followed Xie et al. (2019) and was sequenced by Sangon Biotech (Shanghai) Co. Ltd. The newly generated ITS sequences have been submitted to GenBank.

Data analysis

BLAST searches with the newly-generated ITS sequences were performed against NCBI (https://www.ncbi.nlm.nih.gov/) and UNITE (https://unite.ut.ee/) databases to retrieve similar sequences for the phylogenetic analyses (Table 1). *C. armillatus* (Fr.: Fr.) Fr. and *C. paragaudis* Fr. of section *Armillati* Kühner & Romagn. ex M.M. Moser, Schweiz. Z. Pilzk. were chosen as outgroup. Section *Armillati* belongs to subgenus *Telamonia* sensu stricto and is separated from other sections (Niskanen 2008; Niskanen et al. 2011).

All ITS sequences were aligned and edited with BioEdit 7.0.9 (Hall 1999). ITS1 and ITS2 were delimited by comparison with the sequence KC608590, which is fully an-

Table 1. ITS sequences used in the phylogenetic analysis. New species in bold.

Species	Voucher	GenBank accession No.	Locality	Reference
C. agathosmus TYPE	CFP536	KC608590	Sweden	Niskanen et al. (2013a)
C. ahsii TYPE	MM19650703 (IB)	KX882644	USA	Ammirati et al. (2017)
C. ahsii	JFA10303 (WTU)	KX882649	USA	Ammirati et al. (2017)
C. alboviolaceus	HMJAU44214	MK552393	China	This study
C. alboviolaceus	HMJAU44245	MK234572	China	Xie et al. (2019)
C. alboviolaceus	HMJAU44347	MK552392	China	This study
C. alboviolaceus	F15809	FJ157005	Canada	Harrower et al. (2011)
C. armeniacus	HMJAU44408	MK552394	China	This study
C. armeniacus	F16352	FJ039573	Canada	Harrower et al. (2011)
C. armillatus TYPE	F256861 (S)	NR131891	Sweden	Kytövuori et al. (2005)
C. bulliardii	CFP499 (S)	JX114942	Sweden	Ammirati et al. (2013)
C. caesioarmeniacus TYPE	H7000901	KP137498	Canada	Liimatainen (2014)
C. caesioarmeniacus	HMJAU44409	MK552396	China	This study
C. caesioarmeniacus	HMJAU44403	MK552395	China	This study
C. cinnabarinus	IK85-1517 (H)	JX114943	Finland	Ammirati et al. (2013)
C. cinnabarinus TYPE	CFP379 (S)	JX114944	Sweden	Ammirati et al. (2013)
C. coccineus TYPE	435745 (GK)	JX114945	France	Ammirati et al. (2013)
C. colynbadinus	CFP1130 (S)	JX127302	Sweden	Ammirati et al. (2013)
C. colynbadinus TYPE	F248443 (S)	NR131819	Sweden	Ammirati et al. (2013)
C. fructuodorus	TN09-113	KC608582	USA	Niskanen et al. (2013a)
C. fructuodorus TYPE	H7001104	NR131827	USA	Niskanen et al. (2013a)
C. fuscoperonatus	SSt16-046	MF139754	Sweden	Schmidt-Stohn et al. (2017)
C. fuscoperonatus	CFP1470	JX407330	France	Niskanen et al. (2013b)
C. fuscoperonatus	CFP505	EU433390	Sweden	GenBank/Liimatainen
C. laccariphyllus	**HMJAU44449**	**MK552380**	**China**	**This study**
C. laccariphyllus	**HMJAU44450**	**MK552381**	**China**	**This study**
C. millaresensis	XC2011-200	MH784748	France	Bidaud et al. (2017)
C. millaresensis	XC2013-163	MH784752	France	Bidaud et al. (2017)
C. nolaneiformis	DB886 (BP)	KJ206487	Hungary	Dima et al. (2014)
C. nolaneiformis TYPE	PRM857042	NR131833	Czech Republic	Dima et al. (2014)
C. paragaudis TYPE	F256858 (S)	NR131814	Norway	Niskanen et al. (2011)
C. privignofulvus TYPE	AB00-10-128 (PC)	MH784703	France	Bidaud et al. (2017)
C. privignofulvus	AB04-09-192	MH784714	France	Bidaud et al. (2017)
C. neotorvus	**HMJAU44438**	**MK552383**	**China**	**This study**
C. neotorvus	**HMJAU44441**	**MK552384**	**China**	**This study**
C. neotorvus	**HMJAU44442**	**MK552385**	**China**	**This study**
C. neotorvus	**HMJAU44443**	**MK552386**	**China**	**This study**
C. neotorvus	**HMJAU44437**	**MK552382**	**China**	**This study**
C. rigidipes TYPE	MM1962/0062 (IB)	KJ206504	Switzerland	Dima et al. (2014)
C. rigidipes	IK95-1873 (H)	KJ206506	Germany	Dima et al. (2014)
C. subargyronotus TYPE	H7018127	KP137494	Sweden	Liimatainen (2014)
C. subfuscoperonatus	**HMJAU44446**	**MK552389**	**China**	**This study**
C. subfuscoperonatus	**HMJAU44447**	**MK552390**	**China**	**This study**
C. subfuscoperonatus	**HMJAU44445**	**MK552388**	**China**	**This study**
C. subfuscoperonatus	**HMJAU44444**	**MK552387**	**China**	**This study**
C. subfuscoperonatus	**HMJAU44448**	**MK552391**	**China**	**This study**
C. torvus	TUB 011515	AY669668	Germany	Garnica et al. (2005)
C. torvus	IK98-1973	JX407337	Denmark	Niskanen et al. (2013b)
C. torvus	TF01-035	AJ889977	Denmark	GenBank/Kjoller
C. turgidoides	AB15-09-37	MH784723	France	Bidaud et al. (2017)

Species	Voucher	GenBank accession No.	Locality	Reference
C. turgidoides	AB07-09-121	MH784717	France	Bidaud et al. (2017)
C. uraceomajalis	DB2291 (BP)	KJ206511	Hungary	Dima et al. (2014)
C. uraceomajalis	DB2283 (BP)	KJ206510	Hungary	Dima et al. (2014)
C. uraceomajalis TYPE	DB1623 (BP)	NR131835	Hungary	Dima et al. (2014)
C. uraceonemoralis	ORS-ERDO99-15-1 (BP)	KJ206520	Hungary	Dima et al. (2014)
C. uraceonemoralis TYPE	H7017739	NR131836	Italy	Dima et al. (2014)
C. uraceus TYPE	TN04-872 (H)	NR131837	Finland	Dima et al. (2014)
C. uraceus	IK98-1607 (H)	KJ206525	Finland	Dima et al. (2014)
C. vernalisierraensis TYPE	DBB33386 (UC)	KX882652	USA	Ammirati et al. (2017)
C. vernalisierraensis	DBB15144 (UC)	KX882653	USA	Ammirati et al. (2017)

notated in GenBank. For phylogenetic analyses, both Bayesian Inference (BI) and Maximum Likelihood (ML) methods were used. The analyses were performed with two partitions, one including ITS1 and ITS2, the other including coding sequences (SSU, 5.8S and LSU). The two partitions alignments were concatenated using Phyutility 2.2 (Smith and Dunn 2008). Exactly identical sequences were removed from the data matrix (Vadthanarat et al. 2017). For BI analysis, the best-fit model for each partition was determined using the Akaike Information Criterion (AIC), implemented in MrModeltest 2.3 (Nylander 2004). BI analysis was performed with MrBayes 3.2.6 (Ronquist and Huelsenbeck 2003). Markov Chain Monte Carlo (MCMC) chains were run for 200,000 generations, sampling every 100th generation at which point the average standard deviation of split frequencies was 0.00594. The first 25% of trees were discarded to build the 50% majority rule consensus tree. ML analysis was performed with RAxML (Stamatakis 2014) and implemented in raxmlGUI (Silvestro and Michalak 2012). All parameters in the ML analysis were kept as defaults, except for choosing GTRGAMMAI as the model of sequence evolution. For testing the support of the branches, rapid bootstrap analysis with 1,000 replicates was chosen. The resulting phylogenies were visualised in FigTree 1.4.3 (http://tree.bio.ed.ac.uk/software/figtree/).

Results

Phylogenetic analyses

The dataset for phylogenetic analyses contained 60 ITS sequences, representing 27 species (Table 1). The combined matrix of 33 samples with 583 nucleotide sites (including 366 informative sites) is available from TreeBASE under S26123 (study accession URL: http://purl.org/phylo/treebase/phylows/study/TB2:S26123). GTR+G and JC were chosen as the best-fit model for ITS1+ITS2 partition and SSU+5.8S+LSU partition, respectively. The BI and ML trees showed similar topologies with high statistical support values. The ML tree was selected as the representative phylogeny (Fig. 1). The

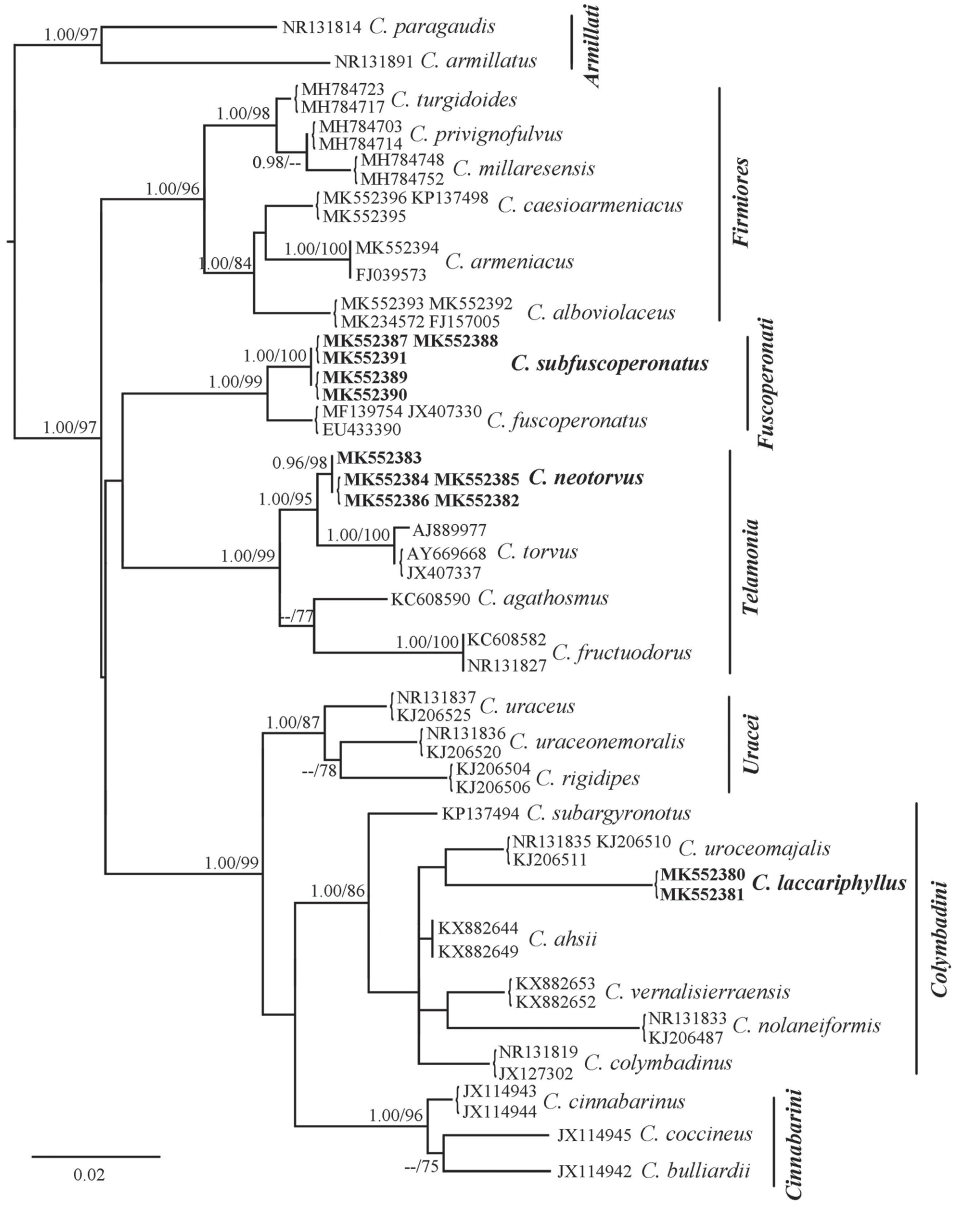

Figure 1. Maximum Likelihood tree inferred from ITS sequences. The tree is rooted with section *Armillati*. Bayesian posterior probabilities (≥ 0.95) and ML bootstrap values (≥ 75%) are shown on each branch (BPP / ML). New species in bold.

Bayesian posterior probabilities (BPP) ≥ 0.95 and ML bootstrap values (ML) ≥ 75% are shown on the branches.

The phylogenetic analyses recovered seven sections, including outgroup (Fig. 1). Three new species were separated into individual lineages with high statistical support

values and were distinct from their closest taxa, respectively. *Cortinarius laccariphyllus* had a distinct position with other species in section *Colymbadini* (BPP = 1.00, MLBS = 86%). The five collections of *C. neotorvus* (BPP = 0.96, MLBS = 98%) formed a sister relationship (BPP = 1.00, MLBS = 95%) with *C. torvus* (Fr.) Fr. in section *Telamonia*. *Cortinarius subfuscoperonatus* (BPP = 1.00, MLBS = 100%) formed a sister relationship (BPP = 1.00, MLBS = 99%) with *C. fuscoperonatus* Kühner in section *Fuscoperonati*.

Taxonomy

***Cortinarius laccariphyllus* Y. Li & M.L. Xie, sp. nov.**
MycoBank No: 830780
Figures 2a, b, 3a, 4a

Diagnosis. Pileus 2.2–6.6 cm in diam., strongly hygrophanous, translucently striate. Lamellae distant, *Laccaria*-like when young. Universal veil white, extremely sparse. Basidiospores 7.7–9.7 × 4.5–5.8 µm. The ITS sequences differ from the sequences of other species of section *Colymbadini* by at least fifteen substitutions and eight indel positions.

Holotype. China. Jilin Province: Antu County, Liangjiang Town, Dongfanghong Village, broadleaf forest (*Quercus mongolica* dominated forest with some *Juglans* and *Acer*), 42°42'51"N, 128°01'10"E, alt. 640 m, 5 August 2017, M.L. Xie, HMJAU44449, GenBank No. (ITS) MK552380.

Etymology. The name refers to the *Laccaria*-like lamellae when young.

Description. Pileus 2.2–6.6 cm in diam., conical when young, then convex, strongly hygrophanous, reddish-brown (9E6–8), dark brown at the centre (8F6–8), margin to half-way translucently striate, rarely fibrillose, margin thin and wavy. Lamellae subadnate to emarginated, distant, *Laccaria*-like (*Laccaria laccata* (Scop.) Cooke) when young, reddish-brown (9E6–8) to rusty brown (6E8), edge slightly serrate. Stipe 4.2–6.6 cm long, 0.4–0.8 cm thick at apex, 0.2–0.5 cm thick at base, cylindrical to tapering towards base, dark brown (7F6) to black brown (7F3), surface with white fibrillose when young, these disappearing with age (excluding the base of stipe). Universal veil white, extremely sparse, soon disappearing. Context dark brown (7F6–8), strongly hygrophanous (pileus and stipe). Odour indistinct. Exsiccata brown (5F8) to black brown (7F5). UV fluorescence yellow on stipe, pileus and lamellar edge, strong at stipe base.

Basidiospores 7.7–9.7 × 4.5–5.8 µm, Q = 1.43–1.84, `X = 8.0–8.5 × 4.8–5.2 µm, `Q = 1.66–1.70 (60 spores, 2 specimens), ellipsoid to amygdaloid, moderately and sharply verrucose, moderately dextrinoid. Basidia 4-spored, clavate, 23–39 × 7–9 µm, thin-walled, hyaline to olivaceous brown in 5% KOH. Lamellar edge fertile, with cylindrical-clavate sterile cells, 14–41 × 7–17 µm, thin-walled, hyaline in 5% KOH. Lamellar trama hyphae regular, pale olivaceous to olivaceous brown in 5% KOH, finely and densely encrusted. Pileipellis: epicutis hyphae cylindrical, 4–9.5 µm wide, dark olivaceous brown in 5% KOH, encrusted; hypocutis well developed, hyphae 11.5–53 µm wide, sub-cellular to cylindrical, slightly olivaceous in 5% KOH, finely

Figure 2. Basidiocarps of three newly-described species. **a, b** *Cortinarius laccariphyllus* (**a, b** HMJAU44449, holotype); **c, d** *Cortinarius neotorvus* (**c** HMJAU44441, holotype; **d** HMJAU44439); **e, f** *Cortinarius subfuscoperonatus* (**e** HMJAU44444, holotype; **f** HMJAU44445). Scale bars: 2 cm (**a, b, d–f**). Photographs by Meng-Le Xie.

encrusted. Pileus trama hyphae thin-walled, hyaline to slightly olivaceous in 5% KOH, smooth to finely encrusted. Clamp connections present.

ITS sequence. The ITS sequences of two specimens are 534 bp long and 100% identical. They differ from the sequences of other species of section *Colymbadini* (Niskanen et al. 2013a; Dima et al. 2014; Ammirati et al. 2017) by at least fifteen substitutions and eight indel positions.

Ecology and distribution. In broadleaf forest (*Quercus mongolica* dominated forest). Gregarious. Known from Jilin Province, China.

Additional specimens examined. China. Jilin Province: Antu County, Liangjiang Town, Dongfanghong Village, broadleaf forest (*Quercus mongolica* dominated for-

est with some *Juglans* and *Acer*), 42°42'51"N, 128°01'10"E, alt. 640 m, 5 August 2017, M.L. Xie, HMJAU44450, GenBank No. (ITS) MK552381.

Comments. *Cortinarius laccariphyllus* has strongly hygrophanous basidiomata, *Laccaria*-like (when young), with distantly-spaced lamellae and an extremely sparse, white veil. Morphologically, *C. nolaneiformis* (Velen.) Dima, Niskanen & Liimat. is similar to *C. laccariphyllus* due to the strongly hygrophanous pileus, similar colouration and similar size of spores. *Cortinarius uraceomajalis* Dima, Liimat., Niskanen & Bojantchev is also similar to *C. laccariphyllus* because of the black brown stipe and the striate pileus. However, both *C. nolaneiformis* and *C. uraceomajalis* have a yellowish veil and medium-spaced lamellae and lamellae not *Laccaria*-like. Furthermore, *C. nolaneiformis* is associated with broadleaf trees and also occurs in coniferous forest; *C. uraceomajalis* has a somewhat lighter brown pileus as well as generally smaller (av. 7.8–8.1 × 4.6–4.7 μm) and narrower (Qav. > 1.7) spores (Dima et al. 2014). In the phylogenetic analyses, *C. laccariphyllus* was well separated from other species in section *Colymbadini*.

***Cortinarius neotorvus* Y. Li, M.L. Xie & T.Z. Wei, sp. nov.**
MycoBank No: 835346
Figures 2c, d, 3b, 4b

Diagnosis. Pileus 2–4.4 cm in diam., weakly hygrophanous, orange grey. Lamellae greyish-red when young. Stipe cylindrical to somewhat tapering towards base. Universal veil greyish-yellow. Context white, sometimes with violet tinge at the stipe apex. Basidiospores 8.5–10.2 × 5.8–6.9 μm. Lamellar edge sterile. The ITS sequence of the holotype differs from the sequences of other species in section *Telamonia* by at least six substitutions and five indels.

Holotype. China. Jilin Province: Antu County, Liangjiang Town, Dongfanghong Village, broadleaf forest (*Quercus mongolica* dominated forest with some *Juglans* and *Acer*), 42°42'51"N, 128°01'10"E, alt. 640 m, 5 August 2017, M.L. Xie, HMJAU44441, GenBank No. (ITS) MK552384.

Etymology. The name refers to *Cortinarius torvus*.

Description. Pileus 2–4.4 cm in diam., hemispherical when young, then convex to almost plane with a low, broad umbo, weakly hygrophanous, orange grey (5B2), paler at the margin, surface with greyish-white fibrillose. Lamellae emarginate, medium-spaced, yellowish-grey (4B2), greyish-red (9B4–6) when young, sometimes with violet tinge when young, margin paler, slightly serrate. Stipe 4.1–10.5 cm long, 0.5–0.7 cm thick at apex, 0.3–0.5 cm thick at base, cylindrical to somewhat tapering towards base, orange grey (5B2) when moist, sometimes with violet tinge at the apex when young, surface with richly whitish fibrillose. Universal veil greyish-yellow (4B3), copious, usually forming a girdle on the upper stipe, cortina white. Context white (A1), marbled watery when moist, sometimes with violet tinge at the apex of the stipe. Odour indistinct. Exsiccata brown (6E5) to dark brown (6F6).

Basidiospores 8.5–10.2 × 5.8–6.9 μm, Q = 1.31–1.67, `X = 9.0–9.9 × 6.1–6.5 μm, `Q = 1.45–1.61 (130 spores, 6 collections), ellipsoid, moderately verrucose, moderate-

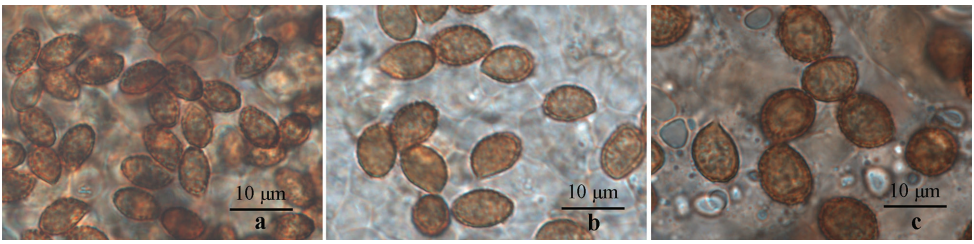

Figure 3. Basidiospores of three newly-described species. **a** *Cortinarius laccariphyllus* (HMJAU44449, holotype); **b** *Cortinarius neotorvus* (HMJAU44441, holotype); **c** *Cortinarius subfuscoperonatus* (HMJAU44444, holotype). Photographs by Meng-Le Xie.

ly dextrinoid. Basidia 4-spored, cylindrical to clavate, 27–53 × 7–12 μm, thin-walled, hyaline to olivaceous brown in 5% KOH. Lamellar edge sterile, sterile cells cylindrical-clavate, 11–26 × 3–9 μm, thin-walled, hyaline in 5% KOH. Lamellar trama hyphae regular, pale olivaceous in 5% KOH, smooth. Universal veil hyphae thin-walled, hyaline to pale olivaceous yellow in 5% KOH. Pileipellis: epicutis hyphae cylindrical, 2–6 μm wide, olivaceous brown in 5% KOH, smooth; hypocutis well developed, hyphae 15–38 μm wide, sub-cellular, thin-walled, hyaline in 5% KOH, smooth. Pileus trama hyphae thin-walled, hyaline to slightly olivaceous in 5% KOH, smooth. Clamp connections present.

ITS sequence. The ITS sequences of *C. neotorvus* are 513–515 bp long (5 collections, Table 1). All four sequences (MK552384 holotype, MK552385, MK552386 and MK552382) are identical and only MK552383 has 2 bp indels. The ITS sequence of *C. neotorvus* (MK552384, holotype) differs from the sequences of other species in section *Telamonia* by at least six substitutions and five indels.

Ecology and distribution. In broadleaf forest (*Quercus mongolica* dominated forest). Solitary or gregarious. Known from Jilin and Heilongjiang Province, China.

Additional specimens examined. China. Heilongjiang Province: Heihe City, Wudalianchi Scenic Area, broadleaf forest (*Quercus mongolica*), 48°39'15"N, 126°28'18"E, alt. 290 m, 16 August 2017, M.L. Xie, HMJAU44442, GenBank No. (ITS) MK552385; 12 August 2018, P.J. Xing, HMJAU44440; Heihe City, Shengshan National Nature Reserve, broadleaf forest (*Quercus mongolica* dominated forest with some *Tilia* and *Alnus*), 49°30'N, 126°43'E, alt. 300 m, 11 September 2017, G.H. Cheng, HMJAU44443, GenBank No. (ITS) MK552386. Jilin Province: Yanji City, Sandaowan Town, broadleaf forest (*Quercus mongolica*), 43°16'10"N, 129°07'19"E, alt. 580 m, 8 September 2018, M.L. Xie, HMJAU44437, GenBank No. (ITS) MK552382, HMJAU44438, GenBank No. (ITS) MK552383, HMJAU44439.

Comments. *Cortinarius neotorvus* is easily confused with *C. torvus* due to highly similar morphology. Morphologically, the lamellae of *C. torvus* are adnate to subdecurrent and distant (Bidaud et al. 1999; Breitenbach and Kränzlin 2000; Soop 2014) and the pileus colour of *C. torvus* is usually darker and with a violet tinge, as well as the stipe usually being bulbous at the base (Consiglio et al. 2003). In mo-

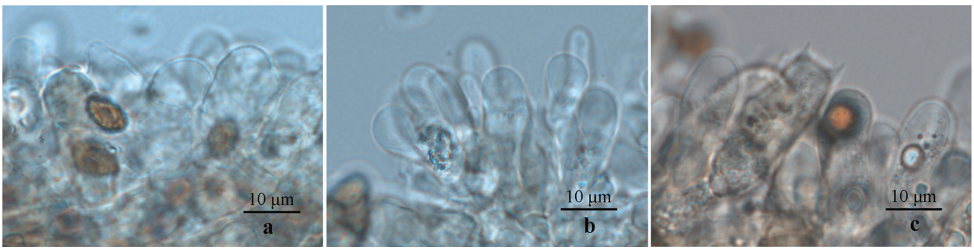

Figure 4. Margin cells of three newly-described species. **a** *Cortinarius laccariphyllus* (HMJAU44449, holotype); **b** *Cortinarius neotorvus* (HMJAU44441, holotype); **c** *Cortinarius subfuscoperonatus* (HMJAU44444, holotype). Photographs by Meng-Le Xie.

lecular data, the ITS sequence of *C. neotorvus* (MK552384, holotype) differ from the sequences of *C. torvus* (AY669668, JX407337) by six substitutions and five indels. In the phylogenetic analyses, the five specimens of *C. neotorvus* were placed in separate monophyletic lineages (BPP = 0.96, MLBS = 90%) and formed a sister relationship with *C. torvus*.

Cortinarius subfuscoperonatus **Y. Li & M.L. Xie, sp. nov.**
MycoBank No: 830782
Figures 2e, f, 3c, 4c

Diagnosis. Pileus 1.6–4.4 cm in diam. Context white, greyish-brown when moist. Basidiospores 9.5–12.1 × 7.9–9.7 µm. The ITS sequence of the holotype differs from other species in section *Fuscoperonati* by at least six substitutions and six indels.

Holotype. China. Gansu Province: Zhangye City, Minle County, Gansu Qilianshan National Nature Reserve, coniferous forest (*Picea crassifolia*), 38°17'55"N, 100°45'54"E, alt. 2860 m, 9 August 2018, M.L. Xie, HMJAU44444, GenBank No. (ITS) MK552387.

Etymology. The name refers to its affinity to *Cortinarius fuscoperonatus*.

Description. Pileus 1.6–4.4 cm in diam., hemispherical when young, then low convex, weakly hygrophanous, pale greyish-brown (6C3), sometimes reddish-brown (9E5–9E6) to dark brown (6F6–6F8), surface with greyish-brown fibrillose, margin wavy with age. Lamellae emarginate, medium-spaced, reddish-brown to rusty brown (7D6–7E7), margin even when young, then slightly serrate. Stipe 2.3–7.5 cm long, 0.8–1.3 cm thick at apex, 1.5–2.5 cm thick at base, clavate, white to pale grey (E2), mycelium white at the base. Universal veil greyish-brown (6C2), rich, usually forming an annular band on the middle part and distinct belts or zones lower down. Context white (A1), greyish-brown (7F8) and marbled watery when moist, strongly hygrophanous near pileus and lamellae. Odour somewhat radish-like. Chemical reaction: pileus and context (fresh basidiomata) are dark black brown (8F3) with 10% KOH. Exsiccata brown (6E5) to dark brown (6F5).

Basidiospores 9.5–12.1 × 7.9–9.7 μm, Q = 1.10–1.45, `X = 10.3–11.2 × 8.0–8.6 μm, `Q = 1.24–1.33 (135 spores, 5 collections), subglobose to broadly ellipsoid, moderately to strongly verrucose, strongly dextrinoid. Basidia 4-spored, clavate, 35–58 × 10–13 μm, thin-walled, hyaline to olivaceous brown in 5% KOH. Lamellar edge fertile, with cylindrical-clavate sterile cells, 13–27 × 6–11 μm, thin-walled, hyaline to slightly olivaceous yellow in 5% KOH. Lamellar trama hyphae regular, pale olivaceous to olivaceous brown in 5% KOH, smooth. Pileipellis: epicutis hyphae cylindrical, 4–12 μm wide, slightly olivaceous brown to olivaceous brown in 5% KOH, some hyphae finely encrusted; hypocutis well developed, hyphae 24–89 × 15–29 μm, sub-cellular to sub-cylindrical, thin-walled, hyaline to slightly olivaceous brown in 5% KOH, smooth. Pileus trama hyphae almost thin-walled, hyaline in 5% KOH, smooth. Clamp connections present.

ITS sequence. The ITS sequences of *C. subfuscoperonatus* are 524–525 bp long (5 collections, Table 1) and distinct from other members of section *Fuscoperonatus*. The ITS sequence of *C. subfuscoperonatus* (MK552387, holotype) differs from *C. fuscoperonatus* by six substitutions and six indels.

Ecology and distribution. In coniferous forest (*Picea crassifolia* dominated forest). Solitary or gregarious. Known from Gansu Province, China.

Additional specimens examined. China. Gansu Province: Zhangye City, Minle County, Gansu Qilianshan National Nature Reserve, coniferous forest (*Picea crassifolia*), 38°17'55"N, 100°45'54"E, alt. 2860 m, 9 August 2018, M.L. Xie, HMJAU44445, GenBank No. (ITS) MK552388; Zhangye city, Su'nan Yugu Autonomous County, Gansu Qilianshan National Nature Reserve, coniferous forest (*Picea crassifolia* dominated forest, occasionally with *Juniperus*), 38°44'57"N, 99°47'56"E, alt. 3010 m, 10 August 2018, M.L. Xie, HMJAU44446, GenBank No. (ITS) MK552389, HMJAU44447, GenBank No. (ITS) MK552390; Zhangye city, Su'nan Yugu Autonomous County, Gansu Qilianshan National Nature Reserve, coniferous forest (*Picea crassifolia* dominated forest, occasionally with *Juniperus*), 38°33'13"N, 100°41'75"E, alt. 2700 m, 11 August 2018, M.L. Xie, HMJAU44448, GenBank No. (ITS) MK552391.

Comments. *Cortinarius subfuscoperonatus* corresponds well to the characteristics of section *Fuscoperonati*, with weak hygrophanous pileus, an annular band on the middle stipe and distinct belts or zones lower down, large spores (> 10 μm long) and grow in coniferous forests. *Cortinarius fuscoperonatus* was previously placed in section *Bovini* M.M. Moser (Bidaud et al. 2009; Soop 2014) and *Armillati* (Brandrud et al. 1992), until Niskanen et al. (2015) placed it in section *Fuscoperonati*. *Cortinarius subfuscoperonatus* has remarkably similar morphological characteristics to *C. fuscoperonatus*, apart from the spores of *C. fuscoperonatus* being narrower (9.7–11.6 × 6.6–7.7 μm), the pileus being chocolate brown to blackish-brown and being fine fibrous to fine scaly (Schmidt-Stohn et al. 2017). In addition, *C. subfuscoperonatus* formed a sister relationship with *C. fuscoperonatus* and was well separated according to the phylogenetic analyses. *C. subfuscoperonatus* could be considered as the second species in section *Fuscoperonati*.

Key to new species and morphologically-similar species in sections *Colymbadini*, *Telamonia* and *Fuscoperonati*

1 Basidiomata medium. Pileus more or less brown, strongly hygrophanous. Stipe usually cylindrical. Universal veil sparse. With positive yellow UV reaction. Associated with coniferous and/or broadleaf trees. Spores ellipsoid to amygdaloid ..... (**section *Colymbadini***) **2**

– Basidiomata medium to large. Pileus more or less brown and hygrophanous. Stipe cylindrical to clavate. Universal veil white to greyish-yellow, sometimes with violet tinge, usually forming a ring at the middle stipe. Associated with coniferous and/or broadleaf trees ..... (**section *Telamonia***) **3**

– Basidiomata medium to large. Pileus brown and weakly hygrophanous. Stipe clavate to slightly bulbous. Universal veil greyish-brown to blackish-brown. Associated with coniferous trees. Spores subglobose to ellipsoid, moderately to strongly verrucose ..... (**section *Fuscoperonati***) **4**

2 Pileus strongly hygrophanous, reddish-brown to dark brown, surface translucently striate. Lamellae distant, *Laccaria*-like when young. Stipe cylindrical to tapering towards base, hollow. Universal veil white, extremely sparse. Odour indistinct. Positively yellow UV fluorescence (exsiccata). Associated with broadleaf trees. Spores ellipsoid to amygdaloid, on average 8.0–8.5 × 4.8–5.2 μm. ..... ***C. laccariphyllus***

– Pileus strongly hygrophanous, yellowish-brown to brown, margin striate. Lamellae medium-spaced. Stipe cylindrical to tapering towards base, not hollow. Universal veil yellow, very sparse. Odour similar to raw vegetables. Usually yellow UV fluorescence at stipe. Associated with broadleaf trees. Spores amygdaloid to narrowly amygdaloid, on average 7.8–8.1 × 4.6–4.7 μm..... ..... ***C. uraceomajalis***

– Pileus strongly hygrophanous, dark greyish-brown to dark brown, margin slightly striate. Lamellae medium-spaced to fairly distant, margin whitish when young. Stipe cylindrical to clavate, sometimes tapering downwards, sometimes hollow. Universal veil yellow. Strong yellow UV fluorescence at stipe, dull yellowish-brown at pileus, lamellae and context. Associated with coniferous and broadleaf trees. Spores amygdaloid to weakly ellipsoid, on average 8.1–8.6 × 4.8–5.1 μm..... ***C. nolaneiformis***

3 Pileus pale greyish-yellow, paler at the margin, weakly hygrophanous. Lamellae emarginate, medium-spaced, greyish-red when young, sometimes with violet tinge. Stipe cylindrical to somewhat tapering towards base, pale greyish-yellow. Odour indistinct. Spores ellipsoid, on average 9.0–9.9 × 6.1–6.5 μm ..... ***C. neotorvus***

– Pileus greyish-brown to chestnut brown, usually with violet tinge at the margin, weakly hygrophanous. Lamellae adnate, subdecurrent to distant, greyish-brown, with violet tinge. Stipe clavate, usually bulb at the base. Odour acidulous. Spores ellipsoid, 8–10.5 × 6–7 μm..... ***C. torvus***

4 Pileus pale greyish-brown, sometimes reddish-brown to dark brown, margin wavy with age, with greyish-brown fibrillose. Stipe clavate. Spores subglobose to broadly ellipsoid, on average 10.3–11.2 × 8.0–8.6 µm..... ..... ***C. subfuscoperonatus***

– Pileus chocolate brown to blackish-brown, pale greyish-brown at the edge, fine fibrous to fine scaly. Stipe clavate, with a bulb at the base. Spores ellipsoid to broadly ellipsoid, 9.7–11.6 × 6.6–7.7 µm ..... ***C. fuscoperonatus***

Discussion

Cortinarius is the most species-rich genus of Agaricales, with most of the described species distributed in the Northern Hemisphere. However, so far, little has been done on *Cortinarius* taxonomy in north-eastern Asia or even in the whole of Asia, leaving an important gap in our knowledge of this genus (Horak 1983). The flora of northern China has a strong affinity shared with the circumboreal areas of Europe and western North America but also harbours some floristic elements with a tropical and subtropical affinity (Wu 1979). Some *Cortinarius* species in northern China are the same as those in Europe and western North America (e.g. Xie 2018; Cheng et al. 2019; Wei and Liu 2019). However, there are also some endemic species in China (Wei and Yao 2015; Xie et al. 2019). Thus far, only 229 *Cortinarius* species (about 10% in the world) have been reported in China. Therefore, studies focusing on Chinese *Cortinarius* are needed.

In this study, we described the phylogenetic relationships amongst the three new species and other species, based on the ITS sequences. However, multiple genes should be used in future studies to describe more complex phylogenetic relationships in *Cortinarius*, which some mycologists have conducted. Peintner et al. (2002) assessed the phylogenetic relationships of *Rozites*, *Cuphocybe* and *Rapacea* by molecular phylogenetic approaches, based on ITS and LSU. Frøslev et al. (2005) analysed the phylogeny of *Cortinarius* subgenus *Phlegmacium*, a taxonomically difficult group, based on ITS, RPB1 and RPB2. They speculated that the sequences from RNA polymerase II genes have the potential for resolving the phylogenetic problems of *Cortinarius*. Later, the study of Frøslev et al. (2007) showed that the delimitation of species, based on ITS sequences, is more consistent with a conservative morphological species concept and there is considerable potential for using ITS sequence data as a barcode for section *Calochroi*. Soop et al. (2019) studied the global supraspecific taxonomy of *Cortinarius* by the phylogenetic approach, based on ITS, LSU, RPB1 and RPB2. Both ITS and LSU datasets and ITS, LSU, RPB1 and RPB2 datasets showed satisfactory results. Although phylogenetic analyses of *Cortinarius* have made significant progress in Europe, North America and even in Australasia, few phylogenetic analyses of *Cortinarius*, based on Chinese materials have been carried out. According to our analysis of ITS data, there are presently less than 200 accessions (excluding sequences obtained from mycorrhiza) from China in GenBank. Thus, the dedicated collection of specimens and studying the phylogeny of *Cortinarius*, based on the ITS or, preferably, multiple genes, are important contributions to the global phylogenetic framework of *Cortinarius*.

Acknowledgements

The study was supported by China Agriculture Research System (No. CARS20), Special Fund for Agro-scientific Research in the Public Interest (No. 201503137), Overseas Expertise Introduction Project for Discipline Innovation (111 Center) (No. D17014), National Natural Science Foundation of China (No. 31270072), the Special Funds for the Young Scholars of Taxonomy of the Chinese Academy of Sciences (No. ZSBR-001). We would like to express our gratitude to the people in the Engineering Research Center of Edible and Medicinal Fungi, Ministry of Education, Jilin Agricultural University, including Dr. Bo Zhang for her suggestions to improve our work, Ms. Yang Yang and Ms. Yu-Xiu Guo for their help during molecular experiments, Mr. Yang Wang, Mr. Zhu-Shan Liu and Mr. Zhi-Hui Luo for their help during the field trips in Jilin and Heilongjiang, as well as Prof. Sheng-Long Wei and Ms. Qian-Qian Liang (Gansu Engineering Laboratory of Applied Mycology, Hexi University, China) for their kind help during the field trips in Gansu. We thank Dr. Frederick Leo Sossah for his kind-hearted and excellent technical assistance with the English language correction. We also thank the reviewers, Bálint Dima, Joseph F. Ammirati and Jerry Adrian Cooper, for their suggestions and corrections to improve our work.

References

Ammirati JF, Hughes KW, Liimatainen K, Niskanen T, Matheny PB (2013) *Cortinarius hesleri* from eastern North America and related species from Europe and western North America. Botany 91:91–98. https://doi.org/10.1139/cjb-2012-0154

Ammirati JF, Niskanen T, Liimatainen K, Bojantchev D, Peintner U, Kuhnert-Finkernagel R, Cripps C (2017) Spring and early summer species of *Cortinarius*, subgenus *Telamonia*, section *Colymbadini* and /*Flavobasilis*, in the mountains of western North America. Mycologia 109(3): 443–458. https://doi.org/10.1080/00275514.2017.1349468

Bessette A, Bessette AR, Fischer DW (1997) Mushrooms of northeastern North America. Syracuse University Press, Syracuse.

Bidaud A, Bellanger JM, Carteret X, Reumaux P, Moënne-Loccoz P (2017) Atlas des Cortinaires XXVI. Éditions Fédération Mycologique Dauphiné-Savoie, Meyzieu.

Bidaud A, Moënne-Loccoz P, Reumaux P (1994) Atlas des Cortinaires. Clé générale des sous-genres, sections, sous-sections et séries. Éditions Fédération Mycologique Dauphiné-Savoie, Meyzieu.

Bidaud A, Moënne-Loccoz P, Reumaux P, Carteret X (2009) Atlas des Cortinaires XVIII. Éditions Fédération Mycologique Dauphiné-Savoie, Meyzieu.

Bidaud A, Moënne-Loccoz P, Reumaux P, Henry R (1999) Atlas des Cortinaires IX. Éditions Fédération Mycologique Dauphiné-Savoie, Meyzieu.

Bojantchev D, Davis RM (2011) *Cortinarius callimorphus*, a new species from northern California. Mycotaxon 117(1): 1–8. https://doi.org/10.5248/117.1

Bougher NL, Hilton RN (1989) Three *Cortinarius* species from Western Australia. Mycological Research 93(4): 424–428. https://doi.org/10.1016/S0953-7562(89)80035-8

Brandrud TE, Frøslev TG, Dima B (2018b) Rare, whitish-pale ochre *Cortinarius* species of section *Calochroi* from calcareous *Tilia* forests in South East Norway. Agarica 38: 3–20.

Brandrud TE, Lindström H, Marklund H, Melot J, Muskos S (1989) *Cortinarius* flora Photographica I. *Cortinarius* HB, Matfors.

Brandrud TE, Lindström H, Marklund H, Melot J, Muskos S (1992) *Cortinarius* Flora Photographica II. *Cortinarius* HB, Matfors.

Brandrud TE, Schmidt-Stohn G, Liimatainen K, Niskanen T, Frøslev TG, Soop K, Bojantchev D, Kytövuori I, Jeppesen TS, Bellù F, Saar, G, Oertel B, Ali T, Thines M, Dima B (2018a) *Cortinarius* section *Riederi*: taxonomy and phylogeny of the new section with European and North American distribution. Mycological Progress 17(12): 1323–1354. https://doi.org/10.1007/s11557-018-1443-0

Breitenbach J, Kränzlin F (2000) Fungi of Switzerland. Vol. 5 Agarics (3rd part) Cortinariaceae. Mycologia Luzern, Lucerna.

Cheng GH, An XY, Xie ML, Li Y (2019) New records of *Cortinarius* species collected from Heilongjiang Province in China. Journal of Fungal Research 17(2): 67–73.

Consiglio G, Antonini D, Antonini M (2003) Il Genere *Cortinarius* in Italia (Parte prima). Associazione Micologica Bresadola, Luglio.

Dima B, Liimatainen K, Niskanen T, Kytövuori I, Bojantchev D (2014) Two new species of *Cortinarius*, subgenus *Telamonia*, sections *Colymbadini* and *Uracei*, from Europe. Mycological Progress 13(3): 867–879. https://doi.org/10.1007/s11557-014-0970-6

Gardes M, Bruns TD (1993) ITS primers with enhanced specificity for basidiomycetes–application to the identification of mycorrhizae and rusts. Molecular Ecology 2(2): 113–118. https://doi.org/10.1111/j.1365-294X.1993.tb00005.x

Garnica S, Schön ME, Abarenkov K, Riess K, Liimatainen K, Niskanen T, Dima B, Soop K, Frøslev TG, Jeppesen TS, Peintner U, Kuhnert-Finkernagel R, Brandrud TE, Saar G, Oertel B, Ammirati JF (2016) Determining threshold values for barcoding fungi: lessons from *Cortinarius* (Basidiomycota), a highly diverse and widespread ectomycorrhizal genus. FEMS Microbiology Ecology 92(4): fiw045. https://doi.org/10.1093/femsec/fiw045

Garnica S, Weiß M, Oberwinkler F (2003) Morphological and molecular phylogenetic studies in South American *Cortinarius* species. Mycological Research 107(10): 1143–1156. https://doi.org/10.1017/S0953756203008414

Garnica S, Weiß M, Oertel B, Oberwinkler F (2005) A framework for a phylogenetic classification in the genus *Cortinarius* (Basidiomycota, Agaricales) derived from morphological and molecular data. Botany 83(11): 1457–1477. https://doi.org/10.1139/b05-107

Gasparini B, Soop K (2008) Contribution to the knowledge of *Cortinarius* (Agaricales, Cortinariaceae) of Tasmania (Australia) and New Zealand. Australasian Mycologist 27(3): 173–203.

Hall TA (1999) BioEdit: A user-friendly biological sequence alignment editor and analysis program for Windows 95/98/NT. Nucleic Acids Symposium Series 41(41): 95–98.

Harrower E, Ammirati JF, Cappuccino AA, Ceska O, Kranabetter JM, Kroeger P, Lim S, Taylor T, Berbee ML (2011) *Cortinarius* species diversity in British Columbia and molecular phylogenetic comparison with European specimen sequences. Botany 89(11): 799–810. https://doi.org/10.1139/b11-065

Harrower E, Bougher NL, Winterbottom C, Henkel TW, Horak E, Matheny PB (2015) New species in *Cortinarius* section *Cortinarius* (Agaricales) from the Americas and Australasia. MycoKeys 11: 1–21. https://doi.org/10.3897/mycokeys.11.5409

He MQ, Zhao RL, Hyde KD, Begerow D, Kemler M, Yurkov A, McKenzie EHC, Raspé O, Kakishima M, Sánchez-Ramírez S, Vellinga EC, Halling R, Papp V, Zmitrovich IV, Buyck B, Ertz D, Wijayawardene NN, Cui BK, Schoutteten N, Liu XZ, Li TH, Yao YJ, Zhu XY, Liu AQ, Li GJ, Zhang MZ, Ling ZL, Cao B, Antonín V, Boekhout T, da Silva BDB, De Crop E, Decock C, Dima B, Dutta AK, Fell JW, Geml J, Ghobad-Nejhad M, Giachini AJ, Gibertoni TB, Gorjón SP, Haelewaters D, He SH, Hodkinson BP, Horak E, Hoshino T, Justo A, Lim YW, Menolli Jr. N, Mešić A, Moncalvo J, Mueller GM, Nagy LG, Nilsson RH, Noordeloos M, Nuytinck J, Orihara T, Ratchadawan C, Rajchenberg M, Silva-Filho AGS, Sulzbacher MA, Tkalčec Z, Valenzuela R, Verbeken A, Vizzini A, Wartchow F, Wei TZ, Weiß M, Zhao CL, Kirk PM (2019) Notes, outline and divergence times of Basidiomycota. Fungal Diversity 99: 105–367. https://doi.org/10.1007/s13225-019-00435-4

Høiland K, Holst-Jensen A (2000) *Cortinarius* phylogeny and possible taxonomic implications of ITS rDNA sequences. Mycologia 92: 694–710. https://doi.org/10.1080/00275514.2000.12061210

Horak E (1983) Mycogeography in the South Pacific region: Agaricales, Boletales. Australian Journal of Botany supplement 10: 1–41.

Kornerup A, Wanscher JHK (1978) The Methuen Handbook of Colour (3rd edn). Eyre Methuen Ltd. Reprint, London, UK.

Kytövuori I, Niskanen T, Liimatainen K, Lindström H (2005) *Cortinarius sordidemaculatus* and two new related species, *C. anisatus* and *C. neofurvolaesus* in Fennoscandia (Basidiomycota, Agaricales). Karstenia 45: 33–49. https://doi.org/10.29203/ka.2005.402

Li GJ, Zhao D, Li SF, Wen HA (2015) *Russula chiui* and *R. pseudopectinatoides*, two new species from southwestern China supported by morphological and molecular evidence. Mycological Progress 14: 33. https://doi.org/10.1007/s11557-015-1054-y

Liimatainen K (2014) Nomenclatural novelties. Index Fungorum. 198: 1–3. http://www.indexfungorum.org/Publications/Index%20Fungorum%20no.198.pdf

Liimatainen K, Niskanen T, Dima B, Kytövuor I, Ammirati JF, Frøslev TG (2014) The largest type study of Agaricales species to date: bringing identification and nomenclature of *Phlegmacium* (*Cortinarius*) into the DNA era. Persoonia 33: 98–140. https://doi.org/10.3767/003158514X684681

Miyauchi S (2001) A new species of *Cortinarius* Section *Hydrocybe* from Japan. Mycoscience 42(2): 223–225. https://doi.org/10.1007/BF02464141

Niskanen T (2008) *Cortinarius* subgenus *Telamonia* pp in North Europe. PhD Thesis, University of Helsinki, Finland.

Niskanen T, Kytövuori I, Bendiksen E, Bendiksen K, Brandrud TE, Frøslev TG, Høiland K, Jeppesen TS, Liimatainen K, Lindström H (2012) *Cortinarius* (Pers.) Gray. In: Knudsen H, Vesterholt J (Eds) Funga Nordica, 2nd revised edition. Agaricoid, boletoid, clavarioid, cyphelloid and gastroid genera, Nordsvamp, Copenhagen, Denmark, 762–763.

Niskanen T, Kytövuori I, Liimatainen K (2011) *Cortinarius* section *Armillati* in northern Europe. Mycologia 103(5): 1080–1101. https://doi.org/10.3852/10-350

Niskanen T, Kytövuori I, Liimatainen K, Ammirati JF (2015) Nomenclatural novelties. Index Fungorum 256: 1–2. http://www.indexfungorum.org/Publications/Index%20Fungorum%20no.256.pdf

Niskanen T, Kytövuori I, Liimatainen K, Lindström H (2013b) The species of *Cortinarius*, section *Bovini*, associated with conifers in northern Europe. Mycologia 105(4): 977–993. https://doi.org/10.3852/12-320

Niskanen T, Liimatainen K, Ammirati JF (2013a) Five new *Telamonia* species (*Cortinarius*, Agaricales) from western North America. Botany 91(7): 478–485. https://doi.org/10.1139/cjb-2012-0292

Nylander JAA (2004) MrModeltest v2. Program distributed by the author. Evolutionary Biology Centre, Uppsala University, Uppsala.

Peintner U, Moser MM, Thomas KA, Manimohan P (2003) First records of ectomycorrhizal *Cortinarius* species (Agaricales, Basidiomycetes) from tropical India and their phylogenetic position based on rDNA ITS sequences. Mycological Research 107(4): 506–508. https://doi.org/10.1017/S0953756203007585

Ronquist F, Huelsenbeck JP (2003) MrBayes 3: Bayesian phylogenetic inference under mixed models. Bioinformatics 19 (12): 1572–1574. https://doi.org/10.1093/bioinformatics/btg180

San-Fabian B, Niskanen T, Liimatainen K, Kooij PW, Mujic AB, Truong C, Peintner U, Dresch P, Nouhra E, Matheny PM, Smith ME (2018) New species of *Cortinarius* sect. *Austroamericani*, sect. nov., from South American Nothofagaceae forests, Mycologia 110(6): 1127–1144. https://doi.org/10.1080/00275514.2018.1515449

Schmidt-Stohn G, Brandrud TE, Dima B (2017) Interessante *Cortinarius*–Funde der Journées européennes du Cortinaire 2016 in Borgsjö, Schweden. Journal des JEC 19: 28–52.

Shao LP, Xiang CT (1997) Forest Mushrooms of China. Northeast Forestry University Press, Haerbin.

Silvestro D, Michalak I (2012) RaxmlGUI: a graphical front-end for RAxML. Org Divers Evol 12:335–337. https://doi.org/10.1007/s13127-011-0056-0

Smith SA, Dunn CW (2008) Phyutility: a phyloinformatics tool for trees, alignments and molecular data. Bioinformatics 24: 715–716. https://doi.org/10.1093/bioinformatics/btm619

Soop K (2005) A contribution to the study of the cortinarioid mycoflora of New Zealand, III. New Zealand Journal of Botany 43(2): 551–562. https://doi.org/10.1080/002882 5X.2005.9512974

Soop K (2014) *Cortinarius* in Sweden (14 edition). Éditions Scientrixk, Sweden.

Soop K, Dima B, Cooper JA, Park D, Oertel B (2019) A phylogenetic approach to a global supraspecific taxonomy of *Cortinarius* (Agaricales) with an emphasis on the southern mycota. Persoonia 42: 261–290. https://doi.org/10.3767/persoonia.2019.42.10

Stamatakis A (2014) RAxML version 8: a tool for phylogenetic analysis and post-analysis of large phylogenies. Bioinformatics 30: 1312–1313. https://doi.org/10.1093/bioinformatics/btu033

Tai FL (1979) Sylloge fungorum sinicorum. Science Press, Beijing.

Teng SC (1963) Fungi of China. Science Press, Beijing.

Vadthanarat S, Lumyong S, Raspé O (2017) First record of *Albatrellus* (Russulales, Albatrellaceae) from Thailand. Phytotaxa 317(2): 104–112. https://doi.org/10.11646/phytotaxa.317.2.2

Valenzuela E, Esteve-Raventos F (1994) *Cortinarius horakii*, a new species from Chile. Mycological Research 98(8): 937–938. https://doi.org/10.1016/S0953-7562(09)80266-9

Wei TZ, Liu TZ (2019) Resource survey of macro-basidiomycetes in southern Greater Khingan Mountains, Chifeng City. Journal of Liaocheng University 32(6): 76–89.

Wei TZ, Yao YJ (2013) *Cortinarius korfii*, a new species from China. Mycosystema 32(3): 557–562.

White TJ, Bruns TD, Lee SB, Taylor JW, Innis MA, Gelfand DH, Sninsky JJ (1990) Amplification and direct sequencing of fungal ribosomal RNA genes for phylogenetics. In: Innis MA, Gelfand DH, Sninsky JJ, et al. (Eds) PCR protocols: a guide to methods and applications: 315–322. Academic Press, New York. https://doi.org/10.1016/B978-0-12-372180-8.50042-1

Wu CY (1979) The regionalization of Chinese flora. Acta Botanica Yunnanica 1: 1–22.

Xie ML (2018) Resources and Taxonomy of *Cortinarius* in Northeast of China. MA thesis, Jilin Agricultural University, China.

Xie ML, Li D, Wei SL, Ji RQ, Li Y (2019) *Cortinarius subcaesiobrunneus* sp. nov., (Cortinariaceae, Agaricales) a new species from northwest China. Phytotaxa 392(3): 217–224. https://doi.org/10.11646/phytotaxa.392.3.4

MycoKeys 69: 111–112 (2020)
doi: 10.3897/mycokeys.69.55264
http://mycokeys.pensoft.net

CORRIGENDA

A peer-reviewed open-access journal
MycoKeys
Launched to accelerate biodiversity research

Corrigendum: Bien S, Damm U (2020) *Arboricolonus simplex* gen. et sp. nov. and novelties in *Cadophora*, *Minutiella* and *Proliferodiscus* from *Prunus* wood in Germany. MycoKeys 63: 163–172. https://doi.org/10.3897/mycokeys.63.46836

Steffen Bien[1], Ulrike Damm[1,2]

1 *Senckenberg Museum of Natural History Görlitz, PF 300 154, 02806 Görlitz, Germany* **2** *International Institute Zittau, Technische Universität Dresden, Markt 23, 02763 Zittau, Germany*

Corresponding author: Ulrike Damm (ulrike.damm@senckenberg.de)

Academic editor: D. Haelewaters | Received 24 June 2020 | Accepted 24 June 2020 | Published @@ ###### 2020

Citation: Bien S, Damm U (2020) Corrigendum: Bien S, Damm U (2020) *Arboricolonus simplex* gen. et sp. nov. and novelties in *Cadophora*, *Minutiella* and *Proliferodiscus* from *Prunus* wood in Germany. MycoKeys 63: 163–172. https://doi.org/10.3897/mycokeys.63.46836. MycoKeys 69: 111–112. https://doi.org/10.3897/mycokeys.69.55264

In the original article, the herbarium code of the Senckenberg Museum of Natural History Görlitz, Germany, was wrongly cited as GLMC. The correct herbarium code of the institution is GLM.

We combined *Margarinomyces bubakii* in the genus *Cadophora*. This was not compliant with the International Code of Nomenclature for algae, fungi and plants article F.5.1 (Turland et al. 2018), because a registration identifier was lacking, which is compulsory since 1 January 2013. The combination is now validated by providing the MycoBank number below.

Taxonomy

Cadophora bubakii **(Laxa) Damm & S.Bien, comb. nov.**
MycoBank No: 835799

Margarinomyces bubakii Laxa, Centralbl. Bakteriol. 2. Abth. 81: 392. 1930. (Basionym)
≡ *Phialophora bubakii* (Laxa) Schol-Schwarz, Persoonia 6 (1): 66. 1970.

References

Turland NJ, Wiersema JH, Barrie FR, Greuter, W, Hawksworth DL, Herendeen PS, Knapp S, Kusber W-H, Li D-Z, Marhold K, May TW, McNeill J, Monro AM, Prado J, Price MJ, Smith GF (2018) International Code of Nomenclature for algae, fungi, and plants (Shenzhen Code) adopted by the Nineteenth International Botanical Congress, Shenzhen, China, July 2017. Regnum Vegetabile 159. Glashütten: Koeltz Botanical Books. https://doi.org/10.12705/Code.2018